Assessment of characteristics and transformations of ultrafine and fine particles in the roadside, ambient, and indoor environment in Hanoi, Vietnam

ベトナムハノイの沿道、一般、屋内環境における超微小粒子および微小粒子の特性と変質に関する研究

By

Truong Thi HUYEN

A dissertation submitted in partial fulfillment of the requirements for the degree of Doctor of Philosophy in Science and Engineering

Examination Committee: Prof. SEKIGUCHI Kazuhiko (Chairperson)
Prof. WANG (O) Qingyue (Seiyo)
Prof. FUJINO Takeshi
Assoc. Prof. YAMAGUCHI Masatoshi

Saitama University
Graduate School of Science and Engineering
Saitama, Japan
September 2022

Acknowledgements

This is an opportunity for me to express my heartfelt gratitude to everyone who supported me during my research time. I would like to thank my advisor Prof. Sekiguchi Kazuhiko who gave me precious guidance and support. Prof. Sekiguchi is a person who works tirelessly and inspires me with his rich research experience. Without his kind support and valuable advice, this work could have been done.

I would like to thank all committee members Prof. Wang (O) Qingyue (Seiyo), Prof. Fujino Takeshi, and Assoc. Prof. Yamaguchi Masatoshi for their helpful comments and suggestions during my whole PhD study period.

My special thanks are extended to the Japanese Government Scholarship (Monbukagakusho: MEXT) for financial support to pursue my PhD at Saitama University.

I want to sincerely thank all lecturers, staff, and students who support me during the field sampling in Hanoi. Specifically, I would like to thank Prof. Nghiem Trung Dung, Assoc. Prof. Ly Bich Thuy, and their students at Hanoi University of Science and Technology for their assistance during the sampling periods.

I would like to express special thanks to my labmates, a doctoral candidate Mr. Kurotsuchi Yuta for his endless assistance and all Sekiguchi's lab members for their support during my research period.

Special thanks are to all secretaries, and staff in the Environmental Science Department, Graduate School of Science and Engineering, Saitama University for their assistance and encouragement.

Finally, I would like to express my gratitude to my family for their continuous encouragement and inspiration to overcome the difficult time when studying abroad.

Abstract

Air pollution is an increasing issue in developing nations. The continuous rising of vehicle numbers in big cities may lead to high levels of pollutants, such as FPs (FPs or $PM_{2.5}$, aerodynamic diameter ≤ 2.5 μm) or UFPs (UFPs or $PM_{0.1}$; aerodynamic diameter ≤ 0.1 μm) posing negative impacts on human health. However, the numbers of studies on different particle size ranges and their chemical compositions have limited in developing countries such as Vietnam. The lack of scientific evidence may lead to difficulty building up air pollution control strategies. Therefore, this study focuses on investigating the seasonal variation of UFPs and FPs concentration and chemical composition, the effects of emission sources and meteorological parameters, and the hypothesis of particle growth from ultrafine to fine-size ranges.

UFPs and FPs were sampled by nanosampler (Model 3182, KANOMAX, Suita, Japan) and cyclone (URG-2000-30EH, University Research Glassware Corp., Chapel Hill, NC, USA), respectively by quartz fiber filter (2500 QAT-UP, Pall Corp., USA). There were five sampling campaigns, conducted from 2020 to 2021, including summer (August 10–24, 2020), the summer-to-winter transitional period (STP; October 14–27, 2020), winter (December 2 – 15, 2020), the winter-to-summer transitional periods (WTP; March 24–April 7, 2021), and the summer of 2021 (July 9 – 24, 2021). UFPs and FPs were monitored in different locations, including the roadside (RS), ambient (AS), and indoor sites. The meteorological parameters (temperature, humidity, number of rainy days, and wind speed) were also acquired. The samples were then analyzed for chemical compositions (carbonaceous and ion species) at Saitama University, Japan.

The results of clarification particle formation and growth in two seasons with different humidity showed that organic carbon (OC) and elemental carbon (EC) were the major compounds in both particle sizes, accounting for up to 56% and 80% of the analyzed components in FPs and UFPs, respectively. Secondary organic carbon (SOC) accounted for 36-41% and 37-47% of the total OC in FPs and UFPs, respectively, indicating the crucial contribution of secondary sources to OC. The strong correlations between water-soluble organic carbon (WSOC) and sulfate and nitrate showed that photochemical reactions contributed considerably to WSOC formation. Furthermore, the correlations between absolute humidity and other chemical components suggest that FPs collected in Hanoi were formed by secondary processes in the aqueous phase on the aerosol surface. In contrast, no correlation was found between the relative humidity and other chemical components. These observations indicate that particle growth depends on the number of water molecules above a certain level under drizzle-like weather conditions particular to the study area.

The UFPs concentration at the AS was in the order of winter > STP > WTP > summer, whereas that of the FPs was winter > WTP > STP > summer. The highest concentration of UFPs and FPs in winter may be due to adverse weather conditions, such as less wet removal and low mixing height layer, which lead to the accumulation of air pollutants and hinder the dilution. A higher concentration of FPs in WTP than in STP was due to a significant increase in ionic species, particularly sulfate, nitrate, and ammonium (SNA). The higher EC level, lower OC/EC ratio, and a higher NO_3^-/SO_4^{2-} ratio indicate that traffic-related emissions were more noticeable in UFPs at the RS than at the AS. The concentrations of analyzed components in UFPs at the RS were generally higher than at the AS, suggesting particle decay from the emission sources. The poor relationships of the chemical components between UFPs at the RS and FPs at the AS suggest the possibility of particle growth. This

growth may explain the difference in size distribution and chemical characteristics of particles in the different sampling locations.

The results of FPs and UFPs at the residential house show that the total concentration of indoor FPs was higher than outdoor FPs. It may be because of the indoor emissions in the residential house. The FPs concentration between the two sampling periods in the summer of 2020 and 2021 insignificantly varied, suggesting stable emission of FPs in the study area. The average ratio between indoor and outdoor concentration (I/O) in FPs was higher than 1.0, indicating the contribution of indoor emissions. The variation of the I/O ratio was insignificant between summer and winter, while the daily variation of the I/O ratio shows the influence of indoor emissions. The sharp increase in the SNA concentration suggests the contribution of secondary particles. However, the variation of the total ion concentration between the two sampling sites was minor. More significant daily variation of ions in outdoor FPs suggests the contribution of the secondary particles under adverse weather conditions (such as low mixing layer and temperature inversion), which impact outdoor FPs more than indoor FPs.

The results of this study contribute to the understanding of the particle characteristics in different locations in Hanoi, Vietnam. The chemical compositions of indoor and outdoor particles may be crucial to assessing the effects on human health, particularly for people living in urban areas or near the roadway. In this study, we also investigate the possibility of particle growth, which may be vital to understanding emission sources and the size distribution of particles. Further investigation is required to get a deeper understanding of the particle's chemical characteristics. Specifically, the sampling period should be longer, and more than two sampling locations should be conducted. The sampling at different determined distances from the traffic emissions is expected to monitor. More types of residential houses and other chemical components should be included in future studies.

Table of Contents

List of Tables

List of Figures

List of Abbreviations

AS	Ambient Site
CEM	Center for Environmental Monitoring
EC	Elemental Carbon
FPs	Fine Particles
I/O	Indoor/Outdoor
MONRE	Ministry of Natural Resources and Environment
OC	Organic Carbon
PM	Particulate Matter
$PM_{0.1}$	Particulate Matter with aerodynamic diameter ≤ 0.1 μm
$PM_{2.5}$	Particulate Matter with aerodynamic diameter ≤ 2.5 μm
PMF	Positive Matrix Factorization
RI	Residential Indoor site
RO	Residential Outdoor site
RS	Roadside Site
SNA	Sulfate, Nitrate, and Ammonium
SOA	Secondary Organic Aerosol
SOC	Secondary Organic Carbon
STP	Summer-to-winter transitional period
UFPs	Ultrafine Particles
USEPA	United States Environmental Protection Agency
VOCs	Volatile Organic Compounds
VR	Vietnam Registration
WHO	World Health Organization
WIOC	Water-insoluble Organic Carbon
WSOC	Water-soluble Organic Carbon
WTP	Winter-to-summer transitional period

Chapter 1

Introduction

1.1 Background

According to the World Health Organization (WHO, 2020), air pollution is one of the primary environmental risks to human health. In 2016, an estimated 7 million deaths were caused by outdoor and indoor air pollution, while in 2012 was 6.5 million (WHO, 2016, 2020). The exposure and effect of air pollution are different in low-, middle-, and high-income countries. People in low- and middle-income countries accounted for more than 90% of fatalities caused by air pollution in 2016 (WHO, 2020). In early research on the impact of air pollution on human health, PM_{10} (particles with aerodynamic diameter ≤10 μm) were common. Fine particles (FPs or $PM_{2.5}$, aerodynamic diameter ≤ 2.5 μm) can penetrate deep into the lung (pulmonary alveoli) and other parts of the human body via the blood. Recent studies on ultrafine particles (UFPs or $PM_{0.1}$; aerodynamic diameter ≤ 0.1 μm) showed that UFPs is more dangerous because they can penetrate deeper into the lung or directly go to other organs without being absorbed by the blood (Oberdörster et al., 2004; Stölzel et al., 2007).

Traffic emission is one of the leading sources of urban air pollution in Asian cities. The development of the economy and increased urbanization led to the growth of population and vehicle numbers. In Vietnam, vehicle numbers increased by approximately 10% of motorcycles and 17% of personal cars from 2013 to 2018 (Vietnam Registration [VR], 2019). A wide array of transport vehicles, such as motorcycles, cars, taxis, vans, and trucks, were found in Vietnam; however, personal motorbikes have dominated. As a result, the high level of air pollution in urban areas such as Hanoi or Ho Chi Minh City was reported, particularly the high concentration of particulate matter (PM).

The studies of FPs have been reported in many regions and countries worldwide. In Asian countries, several studies have been conducted, such as studies on carbonaceous composition (Pachauri et al., 2013; Phairuang et al., 2020; Thuy et al., 2017), soluble inorganic species (Lim et al., 2012; Ying Wang et al., 2005), organic groups and organic compounds (Phuc & Kim Oanh, 2018; Pongpiachan et al., 2013; Truc & Kim Oanh, 2007). However, limited published studies of chemical characteristics of UFPs in different microenvironments in Vietnam have been found, except for our previous studies (Nghiem et al., 2020; Thuy et al., 2018), and the behavior of UFPs related to multiple fundamental chemical components and weather conditions has not been clarified in this city. Determination of chemical compositions and seasonal variation of particles are therefore considered critical steps in evaluating the human health impacts and understanding their emission sources. Furthermore, investigation of the transformation processes, such as the growth, decay, or transport of particles in the atmosphere, could help to explain the variation of chemical compositions, concentration, and size distribution of particles.

1.2 Statement of problems

Hanoi is in the Red River Delta region, located in northern Vietnam and is the country's key economic city and political and cultural center. Hanoi is the second biggest city in Vietnam, with a population of 8,246,5000 (as of December 31, 2020), and an average population density of 2454 people/km^2 (Hanoi Statistical Office, 2021). Similar to many cities in Asian countries, with the rapid population growth and urbanization, Hanoi is facing several environmental issues such as air pollution. According to the national report of the Ministry

of Natural Resources and Environment (MONRE, 2015), more than 50% of total monitoring days in Hanoi had poor air quality and 11 days had very poor air quality, which is mainly related to a high level of $PM_{2.5}$. Compared to Ho Chi Minh City, the biggest city in Vietnam, Hanoi has been frequently reported with more severe air pollution (MONRE, 2015).

Some scattered studies on FPs have been conducted in Vietnam (Hai & Kim Oanh, 2013; Hien et al., 2002; Hopke et al., 2008; Kim Oanh et al., 2006; Ly et al., 2018). The published studies on the chemical composition and characteristics of UFPs have been limited, except for our previous studies (Nghiem et al., 2020; Thuy et al., 2018). In addition, the comparison between indoor and outdoor FPs and UFPs has not yet been comprehensively studied. Therefore, this study focuses on observing UFPs and FPs in different environments (the roadside, ambient, and indoor site), determining the seasonal variation and the contribution of traffic-related emissions to compositions of PM, and evaluating the characteristics of indoor and outdoor particles in the residential building in Hanoi, Vietnam.

1.3 Objectives of the study

The overall purpose of this study is to investigate the variation of chemical compositions and concentrations of UFPs and FPs in different environments in Hanoi, Vietnam. The main objectives are:

1. To determine the seasonal variations of chemical compositions and concentration in UFPs and FPs.
2. To evaluate the effects of traffic-related emissions on the chemical compounds in FPs and UFPs.
3. To assess the characteristics of indoor and outdoor particles.

1.4 Scope of the study

The study simultaneously considered the FPs and UFPs chemical compositions and their variations at multiple sites and periods through three major tasks:

Task 1 focuses on monitoring UFPs and FPs in some selected areas in Hanoi, including the roadside, ambient, and indoor residential site. The monitoring was implemented 23.5 hours a day and seven days a week during five sampling campaigns. Besides the sample collection, the real-time data of $PM_{2.5}$ and meteorological data (temperature and humidity) were recorded by a P-sensor and Thermor recorder, respectively.

Task 2 analyzes the chemical compositions of all collected samples. Carbonaceous components including organic carbon (OC) and elemental carbon (EC), and eight water-soluble ions including chloride (Cl^-), sulfate (SO_4^{2-}), nitrate (NO_3^-), sodium (Na^+), ammonium (NH_4^+), potassium (K^+), magnesium (Mg^{2+}), and calcium (Ca^{2+}) would be analyzed for all samples. The real-time data ($PM_{2.5}$, temperature, and humidity) would be processed, and the $PM_{2.5}$ concentrations and wind speed, measured by the third party, would be collected.

Task 3 focuses on the calculation and visualization of the analysis data according to the major objectives of this study.

1.5 Structure of the dissertation

This study is divided into seven chapters. The content details in each chapter are described as follows:

Chapter 1: Briefly described the background information of the study, the statement of problems, main objectives, and scope.

Chapter 2: Provide the literature review of relevant issues in the study area. It includes emission sources and characteristics of particles, traffic-related air pollution in Vietnam, and indoor and outdoor air pollution. This chapter would give an overview of the pollution situation in Vietnam, basic information on ultrafine and fine particles, and the original motivation to conduct this study.

Chapter 3: Describe generally the sampling locations, sampling devices, and sample analysis in this study. From this chapter, the readers can roughly understand the overall picture of the study.

Chapter 4: This chapter focuses on the effect of absolute humidity on the chemical compositions of ultrafine and fine particles.

Chapter 5: Focuses on the effect of traffic-related emissions on chemical compounds in different particle sizes. The seasonal variation of particles and the possibility of particle growth from ultra- to the fine-size range of particles are also investigated in this chapter.

Chapter 6: Focuses on the indoor and outdoor particle's characteristics. The indoor emission sources and their effects are also assessed.

Chapter 7: Conclude the key findings from this study and recommendations for future studies.

Chapter 2

Literature Review

2.1 Emission sources and characteristic of UFPs

2.1.1 Emission sources of UFPs

There were two important sources of UFPs in the urban areas, primary and secondary sources (Hama et al., 2017). The primary sources of UFPs are mainly combustion processes such as vehicles, coal-fired power plants, gas-fired facilities, and biomass burning (Kumar et al., 2014; Wehner & Wiedensohler, 2003). Indoor combustion was also a source of UFPs, such as stoves, heaters, or smoking. These emissions sources have been reported to impact the particle size distribution, e.g., the size range of particles emitted from diesel engines was different compared to that of gasoline engines. According to Paasonen (2013), road transport was responsible for 60% of the total particle emissions (including UFP and $PM_{0.1-1}$), followed by non-road transport (including other non-road transport and shipping activities) at around 19%. The domestic emissions (cooking, heating) contributed approximately 13% of the total particle number. Other studies also mentioned that traffic is one of the major sources of UFPs (Keogh et al., 2009; Kumar et al., 2014). Particularly, the higher emission of UFPs from traffic is observed in developing countries, e.g., in Delhi, India (Mönkkönen et al., 2004). The secondary sources include the new particle formation in the ambient air, which may be due to the photochemical reaction of gaseous precursors after emissions (Kulmala & Kerminen, 2008). There were two main steps of particle formation, including nucleation of an initial cluster (gas phase compound), and then lead to the particle growth. Sulfuric acid molecules contributed considerably to particle formation and may be in charge of particle growth by condensation.

2.1.2 Characteristics of UFPs

2.1.2.1 Size distribution

The size distribution of UFP can give insights into emission sources as well as the impacts on human health. The accumulation mode (particle size >50 nm) contributes more significantly to the mass concentration of particles. Meanwhile, the higher particle number fraction was observed in the size range of less than 20 nm (nucleation mode). The number of particles in the nucleation mode is much higher than the bigger size. Particles in the nucleation mode had a maximum value on warm days, and the highest mean particle number concentration was in summer (Agudelo-Castañeda et al., 2019). The higher concentration of particles in the nucleation mode may be because of photochemical nucleation, which depends strongly on the intensity of solar radiation. On the other hand, the number concentration of particles with a diameter exceeding 20 nm is higher during winter. It was explained by the lower temperatures promoting nucleation processes and the increase in lifetime, associated with increased traffic exhaust emissions. However, other studies showed that the increase of nucleation mode could happen on both warm and cold days (Wehner & Wiedensohler, 2003).

The particle size distribution also depends on the emissions sources. The size of the particle emitted from diesel engines ranges from 20-130nm, while that from gasoline engines ranges from 20-60nm (Ristovski et al., 2004). Lin et al. (2007) found that the particles had a bi-

modal distribution with one main peak in the fine size (0.56-1 µm at the roadside, and 1-1.8 µm at the rural site) and another peak in the coarse size (3.2-5.6 µm). The smaller size range of UFPs (less than 30 nm) was emitted directly from combustion engines, and the bigger size of UFPs (30-100 nm) formed via coagulation and condensation of primary particles and gaseous pollutants.

2.1.2.2 Chemical concentrations

The EC can be used as a marker for combustion processes, particularly for diesel engines. Besides, ionic species such as SO_4^{2-}, NO_3^-, and NH_4^+ are important components of secondary aerosols. The study of chemical components of UFPs is therefore important to evaluate the emission sources, formation process, and health impacts. According to Sardar et al. (2005), OC accounted for 32-69%; EC from 1-34%; sulfate from 0-24% and nitrate from 0-4% (Figure 2.1). UFP components study by Kim et al. (2011) shows the higher composition of carbonaceous species (83-92% of OC and EC) and lower ionic species (8-17%). A similar result of UFP composition (OC, EC, NH_4^+, NO_3^-, SO_4^{2-}, Cl^-) was reported by Kudo et al. (2011). Lin et al. (2007) conducted a study of the chemical composition of UFPs in different locations (roadside and rural sites), which shows that the primary peak of SO_4^{2-} and NH_4^+ were in the fine particles (0.56-1.0 µm), the second peak in bigger size particles (3.2-5.6 µm) and third peak in UFPs (0.032-0.056 µm). The concentration of NO_3^- in the roadside site was approximately 1.3 times higher than in the rural site, and the peak was found in the particle size range of 1.0-1.8 µm. Other components of UFPs were studied by Corsini et al. (2017), such as polycyclic aromatic hydrocarbons (PAHs) or metals affected by wood burning. PAHs were trace gaseous, contributing <1% of UFP mass concentration.

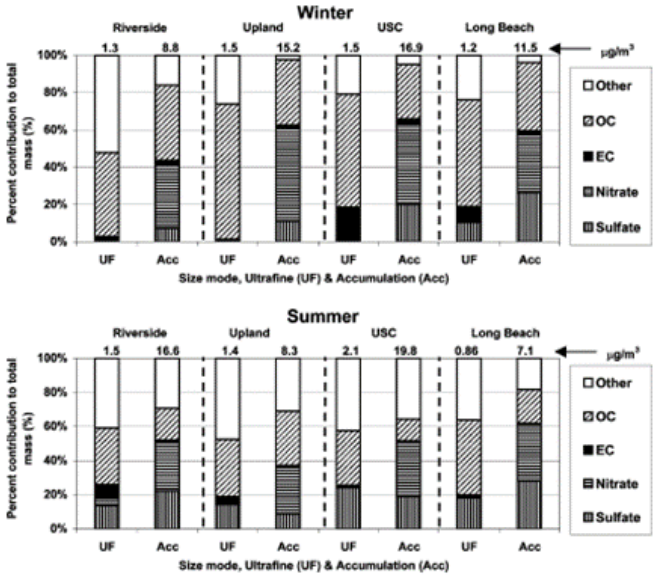

Figure 2.1 Contribution of chemical species to the total particulate mass in ultrafine and accumulation modes *(Source: Sardar et al., 2005)*

2.1.2.3 Temporal variation

Many factors affect the seasonal variation of UFPs, including increasing factors (atmospheric stability and increased emissions) and decreasing factors (better mixing

conditions or lower traffic flow rate during holiday periods). According to Corsini et al. (2017), the total mass concentration of UFPs did not show significant seasonal differences (2.2 μg/m^3, range: 1.6–3.2 μg/m^3 in the winter period and 2.0 μg/m^3, range 1.0–3.1 μg/m^3 in the summer period). However, the variation was observed in the compositions of UFPs, e.g., total PAH concentrations were higher in winter than in summer (Corsini et al., 2017). Kim et al. (2011) reported that the concentration of each component was higher in fall and winter. Similarly, Hussein et al. (2004) showed the lowest number concentration of nucleation mode particles in Helsinki during summer, while the highest concentration was in spring and winter (Figure 2.2). It might be due to higher temperatures, better mixing conditions, and less traffic during summer. Meanwhile, it was lower temperature, low boundary layer height, and high radiation in spring, which was associated with the formation of nucleation mode particles.

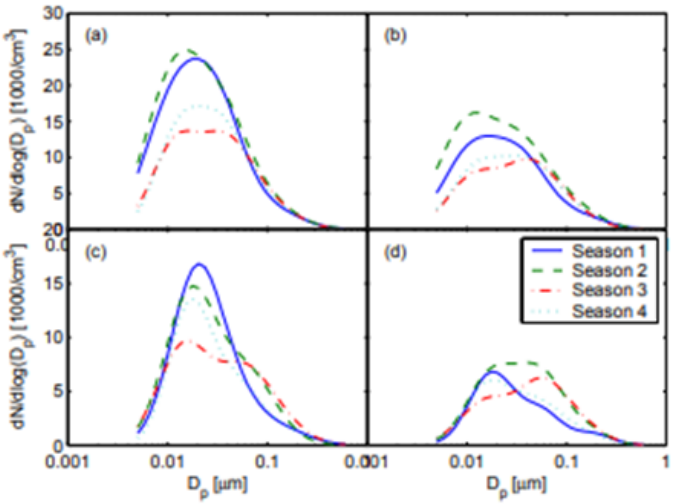

Figure 2.2 Seasonal number size distribution *(Source: Hussein et al., 2004)*
a) workdays and b) weekend at Siltavuori; c) workdays and d) weekend at Kumpula (season 1: Winter; season 2: Spring; season 3: Summer; season 4: Autumn)

Strong diurnal variations of UFP concentrations and compositions were observed, particularly in the urban environment. It was closely related to the variation of traffic density on weekdays or weekends. It has been reported by many studies (Agudelo-Castañeda et al., 2019; Mendes et al., 2018) that the peak of UFP concentrations was related to the traffic rush hour. Figure 2.3-a shows the difference in size range in the metro platform and urban background (Mendes et al., 2018). Three UFP concentration episodes were observed, including (i) the first episode from 6:00 to 9:00 h, which coincides with an increase in morning traffic; (ii) the second one from 12:00 to 16:00 h, which can be related to new particle formation events commonly observed in the urban environment; (iii) the third one during the period from 21:00 to 01:00 h, which might be attributed to a lower mixing height at nighttime. A similar trend has been seen with the number concentration of UFP in the urban background (Figure 2.3-b). Hama et al. (2017) also reported that the maximum number concentration of particles was found around midday (11:00-14:00) when low equivalent black carbon and high ozone levels were recorded. During the cold period (winter), the diurnal variation of particle number concentration had two peaks in the morning and afternoon traffic rush hours. However, the daily cycle was weaker in the warmer period, and the evening peak was not found. The peak of the particles in nucleation mode (20-30 nm) was found during midday during the warm period (June, July, and August).

2.1.3 UFPs in urban environments

2.1.3.1 UFPs near the roadside

The distribution of particles is observed when conducting the sampling at the roadside at a specific distance from the road where the airflow is not disturbed by building or other barriers. The changes in particle size distribution, concentration, or chemical compositions according to the distance from the roadway can be investigated and compared to see the changes of particles after emission. In general, particle concentration decreases with the distance from the roadway. With a distance up to about 300 m, the particle concentrations and the size distribution are nearly similar to the background. According to Zhu et al. (2002), total particle number concentration in the size range of 6 to 25 nm, which accounted for about 70% of total UFPs number concentration, dropped sharply to around 80%, after 100 m. The particles in the size range of 25-50 nm and 50-100 nm experienced a similar trend, which reduced and approached the background concentration at around 150 m from the emission point (Figure 2.3). This phenomenon can be explained by the smaller particles coagulating with these particles to increase their size. Other studies show that particles in nucleation mode dominate in ultrafine particle number near the road and decrease with distance. It is associated with vehicle flow characteristics (the higher the speed, the greater the particle concentration, and the smaller the particle size) (Kittelson et al., 2004). The total concentrations at the roadside were reported to range between 10^4 and 10^6 particles cm^{-3} (Kittelson et al., 2004). The concentration was increasing with increasing traffic rate, and the effect of traffic rate was stronger on particles smaller than 63 nm than on the larger particles.

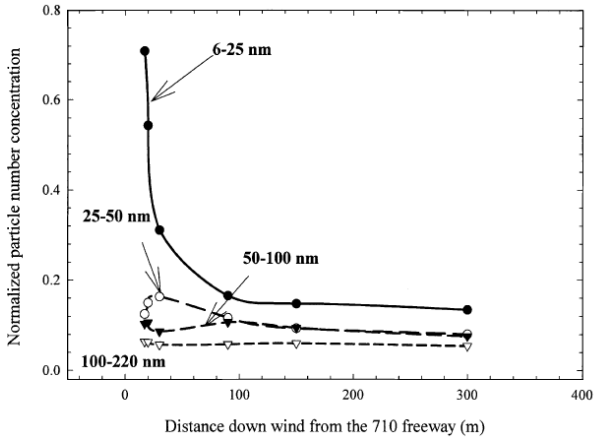

Figure 2.3 Particle number concentration as a function of distance
(Source: Zhu et al., 2002)

In contrast, the concentration of larger particles is independent of distance from the roadway. According to Jacobson et al. (2005), the decay of ultrafine particles is likely a result of a combination of dilution, evaporation, and coagulation. These factors are also proved that associated with the higher decay rate in the study of Zhu et al. (2002), which found that all species decayed rapidly downwind of the roadway with characteristic decay distances ranging from 13 to 46 m. Meanwhile, the longer distance of 92 m has been reported in the study of Jacobson et al. (2005). According to Saha et al. (2018), the changing of particle concentration is the combination of several factors, such as dilution and coagulation, and dilution itself could not explain the decrease in particle concentration.

2.1.3.2 UFPs in different locations in urban areas

Numerous studies monitored particle concentration in different locations in relation to traffic emissions in urban areas. The results of those studies provide the relationship between the concentrations and the distance from a particular roadway or traffic flow. Westerdahl et al. (2005) reported that the concentration of UFPs varied significantly according to the monitoring locations. Particle number concentration decreased as the distance of the monitoring site from the street increased. This observation was also applied for other pollutants, including CO, CO_2, NO, BC, and PAHs. Besides, the variation of UFPs concentration between the sites near and far away from traffic emissions was much more significant than that of bigger particles, such as coarse size particles.

The size distribution of particles stronger fluctuates in urban environments than in rural areas (Ristovski et al., 2004). In the location near the roadway, the particle in nano size (particle diameter <50 nm) is dominant the particle concentration, and it decreases with the distance from the emissions point (Kittelson et al., 2004). The number concentration of nanoparticles in the location near the road (10 m from the roadway) is significantly higher than in the place located 700 m from the road (Figure 2.4).

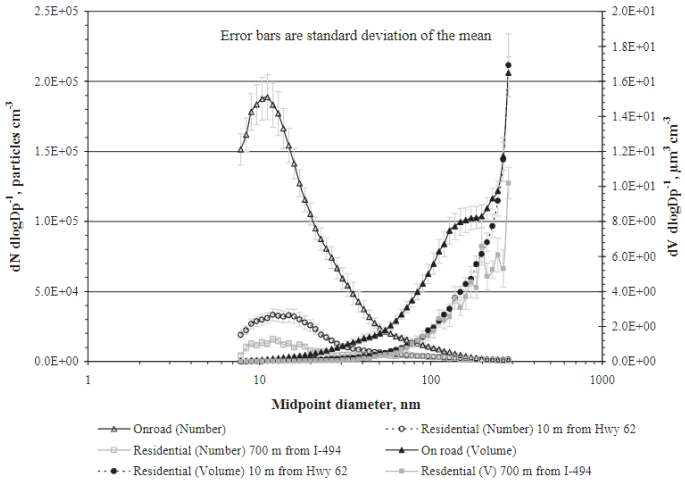

Figure 2.4 Average particle number concentration of size distributions grouped by location *(Source: Kittelson et al., 2004)*

2.2 The characteristics of FPs and the contribution of emission sources in Hanoi

The concentration and chemical compositions of FPs are important to evaluate the impacts on human health, environment, and climate. This information can be also used as an indicator of emission sources and applied further for mitigation measures. In Vietnam, the mean annual FPs concentration has been regulated in the Vietnamese National Standard on ambient air quality since 2013 at 25 µg/m^3, which is higher than the WHO air quality guideline (10 µg/m^3). Available monitoring data show high levels of PM in cities in Vietnam that often exceeded the national ambient air quality standards, particularly in big cities such as Hanoi. According to the database of the US Embassy monitoring station, the yearly average concentration of FPs in Hanoi in 2016 reached 50.5 µg/m^3, approximately two times higher than the Standard (Thuy et al., 2018). In this section, the characteristics and emission sources of FPs in Hanoi are discussed. The effects of traffic emissions on the characteristics of FPs are also reviewed.

2.2.1 Characteristics of FPs

2.2.1.1 FPs concentration

The annual average concentrations of FPs during the period 2010-2017 reported by the Center for Environmental Monitoring (CEM), MONRE were higher than the Vietnamese National Standard of 25 µg/m^3 (Figure 2.5). The FPs concentration was higher in Hanoi than in other cities, such as Hue, Da Nang, Nha Trang, and Ho Chi Minh City. The variation of FPs concentration is different in summer, winter, and transitional periods. A higher concentration was observed during wintertime, particularly during December and January (Cohen et al., 2010; Ly et al., 2018). In contrast, a lower FPs concentration was found during summer (from May to August) (Hien et al., 2002; Ly et al., 2018). The concentration during transitional seasons was higher than in summer and lower than in winter (Figure 2.6). The stable atmosphere conditions (low wind speed and low mixing layer) may lead to a higher concentration of $PM_{2.5}$ during wintertime. This variation trend was also observed in different areas in South East and East Asia, such as in Japan, China, and Thailand, indicating the regional contribution of $PM_{2.5}$ (Ly et al., 2018). Table 2.1 illustrates the FPs concentration collected in different periods in Hanoi. A similar trend of seasonal variation was observed in FPs concentrations in previous studies.

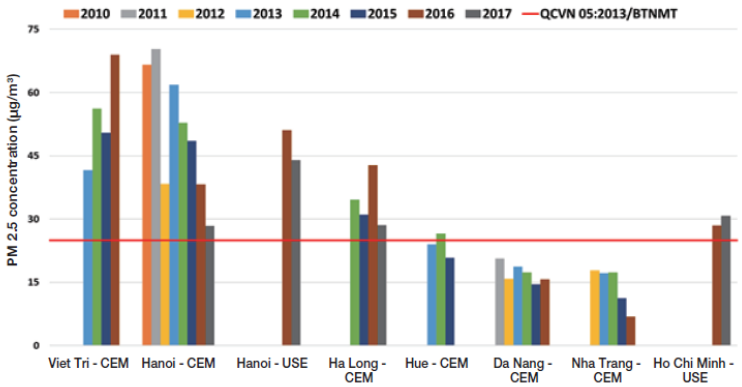

Figure 2.5 Annual average concentration of FPs in Vietnam from 2010-2017
(Source: MONRE, 2017)

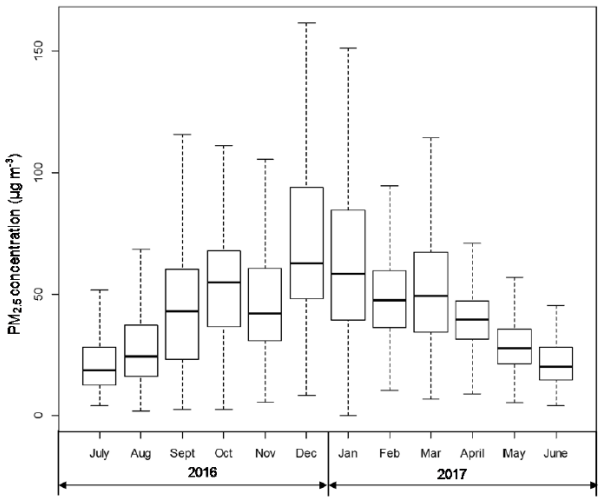

Figure 2.6 Monthly variation of FPs concentration in Hanoi, Vietnam
(Source: Ly et al., 2018)

Table 2.1 Comparison of FPs concentration in different studies

Period	Season	Devices	FPs ($\mu g/m^3$)	References
09/1998-08/1999	Over years	Gent stack filter unit (SFU)	36.1	Hien et al (2002)
2001-2004	Dry (Nov-Mar)	Andersen dichotomous sampler	124	Kim Oanh et al. (2006)
2001-2004	Wet (Apr-Oct)	Andersen dichotomous sampler	33	Kim Oanh et al. (2006)
2001-2008	Over years	$PM_{2.5}$ cyclone	54	Cohen et al. (2010)
12/2006-02/2007	Winter	Andersen dichotomous sampler	76	Hai and Kim Oanh (2013)
12/2016	Winter	Low-cost sensor	76	Ly et al. (2018)
07/2017	Summer	Low-cost sensor	22	Ly et al. (2018)

The diurnal variation of the FPs concentration fluctuates depending on studies and monitoring stations. There was an unclear peak during rush hours measured at the campus of HUST (Ly et al., 2018). The difference in diurnal variation of FPs concentration suggested the effect of traffic emission was not abundant. This result was also found in the study of Nhat et al., (2018) for the FPs concentration measured at the station of the US Embassy in Hanoi. In contrast, the database from the CEM station (556 Nguyen Van Cu, Long Bien, Hanoi) shows that the diurnal variation was closely related to the traffic density fluctuation, which increased during morning and afternoon rush hours (MONRE, 2017). The highest concentrations of FPs were observed during rush hours in the morning (7:00 - 8:00 am) and afternoon (6:00 - 7:00 pm); however, it was low at midday (1:00 - 2:00 pm). It noted that a higher FPs concentration was observed at nighttime (20-22h) at the CEM station. It may be due to nocturnal radiation inversions and subsidence temperature inversions.

2.3.1.2 FPs compositions

According to Cohen et al. (2010), ammonium sulfate accounted for the highest portion of FPs mass concentration of 29 ± 8%, followed by soil (inorganic compound), organic matter, salt, and black carbon (BC). Other studies had different classifications of FPs components to gain insights into the emission sources or other objectives. The compositions of FPs could be divided into different groups, including carbonaceous compounds, ionic species, and elemental components (Hai & Kim Oanh, 2013; Kim Oanh et al., 2006). Ionic species and carbonaceous components were the major compounds, contributing significantly to the mass concentration of FPs (Hai & Kim Oanh, 2013; Kim Oanh et al., 2006; Thuy et al., 2018). Higher mean concentrations of sulfate and nitrate ions were observed during wintertime, which might partly be due to the effects of meteorological conditions, such as less wet removal, and a low mixing layer (Hai & Kim Oanh, 2013). OC and EC concentrations were unchanged in both seasons in Hanoi (Thuy et al., 2018). However, significantly higher OC and EC concentrations were found during the biomass burning periods after the harvest of two rice crops in June and November (Hai & Kim Oanh, 2013; Thuy et al., 2018). Element components including Fe, Zn, Si, Al, Ca, Mg, V, Mn, Ni, Zr, Sn, Sb, Cu, As, Se, Br, Rb, and

Pb could suggest the contribution of several sources such as combustion processes, road dust, construction activities. A higher concentration of Ca, Si, Fe, Zn, Mg, and Al were observed in Hanoi (Gatari et al., 2005; Hai & Kim Oanh, 2013). The seasonal variation of element concentration was the same as the mass concentration. A higher concentration of element was observed in winter (dry season) in Hanoi, approximately two times higher than in summer (wet season) (Kim Oanh et al., 2006).

2.2.2 Emission sources of FPs

Few studies on the contribution of the FPs emission source have been conducted in past years in Hanoi. These studies investigated the emission sources based on the chemical components. Besides, Positive Matrix Factorization (PMF) receptor model has been applied in the study of Cohen et al. (2010); Hai & Kim Oanh (2013). The main emission sources in Hanoi include traffic, industry, construction, soil/road dust, biomass burning, coal combustion, and secondary aerosols (Cohen et al., 2010; Hai & Kim Oanh, 2013; Hopke et al., 2008; Kim Oanh et al., 2006). According to Ly et al. (2018), the emission from local transportation was not dominant, while other local sources and regional-scale backgrounds might contribute more to the FPs level. The study conducted by Hai & Kim Oanh (2013) shows that the main sources of FPs were secondary mixed PM (40%), followed by residential/commercial cooking (16%) and diesel traffic (10%). In contrast, Cohen et al. (2010) confirmed that the major emission source was automobiles (40 ± 10%). The detail of sources and their contribution to the FPs level is shown in Table 2.2.

Table 2.2 Summary of studies on FPs emission sources in Hanoi

Site	Period	Sources	References
Urban site, Hanoi	Northern trajectory (Sep/Oct to Dec 1999)	LRT: 25, LBP emission: 14.9, soil dust: 0.3, LSA: 0.7, marine aerosols: 0.7, Cl^- DMA: 2.6, vehicle/road dust: 2.9 (μ/m^3)	(Hien et al., 2004)
	Northeast trajectory (Jan to Mar/Apr 2001)	LRT: 15.1, LBP emission: 6.4, soil dust: 3.6, LSA: 5, marine aerosols: 0.4, Cl^- DMA: 1.5(μ/m^3)	(Hien et al., 2004)
Urban mixed /residential/commercial sites	2001-2004	Traffic, secondary sulfate and nitrate particles, biomass burning, and soil dust.	(Kim Oanh et al., 2006)
Urban site	2002-2005	Burning biofuel for cooking and home heating, two-stroke engines of motorbike	(Hopke et al., 2008)
Industrial site	Dec 23, 2006 – Jan 7, 2007	secondary mixed PM (40%), diesel traffic (10%), cooking (16%), secondary sulfate (16%), aged sea salt mixed (11%), industry/ incinerator (6%), construction/ soil (1%).	(Hai & Kim Oanh, 2013)
Urban site	Apr 25, 2001 – Dec 31, 2008	automobile (40 ± 10%), soil (3.4 ± 2%), secondary sulfates (7.8 ± 10%), smoke (13 ± 6%), industry (19 ± 8%), and coal (17 ± 7%)	(Cohen et al., 2010)

LRT: Long-range transport; LBP emission: local burning primary emission; LSA: local secondary aerosol; MA: depleted marine aerosols.

2.3 Indoor and outdoor FPs in urban environments

2.3.1 Outdoor FPs

The outdoor FPs emitted from primary sources (including combustion processes, transportation, industry, or construction) and secondary sources (photochemical reactions) (Zhang et al., 2021). Traffic emission is one of the crucial primary sources, accounting for approximately 25% of total FPs emissions in urban ambient air on the global scale (Karagulian et al., 2015). However, in some other regions, traffic contributed more than the global average, e.g., Southeast Asia (36%) or India (37%) (Figure 2.7). The traffic emissions mainly include diesel soot and non-exhaust emissions, such as brakes and tires. Industry and domestic burning were responsible for around 15-20% of the total FPs emission in urban areas (Karagulian et al., 2015). Secondary sources were also important, which accounted for approximately 23% of total FPs emissions in Beijing, China (Yan et al., 2021). These sources formed the particles from precursor gases, such as the oxidation of sulfur and nitrogen oxides into ammonium sulfate and nitrate, respectively. The secondary particles accounted for a very high proportion in some countries, e.g., Canada (62%), the USA (46%), the Republic of Korea (45%), Western Europe (44%), and Turkey (42%) (Karagulian et al., 2015).

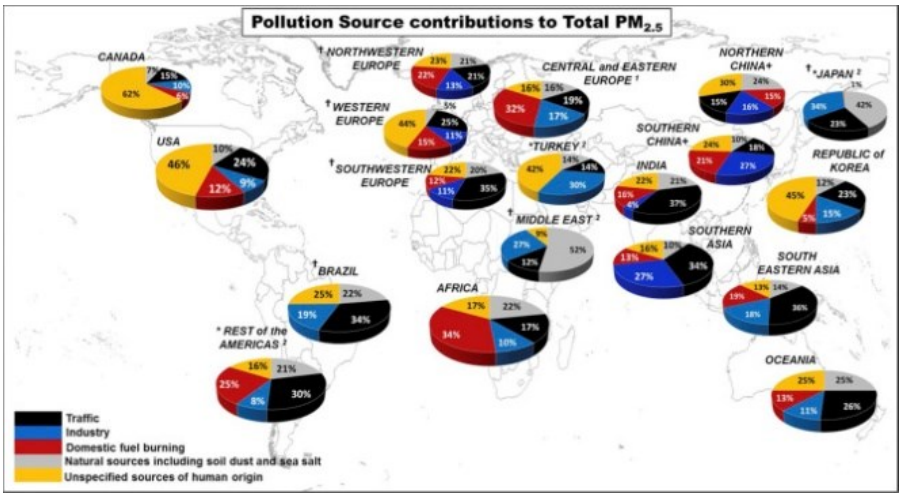

Figure 2.7 Population-weighted averages for relative source contributions to total $PM_{2.5}$ in urban sites *(Source: Karagulian et al., 2015)*

2.3.2 Indoor FPs

Indoor FPs can be emitted by cooking activities, smoking, or the combustion of coal, wood, or other biomass types. Burning coal, wood, or other biomass during winter for heating or cooking purposes are important sources of FPs emissions in China (Li et al., 2016), Nepal (Pokhrel et al., 2015), and other countries. For instance, in Lanzhou, northwest China, the indoor FPs level is higher in winter because of solid biomass burning for priding heat (Figure 2.8). Cooking food at high temperatures may lead to the emissions of particles (Yassin et al., 2012). Other sources of indoor FPs may be incense burning (Kuo et al., 2015), candles (Derudi et al., 2014), and smoking (Sleiman et al., 2014). In the school and office, printers, photocopies, fax machines, and other similar devices have been reported as one the FPs sources, contributing to the increased indoor FPs level (McGarry et al., 2011). Indoor FPs also could be from the sources of cosmetics or other chemicals used in the house such as anti-insect, hair sprayers, perfume, and cleaning agents (Höllbacher et al., 2017). As a result,

the FPs concentration varies in indifferent rooms in the house (e.g., in the kitchen, living room, and bedroom). In addition, FPs from the outdoor environment could enter the indoor by two mechanisms (natural infiltration and mechanical ventilation). Nearly all particles smaller than 1.0 µm and approximately 70% of particles from 1.0-2.5 µm could enter the house (Chen et al., 2012). In the case of mechanical ventilation, the airflow from the outdoor environment could go into the indoor by the fans or air conditioner. If the air conditioner uses the filter cloth, FPs can be partly removed. However, without a filter-based air-conditioner and fans, FPs freely penetrate the buildings. In an indoor environment without smoking or other strong emissions sources, indoor FPs is expected to be the same as, or lower than outdoor concentration. The ratio between indoor and outdoor (I/O) FPs concentration is used to determine the indoor PM pollution evaluation. I/O ratios were lower than 1.0 in the laboratory and office, indicating the lower effect of the outdoor airflow. In contrast, the higher I/O ratios were observed in the kitchen and in the canteen, where the cooking and human activities were presented (Goyal & Kumar, 2013).

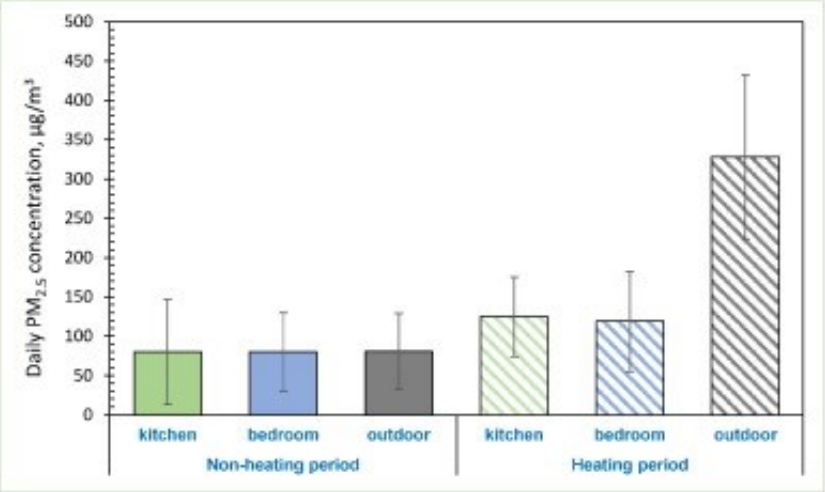

Figure 2.8 Comparison of indoor and outdoor FPs concentrations during the non-heating and the heating sampling periods
(Source: Li et al., 2016)

2.3.3 Regulation of FPs concentration

The FPs concentration has been regulated in the guidelines of WHO for the daily and annual average. The guidelines state that annual average FPs concentrations should not exceed 5 µg/m^3, while 24-hour average exposures should not exceed 15 µg/m^3, and more than 3 – 4 days a year. The different regulations of FPs concentration have been applied worldwide. India and Egypt set the limit of FPs concentration much higher than WHO's guidelines of around 40-50 µg/m^3 on an annual average, while that in China and Hong Kong is 35 µg/m^3 (Cheng et al., 2016). Vietnam, Thailand, and the Republic of Korea regulate the annual mean concentrations of FPs of 25 mg/m^3. Japan, the US, and Canada set the annual mean FPs concentrations of 15, 12, and 10 µg/m^3, respectively. Australia regulates the lowest annual average FPs concentration of 8 µg/m^3, which is even lower than WHO's guidelines. The regulation for indoor FPs is not mentioned in the guidelines of WHO and most countries. However, it has been noted that the ambient concentration of FPs could be used as indoor guidelines, particularly in developing countries where a high level of FPs was found in indoor environments.

Chapter 3

Methodology

3.3 Study area

With a population of 8,246,500 and a high average density of 2,454 person km^{-2} (as of December 31, 2020), Hanoi is the capital city and the commercial and industrial center in northern Vietnam (Hanoi Statistical Office, 2020). The rapid population growth and economic development led to increased vehicle numbers, one of Hanoi's significant sources of air pollution. Other sources, such as open solid waste and biomass burning, construction, industry, and indoor cooking, contribute considerably to air pollution, especially the PM concentration in Hanoi. Thus, Hanoi is expected to have a high PM level of different size ranges, such as $PM_{2.5}$ and $PM_{0.1}$.

Hanoi is influenced by northeast and southeast monsoon, leading to different weather conditions throughout the year. There are two main seasons in Hanoi, summer (May to August) and winter (November to March next year), and two transitional periods between those seasons. In summer, the weather is hot and humid with frequent heavy rain; it is thus called wet summer or wet season. In contrast, the weather is cold and dry in winter affected by the northeast monsoon from mainland China with associated low-mixing height and calm wind. Under this adverse condition, a high level of air pollution was usually observed, particularly $PM_{2.5}$. During the summer-to-winter transitional period (STP), the weather condition is milder; the temperature and humidity are gradually lower. Meanwhile, during the winter-to-summer transitional period (WTP), the southeasterly flow of maritime air becomes dominant, bringing moist and warm air to this area (Hien et al., 2002).

The selected sampling sites are in Hanoi University of Science and Technology (HUST), Hai Ba Trung District, Hanoi, Vietnam (21˚0′20″N, 105˚50′39″E), and a residential house at Truong Dinh St., Hoang Mai District (21˚28′59″N, 105˚24′49″E), approximately 2 km from HUST. The roadside (RS), ambient (AS), and indoor (AI) samples were collected at HUST. The RS samples were collected at the place next to Tran Dai Nghia St., a two traffic lanes road running through three universities and a highly populated area (Figure 2.1). The AS and AI sites are on the rooftop of a four-story building of the School of Materials Science and Engineering, HUST. The AS site is approximately 12 m in height from the ground and is surrounded by diverse institutional and residential areas. The distance from the sampling sites to the three main streets is around 200m, i.e., 200 m from Dai Co Viet St., 250 m from Giai Phong St., and 200 m from Tran Dai Nghia St. (Figure 2.1). The indoor (RI) and outdoor (RO) samples were monitored in a residential house, a terraced house with four floors. The house is in Truong Dinh St., a two-traffic lane (inbound and outbound) street. Both sides of the road have a pavement of about 1.5-2 m in width and are bordered by residential buildings. The devices were placed on the third floor, approximately 9 m from the ground and 1.5m from the floor (Figure 3.1).

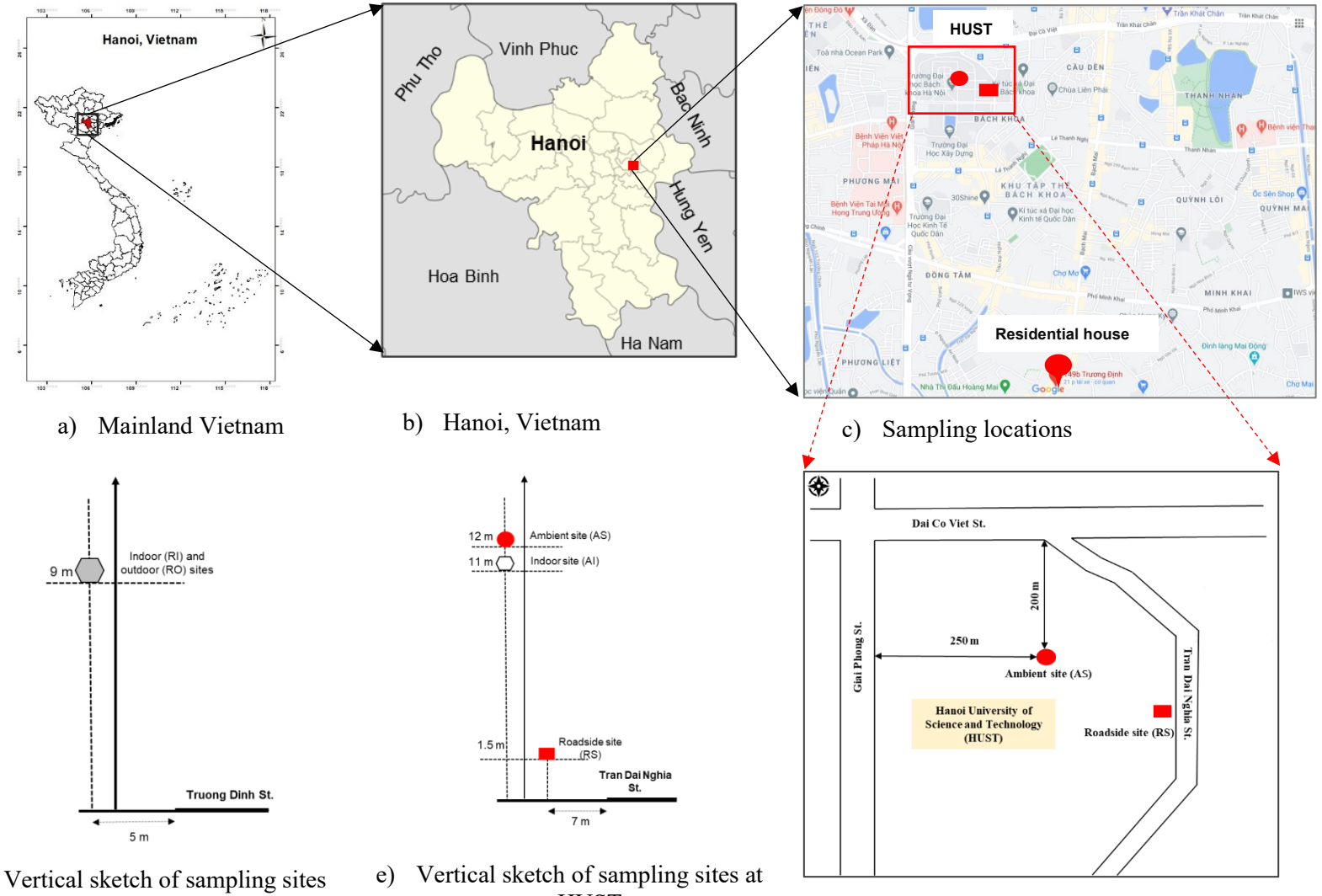

a) Mainland Vietnam

b) Hanoi, Vietnam

c) Sampling locations

d) Vertical sketch of sampling sites at the residential house

e) Vertical sketch of sampling sites at HUST

f) Horizontal sketch of sampling sites at HUST

Figure 3.1 Sampling sites

Table 3.1 Monitoring schedule and number of samples collected

Period	Date	Site	FPs	UFPs	$PM_{2.5}$ sensor	T & RH
			Cyclone	Nanosampler	Sensor	Thermo recorder
August (Summer 2020)	08/10/2020 - 08/24/2020	AS	15	15	15	15
		AI		15	15	
		RS		15		
		RI	6		6	6
		RO	6		6	6
STP, October (Summer to winter 2020)	10/15/2020 - 10/27/2020	AS	14	14	14	14
		RS		14		
December (Winter 2020)	12/02/2020 - 12/15/2020	AS	14	14	14	14
		AI		14	14	
		RS		14		
		RI	14		14	14
		RO	14		14	14
WTP, March (Winter to summer 2021)	03/24/2020 - 04/07/2020	AS	16	15	15	14
		AI		15	15	14
July (Summer 2021)	07/09/2021 - 07/24/2021	AS	16	16		
		RI	16	16	16	16
		RO	16	16	16	14
Total			**147**	**193**	**174**	**141**

T & RH: Temperature and Relative Humidity; STP: summer-to-winter transitional period; WTP: winter-to-summer transitional period; AS: Ambient site; AI: Indoor site at HUST; RS: Roadside site; RI: Indoor sampling at residential house, RO: outdoor sampling at residential house

3.2. Sample collection

The samplings were done simultaneously at all sites in different seasons. In short, five sampling campaigns were from 2020 to 2021, and 340 samples were collected in total. Details of different sampling campaigns and the number of collected samples are illustrated in Table 3.1. Samples of UFPs and FPs were collected by Nanosampler (Model 3182, KANOMAX, Suita, Japan) and cyclone (URG-2000-30EH, University Research Glassware Corp., Chapel Hill, NC, USA), respectively (Figure 3.2). Nanosampler includes five impaction stages to classify particles of different diameters at ≤0.1, 0.1–0.5, 0.5–1, 1–2.5, 2.5–10, and >10 µm. Nanosampler was set up at a flow rate of 40 L/min while cyclone was at 16 L/min. Quartz fiber filter (2500 QAT-UP, Pall Corp., USA) was used for both devices (55-mm filter for Nanosampler and 47-mm filter for cyclone). Before sampling, the filters were baked at 350 ℃ for 2 h to remove possible contaminants. Samples after collecting were placed in a Petri dish and then kept in an airtight aluminum bag at −40 ℃ to avoid additional reactions. Besides, blank samples were prepared and carried out in the same way as the samples. The total blank samples were at least 10% of the total number of samples.

The real-time $PM_{2.5}$ concentrations in different sampling locations were recorded by a $PM_{2.5}$ sensor (P-sensor, Industrial Hygiene Device Calibration, Inc.). Temperature and relative humidity (RH) in the sampling sites were collected by a thermo recorder (TR-72bwb, TECPEL CO., LTD.). $PM_{2.5}$ data measured by a beta attenuation monitor (BAM) at the US Embassy in Hanoi, located approximately 3.1 km from the sampling site, were collected from the AirNow website (https://www.airnow.gov/international/us-embassies-and-consulates/#Vietnam$Hanoi). The data on $PM_{2.5}$ concentration were acquired on an hourly average and then calculated to get the mean concentration of the sampling periods. Thirty-minute average wind speed measured at 6 m in height at Lang station, Hanoi (21.02N 105.80E), located approximately 4.7 km from the sampling point, was obtained from the Wyoming Weather website (https://weather.uwyo.edu).

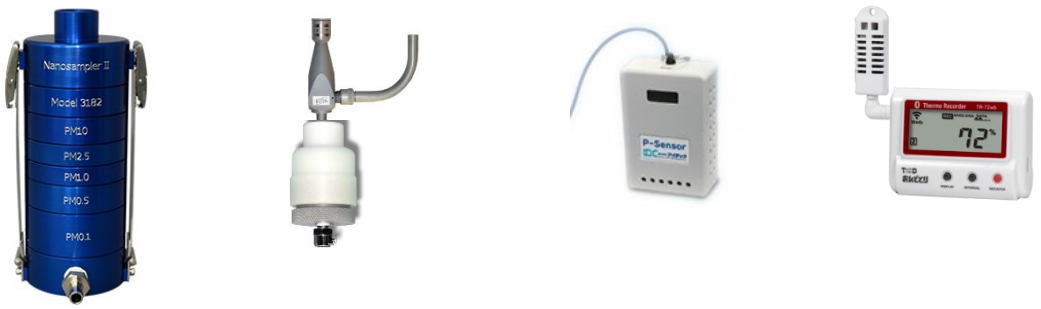

a) Nanosampler b) $PM_{2.5}$ cyclone c) $PM_{2.5}$ sensor d) Thermo recorder

Figure 3.2 Sampling devices

3.3. Analytical methods

A 0.503-cm^2 punched-out filter was used to determine carbonaceous components (OC and EC) by using a carbon analyzer (DRI model 2001, Atmoslytic Inc., Calabasas, CA, USA). The different fractions of OC and EC were analyzed by applying IMPROVE (Interagency Monitoring of Protected Visual Environments) method (Chow et al., 2001). According to IMPROVE method, OC fractions were analyzed at different temperatures of 120, 250, 450,

and 550 °C for OC1, OC2, OC3, and OC4, respectively, in a non-oxidizing helium atmosphere. EC fractions including EC1, EC2, and EC3 were analyzed at higher temperatures of 550, 700, and 800 °C, respectively, in an oxidizing atmosphere (2% O_2, 98% He). OC and EC then were defined as the sum of all OC fractions plus the pyrolysis of organic carbon (PyOC) and the sum of all EC fractions minus PyOC, respectively. PyOC was monitored simultaneously by the reflectance and transmittance of laser signals during the analysis of carbon fractions. Meanwhile, char-EC and soot-EC were further defined as EC1-PyOC and EC2+EC3, respectively (Chow et al., 2004; Han et al., 2007; Zhu et al., 2010). Quality assurance and quality control were ensured by the semiannual calibration of the Potassium Hydrogen Phthalate (KHP) solution. Besides, samples were analyzed times and the difference was smaller than 5% for total carbon (TC), and 10% for OC and EC.

Ionic components were analyzed by an ion chromatography (ICS-1600, Dionex Corp., Sunnyvale, CA, USA) and water-soluble organic carbon (WSOC) by a total carbon analyzer (Multi N/C 3100, Analytik Jena, Jena, Germany). The water-insoluble organic compound (WIOC) concentration is calculated by the total OC minus WSOC (WIOC = OC – WSOC). Before analysis, samples were extracted with 20 mL ultrapure water in 20 mins by an ultrasonic bath. To ensure QA/QC of analysis, all vials and glassware were cleaned by ultrasonic bath and dried by oven before use. An instrument blank was analyzed with field samples to assess the presence of instrument contamination. The coefficient of the standard curves (built by five different concentrations) for anions and cations was more than 0.995. The detected limitation of anions and cations are below 0.0063 mg/L and 0.0071 mg/L, respectively. Furthermore, an instrument blank was analyzed before field samples to assess the presence of instrument contamination. On average, the ion concentrations in the trip blanks were below the detected limitation for Na^+, K^+, Mg^{2+}, and less than 0.004 μg/m^3 for Cl^-, 0.009 μg/m^3 for SO_4^{2-}, NO_3^-, 0.03 μg/m^3 for NH_4^+, and 0.08 μg/m3 for Ca^{2+}. The detail of QA/QC has been described in the study by Wang et al. (2005). The steps of analysis are shown in Figure 3.3.

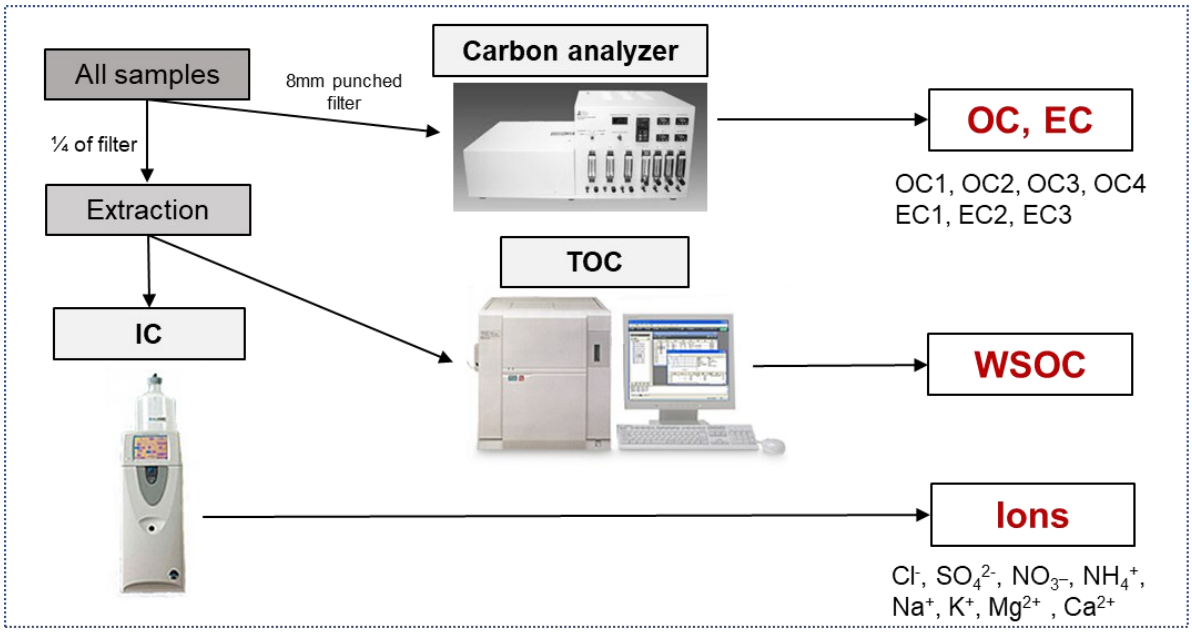

Figure 3.3 Steps of sample analysis

Chapter 4

Impact of absolute humidity on chemical compositions of UFPs and FPs

4.1. Introduction

Atmospheric particulate matter is a major air pollutant and has received increasing attention in recent decades. PM has a wide range of particle sizes, such as PM_{10}, $PM_{2.5}$, and $PM_{0.1}$. It has been reported that high PM levels are related to increases in morbidity, mortality, and several other adverse health effects (Anderson et al., 2005). According to Hofmann (2011), the deposition rate of aerosol in different parts of the respiratory tract depends on the particle size distribution. Although $PM_{0.1}$ accounts for less than 10% of the total particle mass in ambient air (Komppula et al., 2003; Pakkanen et al., 2001), the number concentration is higher, accounting for a higher fraction in ambient air (Tuch et al., 1997). Thus, a larger fraction of UFPs is deposited in the human body than bigger size particles.

Traffic is a crucial primary source of $PM_{0.1}$ in urban areas, particularly emissions from on-road vehicles, such as motorcycles and automobiles (Kittelson et al., 2004; Minoura et al., 2009; Wang Yungang et al., 2012; Y. Zhu et al., 2002). Other primary sources of $PM_{0.1}$ emissions include biomass or coal burning and industrial and cooking activities (Kumar et al., 2014; Wehner & Wiedensohler, 2003). Several studies have indicated that secondary formation via gas-to-particle conversion processes or photochemical transformation contributes considerably to the concentration of UFPs (Agudelo-Castañeda et al., 2019; Kulmala & Kerminen, 2008; Sardar et al., 2005). Precursor gases such as sulfur dioxide (SO_2) or nitrogen oxides (NO_x) play a vital role in these processes and may also govern particle growth by condensation. Besides, the carbonaceous components, including EC and OC, and their fraction in UFPs, can be used to infer the emission source of particles. For example, the origin of EC could be from primary combustion, while OC could be from primary or secondary sources. Therefore, the chemical components of particles can be used as an indicator of their emission sources, their behavior, and their impacts on human health and the environment.

In Vietnam, few studies of UFPs have been conducted, except for our previous studies (Nghiem et al., 2020; Thuy et al., 2018), and the behavior of UFPs related to multiple fundamental chemical components and weather conditions has not been clarified. Thus, information on the chemical concentration of each component in UFPs would be valuable to understanding their particle characteristics and possible emission sources. Additionally, since Hanoi has different weather conditions in different seasons - for example, the summer is rainy with high insolation and high humidity with drizzle-like weather, and winter is dry - it is an important location for confirming the particle growth process.

In this chapter, $PM_{2.5}$ and $PM_{0.1}$ (the latter of which exists stably in high concentrations in urban areas and forms the nucleus of particles) were simultaneously collected in Hanoi during summer and winter, that is, under different weather conditions. The chemical components, including carbonaceous components and water-soluble ions, were analyzed to characterize the particles. The possible emission sources of $PM_{2.5}$ and $PM_{0.1}$ and their behavior associated with secondary formation and growth were examined in the two seasons, which have different humidities.

4.2. Materials and Methods

The sampling periods were in summer 2015 (July 13 to August 2) and winter 2016 (March 2 to 16). The monitoring was designed to evaluate the impact of humidity on the concentration and characteristics of PM. The selected sampling site was on the third floor of the Center of Foreign Languages, HUST, Hai Ba Trung District, Hanoi (Figure 4.1). Hai Ba Trung is one of the central districts of Hanoi with a high population density of 29,581 person/km^2, approximately 13 times higher than the average population density of Hanoi of 2,454 person/km^2 in 2020 (Hanoi Statistical Office, 2021). The sampling site is located near a street with a heavy traffic load (being situated near two busy streets, namely Dai Co Viet and Giai Phong) and is surrounded by institutional buildings, trees, and residential houses. The high traffic volume was found on some major roadways near the sampling sites, around 100,000-150,000 vehicles per day (Phan et al., 2010). Therefore, the PM level and composition at this sampling site could be influenced by different sources, such as transportation, construction, and cooking activities.

$PM_{2.5}$ was collected on a 47-mm quartz fiber filter (2500 QAT-UP, Pall Corp., USA) by cyclone (URG-2000-30EH, University Research Glassware Corp., Chapel Hill, NC, USA). The $PM_{2.5}$ cyclone was operated at a flow rate of 16.7 L/min for 23.5 h. $PM_{0.1}$ was sampled using a prototype nanosampler (hereafter referred to as "pt-nanosampler", Model 3180, Kanomax Japan Inc., Osaka, Japan). The pt-nanosampler included five impaction stages to classify the particles with diameters of 0.1, 0.5, 1.0, 2.5, and 10 μm, respectively (Furuuchi et al., 2010; Otani et al., 2007). The 47-mm quartz fiber filter was used to collect particles in the $PM_{0.1}$ stage. The pt-nanosampler was used to collect particles for 23.5 h at a flow rate of 40 L/min. Before sampling, the quartz fiber filters were prebaked at 350 ℃ for 1 h to remove possible organic carbon contaminants according to the standard method of the Ministry of the Environment, Government of Japan. After sampling, the filter samples were placed into a Petri dish and kept separately in an aluminum bag inside an airtight plastic bag. The samples were stored in a refrigerator at −20 ℃ to avoid volatilization and additional reactions. Field blanks were carried out using the same procedures as the collected samples.

Temperature, relative humidity, and rainfall during the sampling period were obtained to evaluate the impact of the meteorological conditions on the concentration and characteristics of PM. Temperature and relative humidity were obtained from Lang station (21°01'N, 105°48'E), located approximately 6 km from the sapling site. Rainfall data were collected from the Weather Underground website (http://www.wunderground.com) for Noi Bai airport, around 30 km from the sampling site.

OC, EC, WSOC, and ionic species were analyzed for all samples. The IMPROVE (Interagency Monitoring of Protected Visual Environments) method was applied to analyze carbonaceous components. More details of the carbonaceous analysis are available in Section 3.3. For WSOC and ionic species, a quarter of the quartz fiber filter was extracted with ultrapure water for 15 mins and then analyzed with a total carbon analyzer (TOC-V_{CPH}, Shimadzu Corp., Kyoto, Japan) and ion chromatography (ICS-1600, Dionex Corp., Sunnyvale, CA, USA) to monitor WSOC, ionic species, and oxalic acid, respectively. To ensure data quality, the QA/QC procedure was implemented for this analysis. All glassware is to undergo ultrasonic cleaning and oven drying before use. The QA/QC procedures have been described in detail in the previous study (Wang et al., 2005).

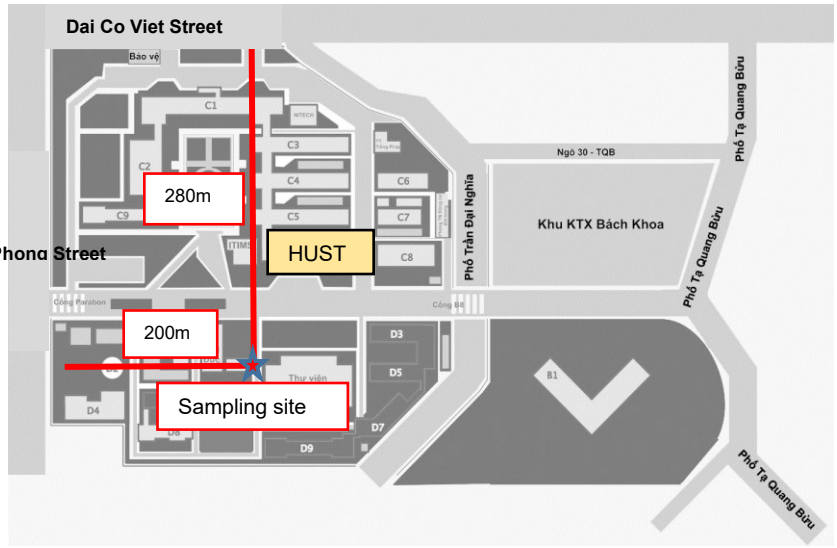

Figure 4.1 Sampling site in Hanoi

4.3. Results and Discussion

4.3.1 Concentration of major components

The total concentrations of measured components (hereafter called the 'concentrations') and the concentration of each component are shown in Table 3.1. Note that the concentrations of FPs and UFPs were judged from the sum of all analyzed components (reconstructed mass approach). Therefore, other components (e.g., elements) were not included in this study, and consequently, the actual FPs and UFPs mass concentration might have been higher than the reported results. The UFPs concentrations were 1.47 ± 0.54 and 1.71 ± 0.61 $\mu g/m^3$ in summer and winter, respectively. In general, the daily average concentration of UFPs was high regardless of the season. The highest concentrations were observed on the days without heavy rain. Rapid increases in concentration were observed after rainy days. The average concentrations of FPs during the summer and winter were 9.38 ± 6.67 and 13.79 ± 8.90 $\mu g/m^3$, respectively. In general, the concentration of FPs tended to be higher during winter. Similar to UFPs, lower FPs concentrations were observed during days of heavy rain. The FPs concentrations observed in this study were lower than the Vietnamese national standard for ambient air quality, which requires an annual average of ≤ 25 $\mu g/m^3$. However, the FPs concentration in the winter sampling period exceeded the guideline of the WHO, which requires an annual mean of ≤ 10 $\mu g/m^3$.

OC and EC were the major compounds in both particle sizes, accounting for up to 56% and 80% of the analyzed components in FPs and UFPs, respectively. Total carbon (TC) contributed approximately 56% and 33% to the concentration of FPs in summer and winter, respectively. The mean OC concentrations in FPs were 3.84 ± 2.12 and 3.34 ± 1.21 $\mu g/m^3$ in summer and winter, respectively, while the mean EC concentrations during the same seasons were 1.37 ± 0.87 $\mu g/m^3$ and 1.15 ± 0.63 $\mu g/m^3$, respectively. OC contributed a higher proportion in TC than EC, comprising more than 80% and 70% of the UFPs concentration in summer and winter, respectively, corresponding to OC and EC concentrations of 1.04 ± 0.35 and 0.18 ± 0.084 $\mu g/m^3$, respectively, in summer, and 1.08 ± 0.32 and 0.14 ± 0.084 $\mu g/m^3$, respectively, in winter. The significant contribution of carbonaceous compounds to the particle concentration indicates that these compounds were abundant in both particle

sizes, particularly UFPs. However, the concentrations of OC and EC in both particle size ranges did not vary significantly between summer and winter, therefore, the variation of reported particle concentration in this study was mainly caused by ionic species. Similarly, Thuy et al. (2018) reported that very small variations of carbonaceous compounds between summer and winter were found in Hanoi, except for the period of biomass burning. These results suggest the presence of stable emission sources in Hanoi during the sampling periods, such as vehicle exhaust, industry, or cooking. The source apportionment studies using Positive Matrix Factorization (PMF) receptor model by Hopke et al. (2008), Cohen et al. (2010), Hai & Kim Oanh (2013), and Nghiem et al. (2020) were also showed that traffic, industry, cooking, and biomass burning were the major primary emission sources in Hanoi. Other studies which using Principal Component Analysis (PCA) to identify the emission sources from the data of carbonaceous compounds, water-soluble inorganic species, and polycyclic aromatic hydrocarbon (PAH) showed that traffic was the main source of emission, following by biomass burning, industry, and sea salt aerosol in Phuket (Choochuay et al., 2020a) and Bangkok, Thailand (ChooChuay et al., 2020b).

Table 4.1 Concentrations of carbonaceous and water-soluble ionic components in FPs and UFPs in Hanoi during summer and winter

	FPs		UFPs	
	Summer (n = 17)	Winter (n = 14)	Summer (n = 18)	Winter (n =15)
	Ave.[a] ± S.D.[b]	Ave.± S.D.	Ave.± S.D.	Ave.± S.D.
OC ($\mu g/m^3$)	3.84 ± 2.12	3.34 ± 1.21	1.04 ± 0.35	1.08 ± 0.32
EC ($\mu g/m^3$)	1.37 ± 0.87	1.15 ± 0.63	0.18 ± 0.084	0.14 ± 0.084
TC ($\mu g/m^3$)	5.21 ± 2.95	4.49 ± 1.81	1.22 ± 0.42	1.22 ± 0.39
WSOC ($\mu g/m^3$)	1.93 ± 1.41	1.64 ± 0.96	0.51 ± 0.21	0.51 ± 0.21
WIOC ($\mu g/m^3$)	1.91 ± 0.77	1.70 ± 0.47	0.53 ± 0.21	0.57 ± 0.18
Na^+ ($\mu g/m^3$)	0.05 ± 0.031	0.17 ± 0.22	-[c]	-[c]
NH_4^+ ($\mu g/m^3$)	0.82 ± 0.99	2.35 ± 1.73	0.072 ± 0.032	0.12 ± 0.92
K^+ ($\mu g/m^3$)	0.19 ± 0.13	0.14 ± 0.10	0.009 ± 0.01	0.014 ± 0.011
Mg^{2+} ($\mu g/m^3$)	0.034 ± 0.02	0.054 ± 0.036	-[c]	-[c]
Ca^{2+} ($\mu g/m^3$)	0.56 ± 0.20	0.45 ± 0.17	-[c]	-[c]
Cl^- ($\mu g/m^3$)	0.16 ± 0.14	0.70 ± 0.60	0.009 ± 0.003	0.014 ± 0.014
SO_4^{2-} ($\mu g/m^3$)	1.97 ± 2.33	3.98 ± 3.65	0.10 ± 0.07	0.20 ± 0.13
NO_3^- ($\mu g/m^3$)	0.40 ± 0.50	1.46 ± 1.09	0.063 ± 0.031	0.14 ± 0.095
PM concentration[d] ($\mu g/m^3$)	**9.38 ± 6.67**	**13.79 ± 8.90**	**1.47 ± 0.54**	**1.71 ± 0.61**

[a] Average concentration
[b] Standard deviation
[c] Below detection limit
[d] Sum of the analyzed compounds

Inorganic ions contributed up to 67% of the $PM_{2.5}$ concentration and 29% of the UFPs concentration. The lower proportion of ionic species in UFPs could be explained by the secondary aerosol formation from the precursor gases such as SO_2 (Kumar et al., 2014). According to Yang et al. (2021), the condensation of sulfuric acid and nitric acid could impact the particle growth from nano-sized particles to FPs. The three major ions in both FPs and UFPs were SO_4^{2-}, NH_4^+ and NO_3^-, which together accounted for around 80% of the total ionic concentration in FPs and more than 90% in UFPs. The concentrations of these ions were significantly higher in winter; the mean concentration of SO_4^{2-} was 1.97 ± 2.33 $\mu g/m^3$ in summer and 3.98 ± 3.65 $\mu g/m^3$ in winter (Table 3.1). High concentrations of these ions could be the result of rapid emissions of precursor gases such as SO_2 or NO_x from vehicular exhausts under adverse weather conditions in winter. Hien et al. (2014) reported that concentrations SO_2 and NO_2 were several times higher in the winter compared to summer. The average concentrations of SO_2 and NO_2 have been recorded in some Districts in Hanoi ranged from 11.7 - 47.4 $\mu g/m^3$ and 17.9 – 65.9 $\mu g/m^3$, respectively (Hien et al., 2014). Similarly, it has been reported that concentrations of NO_2 and NO_x reached higher levels during winter in Hanoi (Sakamoto et al., 2018).

4.3.2 Carbonaceous compounds

The OC and EC fractions in $PM_{2.5}$ and $PM_{0.1}$ are shown in Figure 4.2. The carbonaceous content in $PM_{2.5}$ was approximately four times higher than that in $PM_{0.1}$. The contributions of carbonaceous component in $PM_{2.5}$ were: EC1>OC3>OC2>PyOC>OC4>EC2>OC1>EC3; and in $PM_{0.1}$: OC3>OC2>OC4>EC1>EC2>PyOC>OC1>EC3. The main carbon fractions in $PM_{2.5}$ were EC1 and OC3, which accounted for approximately 25% and 20% of the total carbonaceous concentration, respectively. OC1 and EC3 contributed less than 2% to the total concentration in both seasons while OC2, OC4, EC2, and PyOC contributed between 7% and 16%. In $PM_{0.1}$, OC2 and OC3 were the main contributors, accounting for around 25% to 30% of the carbonaceous concentration; meanwhile, OC4, EC1, EC2, and PyOC contributed approximately 8-14%. The highly volatile OC1 contributed smaller fraction of 1-4% while EC3, a carbon polymer that does not burn easily, accounting for only 0.8-1.2% of total carbonaceous concentration (Figure S3-b). The EC fractions in $PM_{2.5}$ were higher than that in $PM_{0.1}$, particularly EC1 (Figure S3). It could be explained by the formation of particles during the combustion process. EC is emitted as tiny spherules during combustion and then aggregated to form particles of larger size from 0.1 to 1 μm which is the subclass of $PM_{2.5}$ (United States Environmental Protection Agency [USEPA], 2012). According to Chow et al. (2004), OC3 was mainly produced by cooking activities, while a smaller fraction is produced by gasoline motor vehicle exhaust and around 1% is contributed by road dust. Meanwhile, EC1 was mainly contributed by motor vehicle emissions, vegetative burning, and coal burning (Cao et al., 2005; Chow et al., 2004; Phairuang et al., 2020). OC2 was mainly found in the coal combustion sample (> 45%), in biomass burning, or from SOC (Cao et al., 2005; Chow et al., 2004). The main carbonaceous components in $PM_{2.5}$ and $PM_{0.1}$ indicate possible emission sources such as gasoline motor vehicles, cooking activities (LPG burning), biomass, and coal combustion.

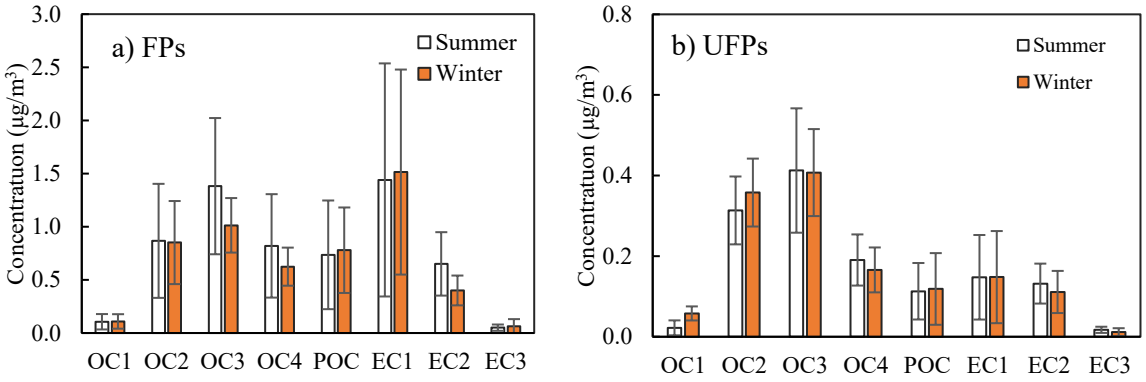

Figure 4.2 Fractions of OC and EC in FPs (a) and UFPs (b)

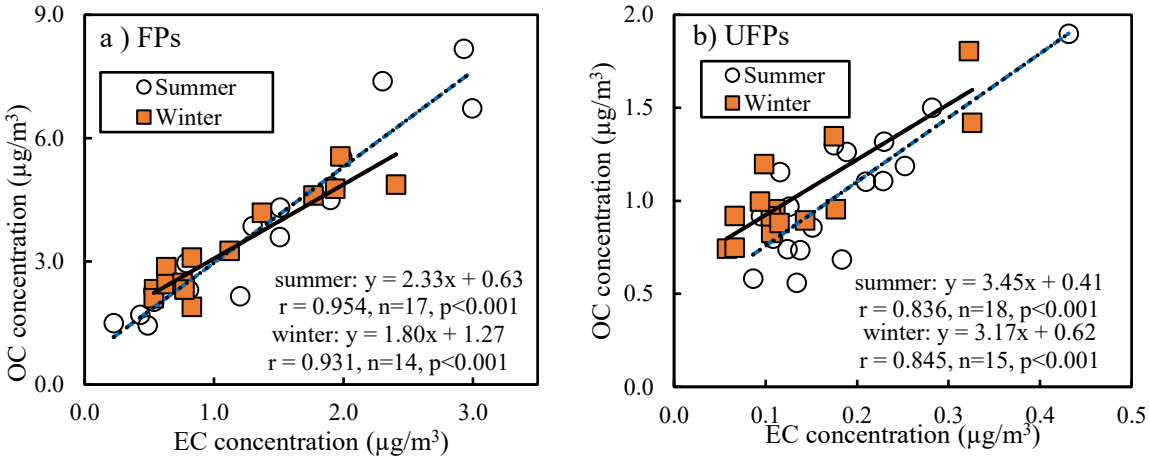

Figure 4.3 Relationships between OC and EC in FPs (a) and UFPs (b)

The correlation between OC and EC in $PM_{2.5}$ and $PM_{0.1}$ is shown in Figure 4.3. In both seasons of the sampling period (winter and summer), a strong correlation was observed between OC and EC in $PM_{2.5}$ ($r > 0.9$). A strong correlation was also found between OC and EC in $PM_{0.1}$ both seasons ($r \approx 0.84$). The high r value indicates that there were common dominant sources of OC and EC in particles at the sampling site. However, the lower correlation between OC and EC in $PM_{0.1}$ suggests that the various sources of $PM_{0.1}$ may have a stronger effect on the characteristics of OC and EC in $PM_{0.1}$ than in $PM_{2.5}$.

The rank of carbonaceous components indicated the possible sources of PM, whereas the OC/EC ratio confirmed the major emission sources and the characteristics of variation in carbonaceous aerosols. Thus, the average OC/EC ratios were calculated for both $PM_{2.5}$ and $PM_{0.1}$ for the two sampling periods to determine the emission sources in the sampling area (Table 3.2). The EC fraction was emitted from primary sources while OC may have been emitted from both primary and secondary sources; that is, a smaller OC/EC ratio was found near the emission source (Pio et al., 2011). The OC/EC ratio in $PM_{2.5}$ from motorcycle exhaust ranged from 1 to 4.2 (Panicker et al., 2015). A ratio between 2.5 and 10.5 represented residential coal burning (Chen et al., 2006), a ratio between 3.8 and 13.2 indicated emissions from biomass burning, and a ratio of 4.3-7.7 suggests a contribution from cooking activities (Pachauri et al., 2013). In this study, the mean OC/EC ratios of $PM_{2.5}$ in summer and winter

were 3.19 ± 1.12 (range 1.79-6.67) and 3.20 ± 0.77 (range 2.03-4.54), respectively. In contrast, the ratios for $PM_{0.1}$ were significantly higher, at 6.15 ± 1.75 (range 3.73-9.96) in summer and 8.70 ± 2.88 (range 4.36-13.87) in winter. The range of carbonaceous ratios in this study suggest the contributions of coal burning, cooking activities, biomass burning, and motorcycle exhaust. A similar average OC/EC ratio of 3.52 ± 1.41 was found in $PM_{2.5}$ in the study of ChooChuay et al. (2020b) for Bangkok, Thailand. The source apportionment by PCA was shown that the emission sources in Bangkok, Thailand were vehicular exhausts, biomass burning, sea salt aerosols, power plants, and industrial emissions (ChooChuay et al., 2020b). The previous study by using PMF model for Hanoi, Vietnam reported that local burning and vehicle/road dust were the main anthropogenic emission sources (Hien et al., 2004). In the study of Cohen et al. (2010), the automobile contributed up to 40% of total emission, following by secondary sulfate aerosol and industry. The reported results of emission sources in this study are also consistent with the characteristics of the sampling site at HUST. This site is considered as a mixed site surrounded by residential houses, buildings, and busy streets; therefore, it might be affected by emissions from domestic cooking, construction, transportation, and coal or biomass burning.

The OC/EC ratios were more than 2.0, indicating the existence of SOA in the particles (Pachauri et al., 2013). The rapid increase of secondary OC, which resulted from photochemical reactions and self-condensation, caused the increase in the OC/EC ratio (Pio et al., 2011; Plaza et al., 2011). In this study, the OC/EC ratios of both FPs and UFPs were greater than 2.0; thus, the emission sources of such PM might be primary emissions (as mentioned above) or secondary sources (secondary particles). Furthermore, the OC/EC ratio was generally higher during the winter sampling period, especially for $PM_{0.1}$. Higher OC/EC ratios in winter have also been reported in other studies for Shanghai, China (Feng et al., 2009), Taiyuan, China (Meng et al., 2007), and Agra, India (Pachauri et al., 2013). Several factors might be responsible for this result, such as the stagnant condition of the atmosphere (low mixing height and calm wind) or the condensation of semi-volatile organic compounds at lower temperatures.

The average concentrations of char-EC and soot-EC in $PM_{2.5}$ were respectively 0.70 ± 0.62 $\mu g/m^3$ and 0.67 ± 0.32 $\mu g/m^3$ in the summer sampling period and 0.74 ± 0.57 $\mu g/m^3$ and 0.41 ± 0.15 $\mu g/m^3$ in the winter sampling period. Meanwhile, the average concentrations of char-EC and soot-EC in $PM_{0.1}$ were respectively 0.05 ± 0.04 $\mu g/m^3$ and 0.15 ± 0.05 $\mu g/m^3$ in summer and 0.04 ± 0.03 $\mu g/m^3$ and 0.11 ± 0.06 $\mu g/m^3$ in winter (Table 3.2). A higher char-EC fraction was found in $PM_{2.5}$, while soot-EC was dominant in $PM_{0.1}$. This result is consistent with previous studies that reported abundant char-EC in FPs and abundant soot-EC in UFPs (Han et al., 2007; Zhu et al., 2010).

The concentration of SOC in $PM_{2.5}$ was calculated based on the indirect method, namely, the EC-tracer method. This method uses EC as the tracer for primary organic carbon because EC is emitted mainly from primary sources with other primary organic components (Turpin & Huntzicker, 1995). The SOC concentrations in $PM_{2.5}$ were 1.46 ± 0.73 $\mu g/m^3$ in summer and 1.09 ± 0.37 $\mu g/m^3$ in winter (Table 3.2). These values for SOC accounted for approximately 41% and 36% of the OC concentration in summer and winter, respectively. In contrast, the concentration of SOC in $PM_{0.1}$ was found to be 0.38 ± 0.17 $\mu g/m^3$ in summer and 0.48 ± 0.16 $\mu g/m^3$ in winter, representing 37% and 47% of the OC concentration in each season, respectively. In general, the formation of SOC by photochemical reactions occurred more in the summer owing to the high intensity of solar radiation. However, in this study, no significant difference was found between the SOC concentration in summer and winter

in either FPs or UFPs. A slightly higher concentration of SOC was observed in $PM_{2.5}$ during the summer sampling period, while the SOC concentration in $PM_{0.1}$ slightly increased during winter. It has previously been shown that the stable atmospheric condition and low temperature in winter strengthen the oxidation and condensation processes, leading to the formation of SOC (Kudo et al., 2011; Thuy et al., 2018); this might explain the higher SOC/OC ratio during the winter sampling period in the present study. The high proportion of SOC in both particle size ranges indicates a considerable contribution of SOC to the OC concentration. These results are consistent with other studies that reported a considerable contribution of SOC to the OC in PM in locations such as in Shanghai, China ($PM_{2.5}$, annually, 27-33%; Feng et al., 2009), Agra, India ($PM_{2.5}$, wintertime, 18-60%; Pachauri et al., 2013), and Southern Thailand ($PM_{0.1}$, monsoon season, 43%; Phairuang et al., 2020).

Table 4.2 OC/EC ratio, concentrations of char-EC, soot-EC, SOC, and the SOC/OC ratio in FPs and UFPs

	FPs		UFPs	
	Summer	Winter	Summer	Winter
OC/EC	3.19 ± 1.12	3.20 ± 0.77	6.15 ± 1.75	8.70 ± 2.88
Char-EC ($\mu g/m^3$)	0.70 ± 0.62	0.74 ± 0.57	0.05 ± 0.04	0.04 ± 0.03
Soot-EC ($\mu g/m^3$)	0.67 ± 0.32	0.41 ± 0.15	0.15 ± 0.05	0.11 ± 0.06
SOC ($\mu g/m^3$)	1.46 ± 0.73	1.09 ± 0.37	0.38 ± 0.17	0.48 ± 0.16
SOC/OC (%)	41.2	35.8	37.1	47.4

The correlations of char-EC with OC and EC, and of soot-EC with OC and EC, were plotted to illustrate the relationships between those components, as shown in Figure 4.4. In FPs, compared with soot-EC, char-EC had a stronger correlation with both OC and EC ($r > 0.9$) in both seasons (Figure 4.4-a and 4.4-c). The strong relationship between char-EC and OC indicated that char-EC contributed more to the total EC than did soot-EC and was closely related to the OC concentration. In UFPs, char-EC had a moderate correlation with both OC and EC (Figure 4.4-b and 4.4-d). In contrast, the relationships between soot-EC and OC and EC were more complicated. Moderate correlations between soot-EC and OC and EC were observed in $PM_{2.5}$ in the summer sampling period (during which time humidity was higher), whereas poor correlations were observed during the winter sampling period.

The strongest correlations between soot-EC and OC and EC were obtained in $PM_{0.1}$ (Figure 4.5). In particular, there was a strong relationship between soot-EC and EC for $PM_{0.1}$ ($r \approx 0.9$). These results suggest that the EC in FPs was dominated by char-EC while the EC in UFPs mainly comprised soot-EC. The correlations observed in this study were in agreement with the findings of previous studies that reported a smaller proportion of soot-EC than char-EC in FPs in Japan (Kim, Sekiguchi, Furuuchi, et al., 2011) and China (Han et al., 2009). Additionally, UFPs may exist as a stable mixture of char-EC and soot-EC (Kim, Sekiguchi, Furuuchi, et al., 2011). In the present study, OC and EC showed a moderate correlation with soot-EC in $PM_{2.5}$ in the humid summer, suggesting that UFPs containing soot grow in humid conditions and contribute to FPs.

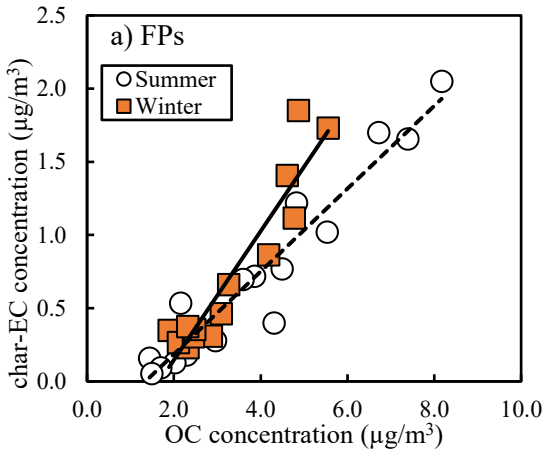

summer: $y = 0.28x - 0.38$, $r = 0.959$, $n = 17$, $p < 0.001$
winter: $y = 0.44x - 0.73$, $r = 0.940$, $n = 14$, $p < 0.001$

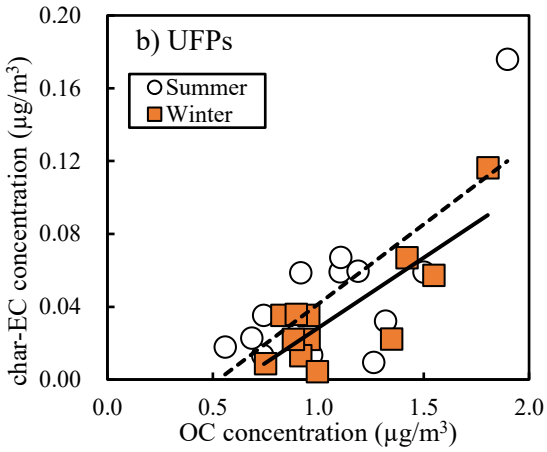

summer: $y = 0.09x - 0.05$, $r = 0.740$, $n = 13$, $p < 0.001$
winter: $y = 0.08x - 0.05$, $r = 0.827$, $n = 12$, $p < 0.05$

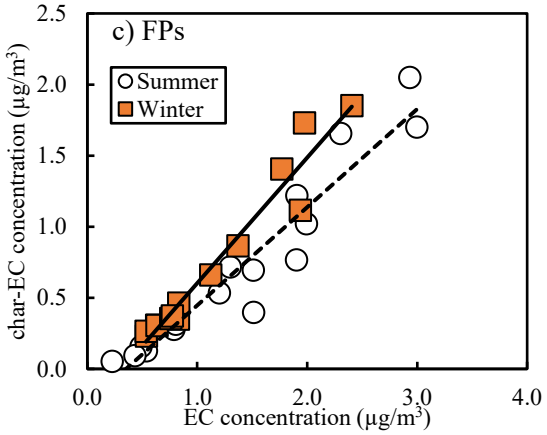

summer: $y = 0.69x - 0.24$, $r = 0.958$, $n = 17$, $p < 0.001$
winter: $y = 0.88x - 0.28$, $r = 0.974$, $n = 14$, $p < 0.001$

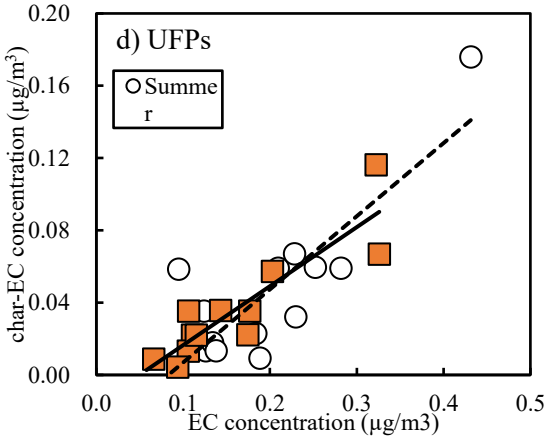

summer: $y = 0.40x - 0.03$, $r = 0.824$, $n = 13$, $p < 0.001$
winter: $y = 0.33x - 0.02$, $r = 0.893$, $n = 12$, $p < 0.001$

Figure 4.4 Relationships between char-EC and OC and EC in FPs and UFPs

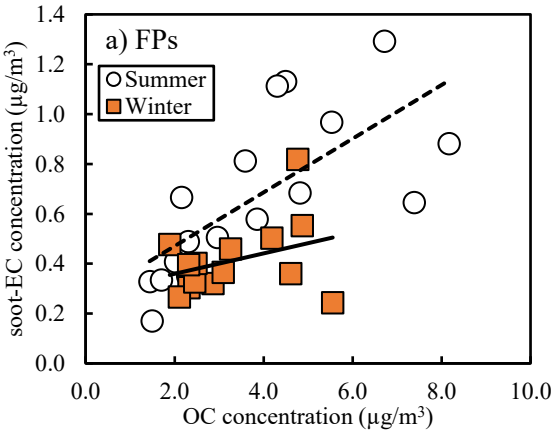

summer: $y = 0.11x + 0.26$, $r = 0.706$, $n = 17$, $p < 0.05$
winter: $y = 0.04x + 0.28$, $r = 0.337$, $n = 14$, $p > 0.23$

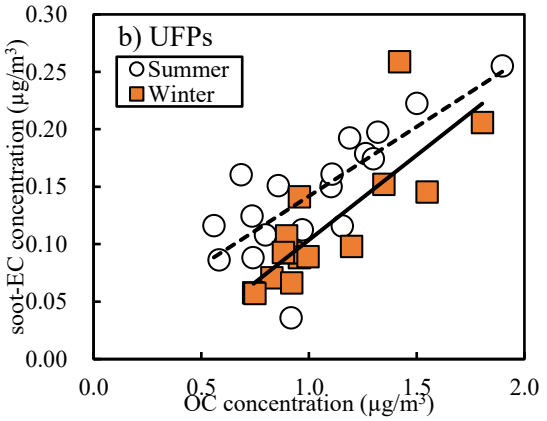

summer: $y = 0.12x + 0.02$, $r = 0.782$, $n = 18$, $p < 0.001$
winter: $y = 0.15x - 0.04$, $r = 0.817$, $n = 15$, $p < 0.001$

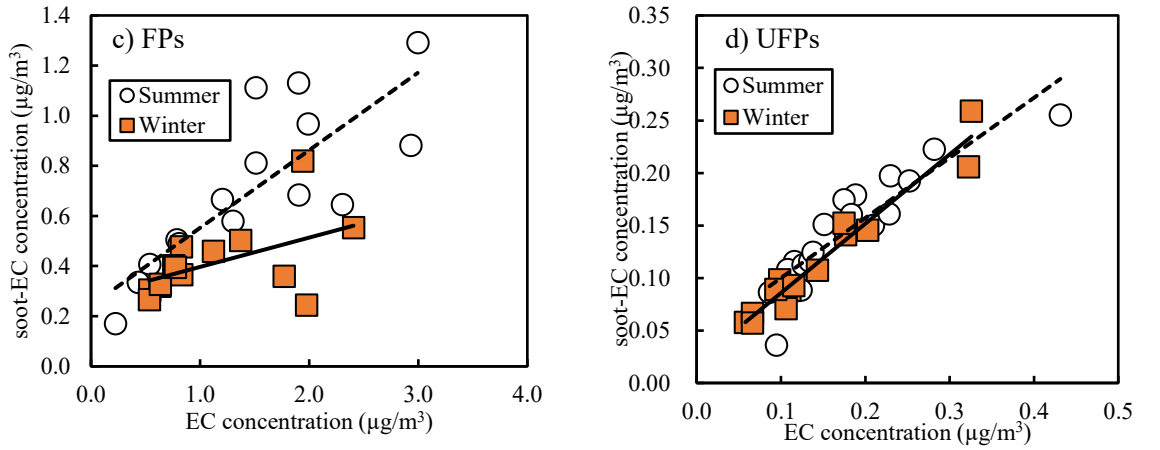

summer: $y = 0.31x + 0.24$, r =0.831, n=17, $p < 0.001$
winter: $y = 0.12x + 0.28$, r = 0.497, n=14, $p < 0.1$

summer: $y = 0.57x + 0.04$, r=0.899, n=18, $p < 0.001$
winter: $y = 0.66x + 0.02$, r = 0.973, n = 15, $p < 0.001$

Figure 4.5 Relationships between soot-EC and OC and EC in FPs and UFPs

4.3.3 Relationship between WSOC and PM components

Most SOA consists of water-soluble compounds with polar functional groups such as hydroxyl, carbonyl, or carboxyl, leading to their solubility. Although some SOA contains large carbon-hydrogen functional groups (which are insoluble), the largest fraction of SOA comprise WSOC (Miyazaki et al., 2006). Therefore, WSOC has been used as a marker of SOA when studying SOA formation. Some previous studies noted that SOA can be formed by oxidation processes in ambient air (Miyazaki et al., 2006) or can be produced by primary combustion such as of fossil fuel or in biomass burning (Mayol-Bracero et al., 2002; Tang et al., 2016). Clarifying the sources of WSOC is important for understanding the behavior of carbonaceous components in ambient air.

The correlations between WSOC and SO_4^{2-}, NO_3^-, K^+, and oxalic acid (C_2) were plotted to identify the origin of WSOC in both FPs and UFPs. A strong positive correlation was observed between WSOC and SO_4^{2-}, NO_3^-, K^+, and oxalic acid (C_2) in $PM_{2.5}$ during both the summer and winter sampling periods (Figure 4.6). The secondary components (SO_4^{2-} and NO_3^-) were used as the indicators of photochemical reactions. When a high concentration of these compounds is observed, the atmosphere can be considered as photochemically active and WSOC may be formed (Kumagai et al., 2009). Strong correlations were observed between WSOC and SO_4^{2-} and NO_3^- in $PM_{2.5}$ (Figure 4.6-a and 4.6-b), indicating that the WSOC might have been formed by secondary reactions. K^+ has been shown to be a primary product of coal and biomass burning (Kumagai et al., 2009, 2010; Watson et al., 2001), while oxalic acid can be emitted from both primary (e.g., vehicular exhaust and coal and biomass combustion) and secondary (e.g., the photochemical oxidation of organic precursors) sources. The strong relationship between WSOC and K^+ suggests that combustion processes may contribute to the WSOC in $PM_{2.5}$ (Figure 4.6-c). In this study, a significant correlation was observed between WSOC and oxalic acid in $PM_{2.5}$ in both summer (r = 0.968) and winter (r = 0.940) (Figure 4.6-d). This result implies that the sources of oxalic acid were stable during the sampling periods, and therefore this compound may have been produced by both primary and secondary sources.

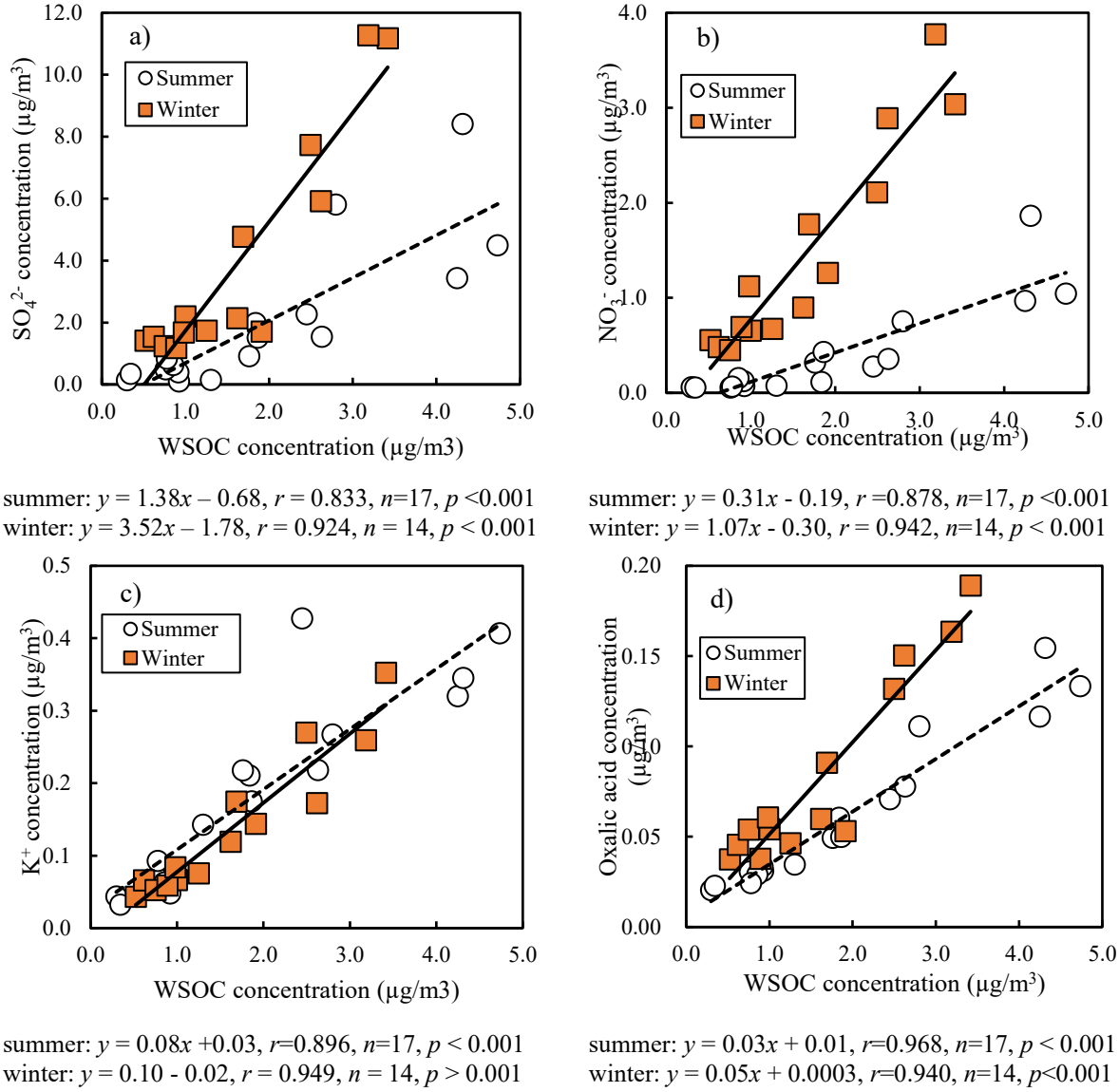

Figure 4.6 Relationships between WSOC and K^+, SO_4^{2-}, NO_3^-, and oxalic acid (C_2) in FPs

Strong correlations were found between WSOC and other components in $PM_{2.5}$ and $PM_{0.1}$, except for the correlation between WSOC and SO_4^{2-} (both summer and winter) and NO_3^- (wintertime) in $PM_{0.1}$ (Figure 4.7). Compared with winter, stronger correlations were observed between WSOC and SO_4^{2-} (Figure 4.7-a) and NO_3^- (Figure 4.7-b) in summer, demonstrating the contribution of secondary formation. Agudelo-Castañeda et al. (2019) found that the number of particles in the nucleation mode was highest on warm days and that the highest mean particle number concentration occurred in summer. The higher concentration of particles on warmer days has been shown to be caused by the photochemical reaction of gaseous precursors such as SO_2 or NO_x after their emission (Kulmala & Kerminen, 2008). Therefore, it was considered that the contribution of secondary generation to UFP was low. On the other hand, since the correlation between WSOC and NO_3^- was higher in summer, it is possible that NO_x and organic components derived from combustion (e.g., traffic and coal combustion) were mixed with UFPs under high-humidity conditions. The relationship between WSOC and K^+ was not significantly different between winter and summer, suggesting stable sources of K^+. Additionally, the stronger correlation between

WSOC and oxalic acid in summer (r = 0.905) compared with that in winter (r = 0.730) implies the contribution of photochemical reactions to PM during summer.

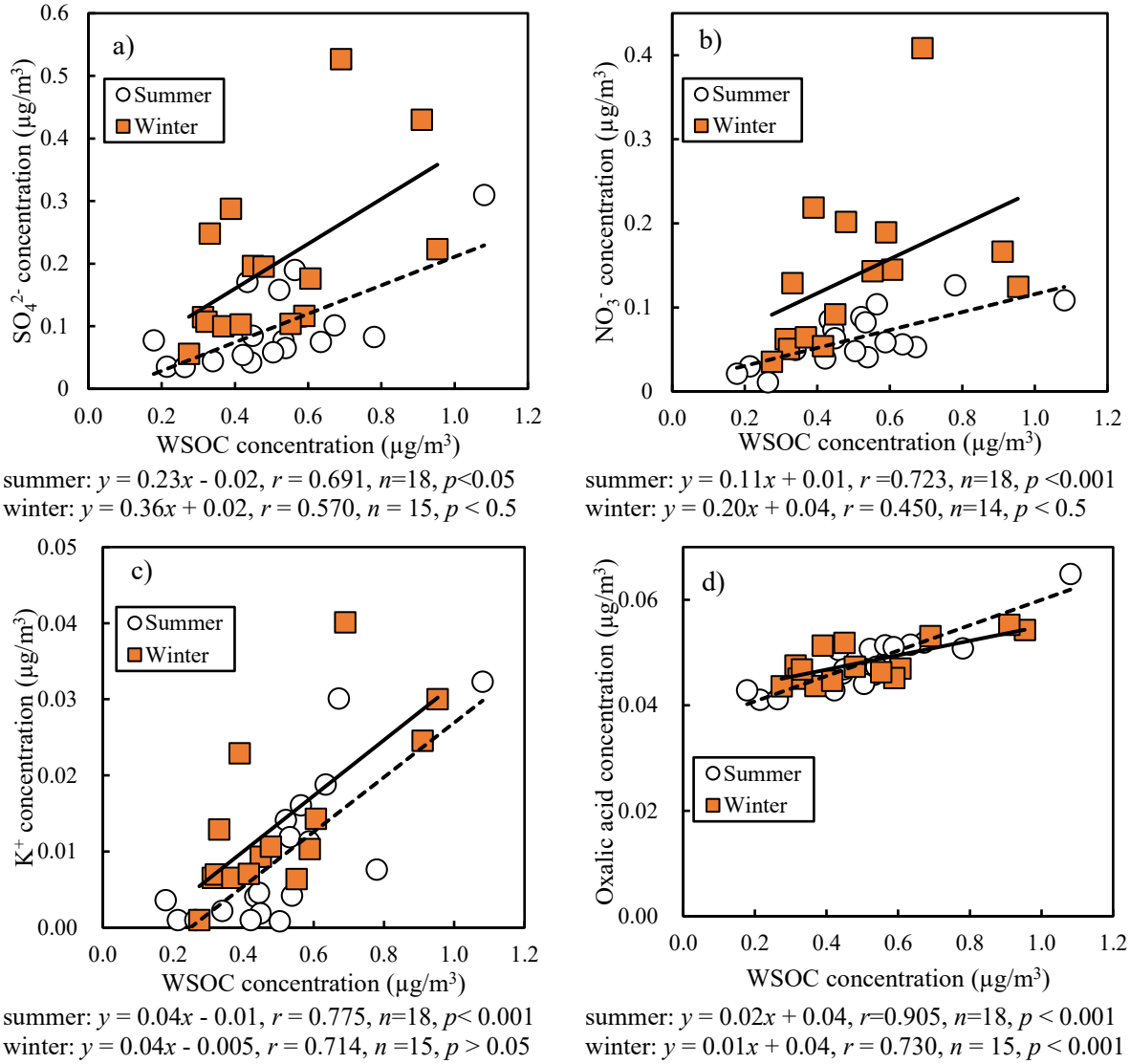

Figure 4.7 Relationships between WSOC and K^+, SO_4^{2-}, NO_3^-, and oxalic acid (C_2) in UFPs

Based on this observation, the primary sources of PM in Hanoi are hypothesized to be from traffic, coal, and biomass combustion. It has been reported that the air quality in Hanoi is affected by biomass burning, particularly the burning of rice straw after rice cultivation (Hai & Kim Oanh, 2013). Additionally, since coal is used for cooking in Hanoi and the city is surrounded by coal power plants, this could also be a considerable emission source. Furthermore, a large number of motor vehicles in Hanoi might represent another important source. In this study, the relationships between WSOC and K^+ did not vary significantly between summer and winter for both FPs and UFPs. These results suggest that the contribution of biomass burning during the sampling period was insignificant compared to traffic and industry emissions. It should be noted that vehicular exhaust, industry, biomass burning, and residential/commercial cooking were important sources in Hanoi as mentioned in several studies (Cohen et al., 2010; Hai & Kim Oanh, 2013; Hopke et al., 2008; Nghiem et al., 2020). The sampling periods in this study did not cover the intensive rice-straw burning

periods, which occur around June and November each year (Hai & Kim Oanh, 2013). However, to clarify the contribution of each source in detail, it is necessary to analyze more components such as levoglucosan (a marker of biomass burning) or polycyclic aromatic hydrocarbons, which are derived from fossil fuel combustion. Future studies are expected to enhance the understanding of emission sources and their contribution to PM in Hanoi.

4.3.4 Relationship between absolute humidity and particle formation

The impact of RH was first plotted; however, no correlation was found between RH and particle components. High RH has been proven to increase the size of particles in the atmosphere (Kozáková et al., 2017; X. Wang et al., 2012; Xiang et al., 2017). However, very high RH (> 85%) has been shown not to affect the increase in the concentration of particles (L. Zhang et al., 2017). It has also been shown that high RH (>80%) can cause the depletion of oxidants, leading to the reduction of the intensity of the oxidation reaction between volatile organic compounds (VOCs) and the oxidants (Xiang et al., 2017). In this study, the RH was more than 85% on 12 of the 36 analysis days, particularly on rainy days. A previous study found that rainfall can reduce the particle level and therefore lead to a negative correlation between RH and particle concentration (Vecchi et al., 2004). This phenomenon could explain the lack of correlation between RH and particle components in this study.

More interestingly, a correlation was observed between particle components and the absolute humidity (AH), the total mass of water vapor present in a volume of air. Figure 4.8 illustrates the relationships between SO_4^{2-}, NO_3^-, WSOC, char-EC, soot-EC, and AH. During the summer, positive correlations were observed between AH and SO_4^{2-}, NO_3^-, and WSOC in FPs. The strongest correlation was found between AH and WSOC (r = 0.850), followed by the correlation between AH and SO_4^{2-} (r = 0.808). According to Wang et al. (2012), the water in aerosol is the limiting factor for the occurrence of the uptake of precursor gases on the aerosol surface. This was associated with the formation of secondary aerosol in the condition of the abundant precursor gases, liquid water content and large surface area of aerosol. The strong correlations between AH and SO_4^{2-} and NO_3^- demonstrate that SO_4^{2-} and NO_3^- were formed in the aqueous phase during the summer sampling period. A strong correlation was also found during summer between AH and char-EC (r = 0.825) and soot-EC (r = 0.740). In contrast, no correlation was found between AH and other components in winter, under the condition of low AH.

In UFPs, a positive correlation between AH and NO_3^- (r = 0.809) and a lower positive correlation (r = 0.508) between AH and SO_4^{2-} were observed in summer. There was a tendency for high concentrations of soot-EC and WSOC under high AH conditions; however, the correlations between AH and soot-EC and WSOC were lower (r = 0.441 and r = 0.337, respectively). These results suggest that the contribution of secondary generation to UFPs was low in Hanoi, as described above, but that NO_x, soot-EC, and WSOC derived from combustion might be incorporated under high-humidity conditions. The family of NO_x compounds includes several different oxides which are formed when burning fossil fuel at high temperatures. NOx is emitted from on-road vehicles (e.g., motorbikes, automobiles, buses, trucks, etc.), non-road vehicles (e.g., boats, equipment, etc.), or industrial sources. NO_x is primarily emitted in the form of nitric oxide (NO) which is then oxidized within hours to nitrogen dioxide (NO_2). NO_2 is further oxidized to dinitrogen pentoxide (N_2O_5) or nitric acid (HNO_3) (USEPA, 1999). In an environment near roads where NOx production is abundant, it is rapidly oxidized and produced by interacting with water molecules to form NO_3^-. Therefore, the correlation between NO_3^- and AH is high in UFP due to its

hydrophilicity. In contrast, soot-EC and WSOC had low correlations with AH in UFPs but high correlations in FPs because it took some time to interact with water molecules owing to their hydrophobic properties. A high correlation was observed between AH and all components in FPs, including soot-EC and WSOC, meaning that significant particle growth from UFPs to FPs may have occurred via water molecules under high-AH conditions. AH has different influences on particle sizes (FPs and UFPs). It is considered that the influence of AH on particle size may occur in areas where a large amount of exhaust gas is emitted (e.g., motorcycles) under high-humidity conditions (e.g., drizzle).

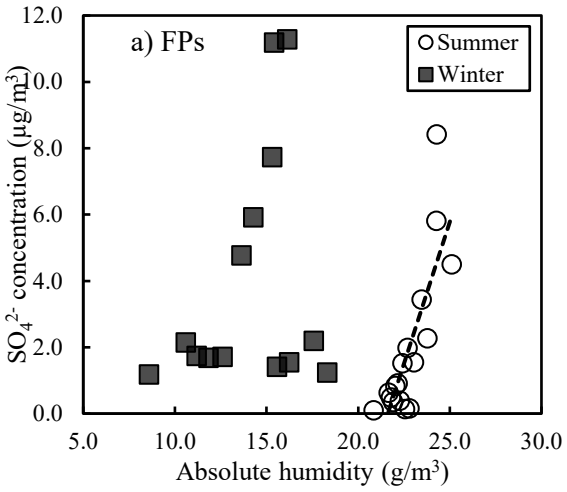

Summer: $y = 1.71x - 36.91$, $r = 0.808$, $n = 17$, $p < 0.001$

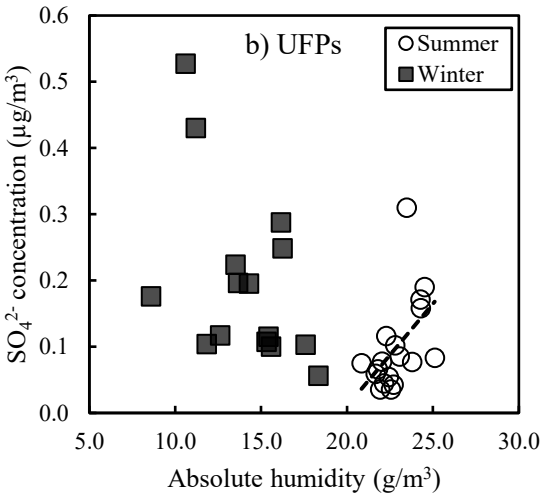

Summer: $y = 0.03x - 0.61$, $r = 0.508$, $n = 18$, $p < 0.05$

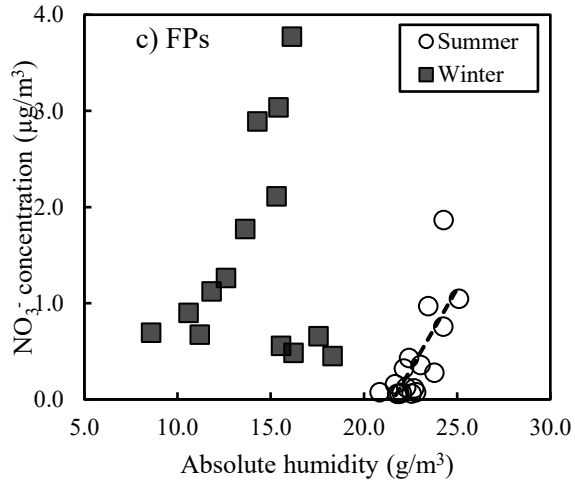

Summer: $y = 0.34x - 7.24$, $r = 0.748$, $n = 17$, $p < 0.001$

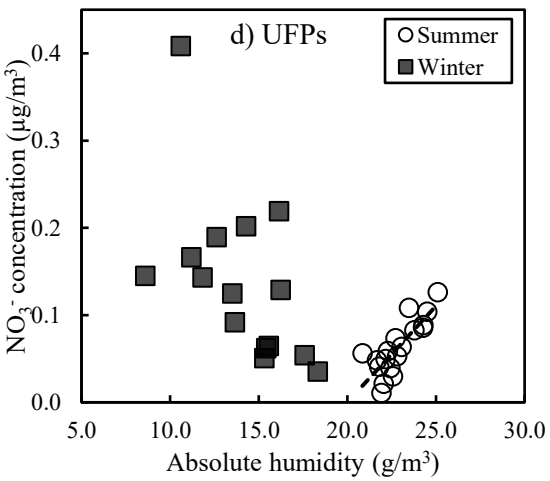

Summer: $y = 0.02x - 0.44$, $r = 0.809$, $n = 18$, $p < 0.001$

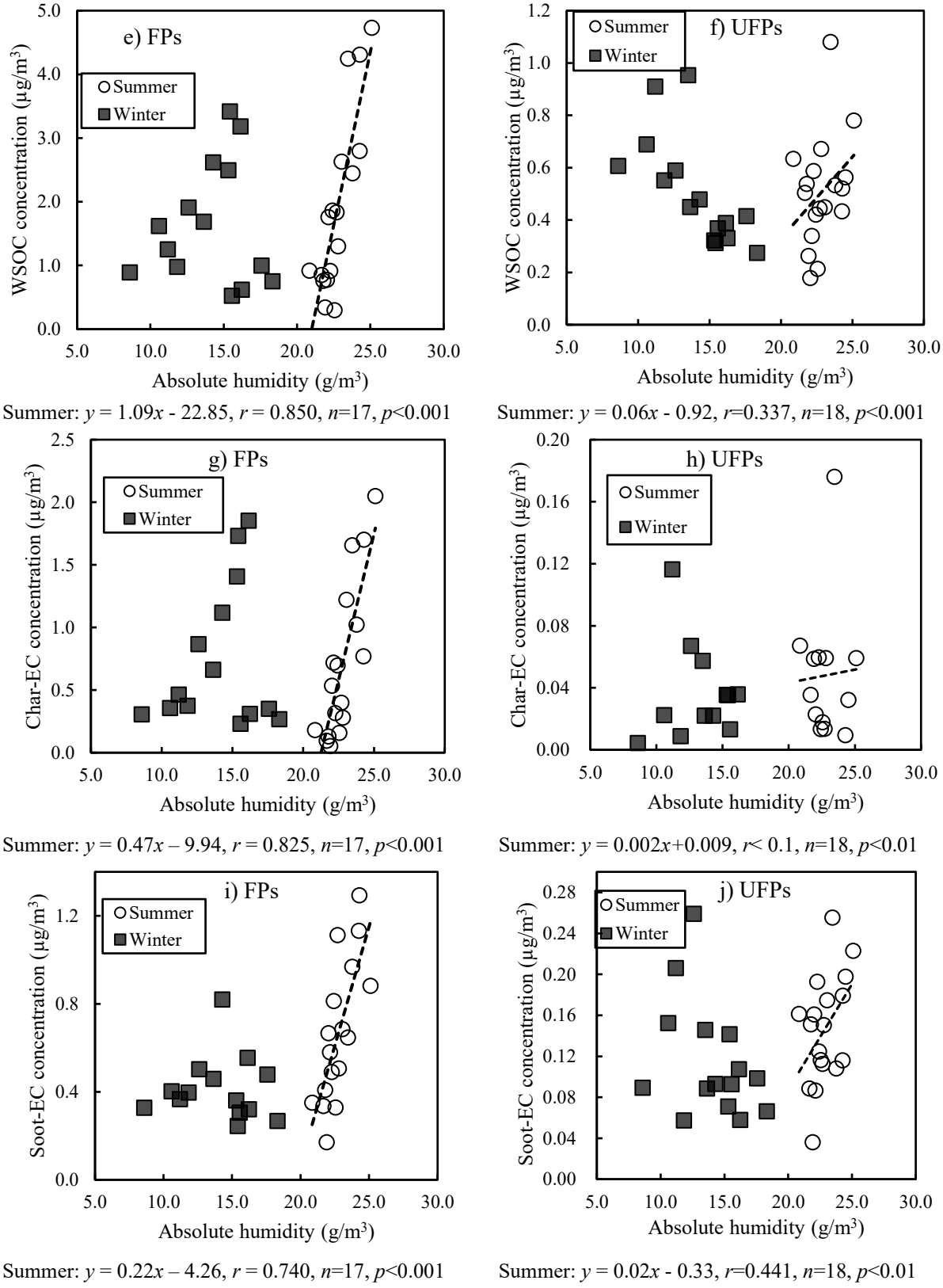

Figure 4.8 Relationships between AH and SO_4^{2-}, NO_3^-, WSOC, char-EC, and soot-EC in FPs and UFPs

4.4 Conclusion

In general, the concentration of FPs tended to be higher in winter. An insignificant variation in the UFPs concentration was observed between summer and winter. A lower concentration of UFPs was observed during rainy days; however, after the rain stopped, the concentration of UFPs quickly increased. Carbonaceous material (OC and EC) was the main component of particles, comprising up to 56% and 80% of FPs and UFPs, respectively. SO_4^{2-}, NO_3^-, and NH_4^+ were the main ionic species in both size ranges; the high concentrations of these ions suggest the influence of secondary formation processes.

The main carbon fractions were different in FPs and UFPs. EC1 and OC3 were the major fractions in FPs, while OC2 and OC3 accounted for higher shares in $PM_{0.1}$. The OC/EC ratio in FPs and UFPs did not vary significantly between summer and winter. The OC/EC ratios were used to infer the contribution of primary sources and the presence of SOA during the sampling period. Abundant char-EC was found in FPs, while soot-EC was dominant in UFPs. Secondary formation contributed considerably to the OC concentration, accounting for 36-41% and 37-47% of FPs and UFPs, respectively.

In FPs, WSOC correlated with SO_4^{2-}, NO_3^-, K^+, and oxalic acid in both seasons. In UFPs, strong correlations were observed between WSOC and SO_4^{2-}, NO_3^-, and oxalic acid in summer, whereas moderate correlations were observed between WSOC and K^+ in both summer and winter. The results imply that WSOC may be emitted from the combustion of coal or other fossil fuels and may be from photochemical reactions.

No relationship between RH and particle components was found in this study. However, strong correlations were observed between AH and SO_4^{2-}, NO_3^-, WSOC, char-EC, and soot-EC during summer. This finding may be explained by the very high RH (>85%) and rainy conditions that occur in summer in the study region. The strong correlations between AH and other components during summer might be related to secondary transformation processes involving water molecules, regardless of temperature. Therefore, it is necessary to consider the particle formation via water molecules that can occur in highly contaminated areas under high humidity environments. A different influence of AH on the WSOC concentration was seen in FPs and UFPs. It was found that the AH had a stronger effect on the WSOC concentration in FPs than in UFPs.

Chapter 5

Assessment of traffic-related chemical components in UFPs and FPs

5.1 Background

The characteristics of particles vary significantly depending on the size ranges. Particles with diameters above 30 μm can easily sediment by gravity, whereas $PM_{2.5}$ remain in the air for a long time. $PM_{2.5}$ can also travel longer distances than coarse particles. In early research on the impact of air pollution on human health, PM_{10} was common. It is now known that $PM_{2.5}$ can penetrate deep into the lung (pulmonary alveoli) and other parts of the human body via the blood. Recent studies on $PM_{0.1}$ and human health showed that $PM_{0.1}$ is more dangerous because it can penetrate deeper into the lung or directly go to other organs without being absorbed by the blood (Dumkova et al., 2016; Oberdörster et al., 2004; Stölzel et al., 2007).

Various emission sources of particles such as vehicular exhaust, construction activities, industry, and coal and biomass burning in urban areas have been reported (ChooChuay et al., 2020; Hai & Kim Oanh, 2013; Hopke et al., 2008; Vu et al., 2015). Traffic emissions have been mentioned as an important source of UFPs (Minoura et al., 2009; Nghiem et al., 2020; Yungang Wang et al., 2012). The emissions from traffic include particles in the solid phase, low-volatile liquid, and gaseous pollutants such as NO_x, SO_2, and VOCs (Jacobson et al., 2005; Khalek et al., 2015; Rivas et al., 2020). The mixture of gases and particles from traffic emissions and other sources are favorable conditions for physicochemical processes, which affect the concentration and composition of particles, particularly the ultra-size range particles. For instance, the gases emitted from vehicles or other combustion sources might condense immediately to form particles or generate secondary particles by photochemical reactions. Therefore, the temporal and spatial variations of UFPs are expected to be more complicated than bigger size particles.

In a study of UFPs at roadsides, a decrease in particle concentration with distance from the road was observed. With a distance of up to approximately 300 m, the particle concentrations and size distribution are nearly similar to the background (Zhu et al., 2002). This phenomenon is explained by several processes, such as the dilution, coagulation, and evaporation of particles (Jacobson et al., 2005; Saha et al., 2018). Those results show the critical contribution of traffic-related emissions to the UFPs in urban areas, particularly in populated cities such as Hanoi, Vietnam. Limited published studies on the chemical composition and the transformation of particles near the roadside are available. The spatial variation of chemical properties and concentration of particles near busy roadways is crucial because of its potential health impacts on people (Jeong et al., 2015). Thus, observing particles near the road is vital to determine the change of concentration and compositions from the emission source to the ambient air. It would reveal the particles' growth or decay processes, explaining the differences in particle concentration and size distribution in different sampling locations.

UFPs and FPs were simultaneously collected in Hanoi during different seasons at the roadside and ambient sites. The chemical components, including carbonaceous and ionic species, were measured to characterize particles, evaluate the seasonal variation, and the spatial difference between RS and AS. Furthermore, the relationship between UFPs from the roadside and FPs in the ambient site was examined to observe the chemical composition changes and the contribution of particle growth processes.

5.2 Methods

5.2.1 Sampling site description

Two selected sampling sites were at HUST, Hai Ba Trung District, Hanoi, including a roadside (RS) and ambient (AS) site. The RS is next to Tran Dai Nghia St., a two traffic lanes road, running through three universities and a highly populated area (Figure 5.1). Tran Dai Nghia St. is two traffic lanes road, approximately 8-10 m in width. Both sides of the street have a pavement of about 2.5-3m in width. Traffic volume in Tran Dai Nghia St. was not counted in this study. However, around 100,000–150,000 vehicles per day are expected on this street. This traffic volume was observed in similar roadways near the sampling locations in the study by Phan et al. (2010). The AS site is on the rooftop of a four-story building of the School of Materials Science and Engineering, HUST, approximately 12 m in height from the ground. This site is around 200 m from Dai Co Viet St., 250 m from Giai Phong St., 200 m from Tran Dai Nghia St., and surrounded by diverse institutional and residential areas (Figure 5.1).

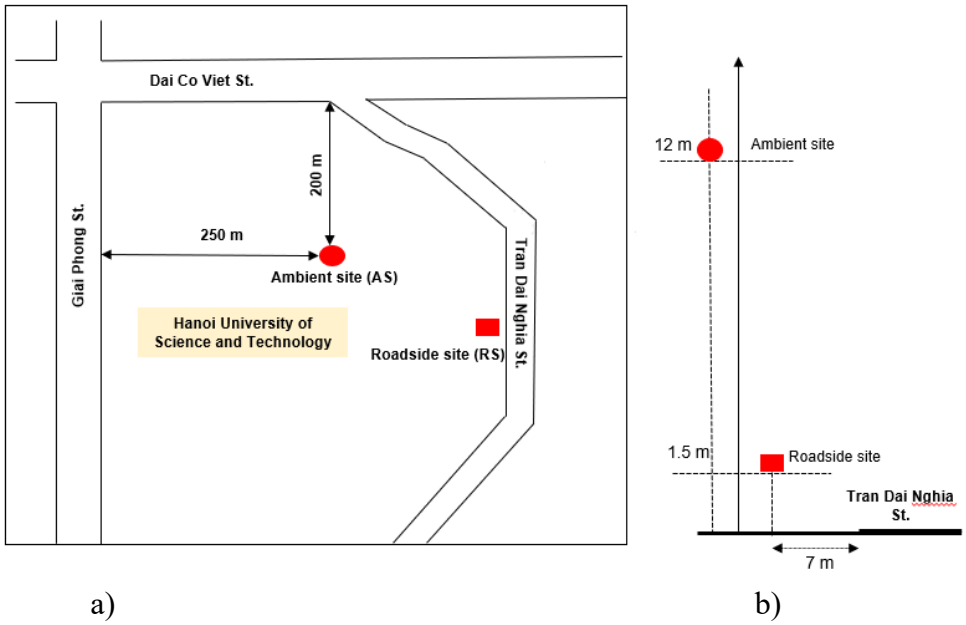

Figure 5.1 Horizontal sketch (a) and Vertical sketch (b) of sampling sites

5.2.2 Sample collection and analysis

The sampling was done simultaneously in different seasons at the RS and AS. At the AS, daily samples (23.5 h) of UFPs and FPs were collected in summer (August 10–24, 2020), STP (October 14–27, 2020), winter (December 02–15, 2020), and WTP (March 24–April 7, 2021). At the RS, due to the limitation of sampling devices, only UFPs were collected. The roadside samples were collected in summer, STP, and winter, except for the WTP sampling due to the construction activities at the site. The sampling equipment at the RS was set up approximately 7 m away from the traffic lane at the street's outer edge. All the sampling devices were placed at 1.5 m in height from the floor and at least 1 m from any barriers such as walls, doors, and windows. UFPs and FPs were collected by Nanosampler (Model 3182, KANOMAX, Suita, Japan) and cyclone (URG-2000-30EH, University Research Glassware Corp., Chapel Hill, NC, USA), respectively. Nanosampler includes five impaction stages to

classify particles of different diameters at ≤0.1, 0.1–0.5, 0.5–1, 1–2.5, 2.5–10, and >10 µm. Nanosampler was operated at a flow rate of 40 L/min while cyclone was at 16 L/min. Quartz fiber filter (2500 QAT-UP, Pall Corp., USA) was used for both devices (55 mm filter for Nanosampler and 47-mm filter for cyclone). Before sampling, the filters were baked at 350 ℃ for 2 h to remove possible contaminants. After collection, the samples were placed in a Petri dish and then kept in an airtight aluminum bag at −40 ℃ to avoid any reactions. Blank samples were prepared and treated the same way as the samples. The total number of blank samples was at least 10% of the total number of samples. $PM_{2.5}$ measured by BAM at the US Embassy in Hanoi, located approximately 3.1 km from the sampling site, were collected from the AirNow website (https://www.airnow.gov/international/us-embassies-and-consulates/#Vietnam$Hanoi). A thermo recorder was set up in the same location as the other devices to record the temperature and relative humidity. The wind speed during the sampling periods, measured at Lang station in Hanoi (21.02N 105.80E), approximately 4.7 km from the sampling site, was obtained from the Wyoming Weather website (https://weather.uwyo.edu/surface/meteorogram/seasia.shtml).

A 0.503 cm^2 punch-out filter was used to determine the carbonaceous components (OC and EC) using a carbon analyzer (DRI model 2001, Atmoslytic Inc., Calabasas, CA, USA). The different fractions of the OC and EC were analyzed following the Interagency Monitoring of Protected Visual Environments (IMPROVE) method (Chow et al., 2001). Details of each carbonaceous fraction analysis are further discussed in Section 3.3. Quality assurance and quality control were ensured by the semiannual calibration of the Potassium Hydrogen Phthalate (KHP) solution. In addition, the samples were analyzed twice, and the difference was smaller than 5% for total carbon (TC = OC + EC). Further, QA/QC procedures were discussed in the study by Huyen et al. (2021). Ionic components were analyzed by ion chromatography (ICS-1600, Dionex Corp., Sunnyvale, CA, USA) and water-soluble organic carbon (WSOC) by a total carbon analyzer (Multi N/C 3100, Analytik Jena, Jena, Germany). Before analysis, the samples were extracted with 20 mL ultrapure water for 20 min in an ultrasonic bath. To ensure QA/QC of the analysis, all the vials and glassware were cleaned by ultrasonic bath and oven-dried before use. An instrument blank was analyzed with field samples to assess the presence of instrument contamination. The detail of QA/QC has been described in the study by Wang et al. (2005).

5.3 Results and Discussion

5.3.1 UFPs at RS

5.3.1.1 OC and EC fraction

The OC and EC concentrations in UFPs in this study were compared with that of other published studies (Table 5.1). The mean OC concentration at RS during summer was comparable to those from similar samples in Japan, Germany. Meanwhile, the OC concentration in winter was approximately two times higher than that in the samples collected during summer in Japan, Germany, and for the whole year in Taiwan and Thailand. The high OC concentration during winter may be associated with the effect of long-range transportation, the rice straw burning in surrounding agriculture areas (Hai & Kim Oanh, 2013; MONRE, 2017), or meteorological conditions (Hien et al., 2011; Kim, Sekiguchi, Furuuchi, et al., 2011). The mean concentration of OC for all the sampling periods was 1.61 ± 0.67 µg/m^3. It was higher than the annual average OC concentration in UFPs from the AS (1.48 ± 0.67 µg/m^3) and samples collected in Phuket, Thailand (0.68 ± 0.60 µg/m^3). In

contrast, the mean EC concentration for all the sampling periods in this study was 0.46 ± 0.22 μg/m^3, approximately four times higher than in Japan and Germany and 1.3 times higher than in Taiwan. The high EC level might be due to the fuel quality, the low engine standards, and the lack of control technology for existing vehicles in the study area. In Vietnam, following Decision number 49/2011/QD-TTg, four fuel types are available that comply with Euro II, III, IV, and V (as of 2022). Euro IV and V standards for imported and newly assembled automobiles have been applied since 2017 and 2022, respectively, and Euro III for motorcycles since 2017. Motorcycles and automobiles assembled or imported before 2017 have been following Euro II standards. As a result, even though the Euro IV and IV have been in place, the majority of the vehicle fleet in circulation only meet Euro II standards, particularly motorcycles. These factors could have led to the high emissions of other pollutants such as VOCs and BTEX (a mixture of benzene, toluene, ethylbenzene, and xylene) (Phuc & Kim Oanh, 2018; Trang et al., 2015).

Table 5.1 Comparison of OC and EC concentrations in UFPs from different locations

Sampling site	Sampling periods	Devices	OC (μg/m^3)	EC (μg/m^3)	References
RS, Hanoi, Vietnam	Summer Aug 10 - 24, 2020	Nanosampler 3182	1.30 ± 0.26	0.36 ± 0.10	This study
	STP Oct 14 - 27, 2020		1.44 ± 0.91	0.45 ± 0.27	This study
	Winter Dec 02 - 15, 2020		2.10 ± 0.40	0.59 ± 0.21	This study
	Average		1.61 ± 0.67	0.46 ± 0.22	This study
AS, Hanoi, Vietnam	Annual average	Nanosampler 3182	1.48 ± 0.67	0.35 ± 0.20	This study
Roadside, Japan	Summer Jul-Aug 2009	Inertial filter (INF)	1.01 ± 0.16	0.08 ± 0.05	(Kudo et al., 2012)
Roadside, Germany	Summer Aug-Sep 2009	Inertial filter (INF)	1.21 ± 0.43	0.14 ± 0.06	(Kudo et al., 2012)
Roadside, Taiwan	Annual average Jan - Dec 2008	MOUDIs	0.54 ± 0.07	0.36 ± 0.17	(Chen et al., 2010)
Ambient site, Phuket, Thailand	Annual average Jan - Dec 2018	Inertial filter	0.68 ± 0.60	0.23 ± 0.14	(Phairuang et al., 2020)

OC and EC concentrations are written as Average concentration ± Standard deviation

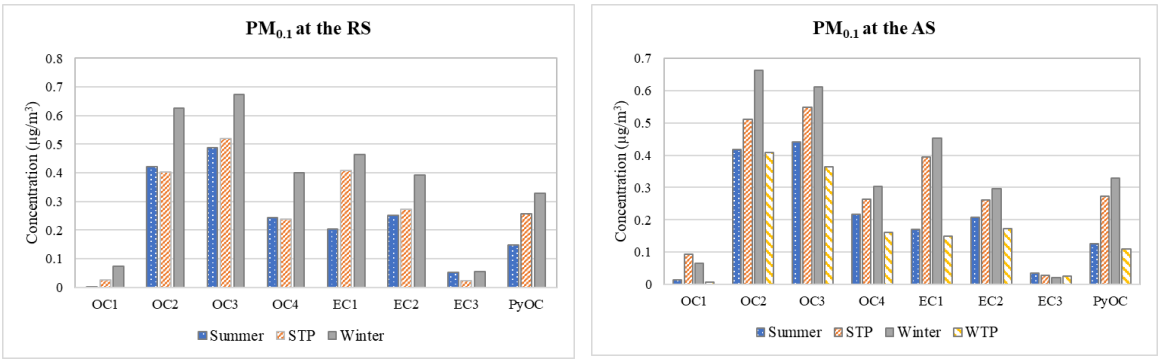

Figure 5.2 Seasonal variation of carbon fractions in UFPs at RS and AS

The average contributions of each component in UFPSs at RS for all seasons (summer, winter, and STP) were OC3 (24.1%) > OC2 (20.8%) > EC1 (15.4%) > EC2 (13.2%) > OC4 (12.6%) > PyOC (10.5%) > EC3 (1.9%) > OC1 (1.4%). OC2 and OC3 were the major carbonaceous components in UFPs, where OC3 was emitted mainly from cooking, motorbike exhaust, and a small fraction from road dust (Cao et al., 2005; Gu et al., 2010; Panicker et al., 2015), and OC2 was found in the coal or biomass combustion (Cao et al., 2005; Gu et al., 2010). EC1, produced by motorbike emission, coal, and vegetative burning (Cao et al., 2005; Phairuang et al., 2020), also accounted for 13%–15%. The OC and EC fractions ranking provided the sign of multiple emission sources in the study area, including motorbike exhaust, coal and biomass combustion, and cooking activities. The seasonal variations of each carbon fraction in UFPs at RS and AS are shown in Figure 5.2.

The concentrations of OC, EC, char-EC, soot-EC, and their ratios in UFPs at RS in the different sampling periods are shown in Table 4.2. The OC concentrations at RS were 1.30 ± 0.26, 1.44 ± 0.91, and 2.10 ± 0.40 µg/m^3 and the EC concentrations were 0.36 ± 0.10, 0.45 ± 0.27, and 0.59 ± 0.21 µg/m^3 in summer, STP, and winter, respectively. The highest concentrations of OC and EC were found in winter and the lowest in summer. The seasonal variation of OC and EC in UPFs at RS was consistent with the PM concentration, which was higher in winter than in summer. The OC and EC concentrations in UFPs at RS were higher than those collected from the AS, except for the OC concentration during STP. Even though the OC and EC concentration varied from summer to winter, the contribution of those components to TC was virtually unchanged. For instance, OC concentration accounted for approximately 76%–78% of TC, irrespective of the season change. The contribution of EC to TC was around 22%–24%. This was higher than UFPs at the AS of 18%–20%. The higher EC concentration and contribution to TC in the RS samples indicated that the vehicular exhaust's effect on the RS samples was stronger than that on the AS samples.

The ratio between OC and EC concentrations has been used in numerous studies to identify the effect of traffic-related emissions. The OC/EC ratio in FPs at the roadside was 1.64 in Japan (Kudo et al., 2012) and 1.0 in Hong Kong (Cao et al., 2006). The ratio in FPs at the tunnel in Guangzhou, China was 0.56 (Huang et al., 2006), while that in Xueshan Tunnel, Taiwan was 1.26 (Zhu et al., 2010). In general, low OC/EC ratios at the tunnel or the roadside were observed because of traffic-related emissions (primary emissions of OC and EC). Meanwhile, the OC/EC ratios in FPs at the ambient site were higher, e.g., the ratio of OC/EC was 3.52 in Bangkok, Thailand (ChooChuay et al., 2020a), 2.03 in Saitama, Japan (Kim et al., 2011), and 3.2 in Hanoi, Vietnam (Huyen et al., 2021). Higher OC/EC ratios at the ambient site may be due to secondary organic particle formation or other primary OC-rich sources such as biomass burning (Kudo et al., 2012). Kim et al. (2013) reported that the

OC/EC ratio in UFPs during daytime was lowest at the site located 5m away from the intersection (5.52), while the highest ratio was found at the site located 150 away from the intersection (6.76). The study by Thuy et al. (2018) shows that a slightly lower OC/EC ratio in UFPs was observed in the place near the road (3.79–4.67) in comparison with the ambient site (4.78–5.68) in Hanoi, Vietnam. In this study, the OC/EC ratios in $PM_{0.1}$ at RS were 3.73 ± 0.64 in summer, 3.39 ± 0.82 in STP, and 3.84 ± 0.83 in winter (Table 4.2). These OC/EC ratios were lower than $PM_{0.1}$ at the AS in all the sampling periods, ranging from 4.72 to 5.10. The higher OC/EC ratios at the AS indicated that OC and EC in $PM_{0.1}$ samples at RS were affected more by the primary sources, i.e., vehicular exhaust while OC in the $PM_{0.1}$ samples at the AS may be influenced by secondary formation from the gaseous phase or other primary sources such as biomass combustion.

Table 5.2 Average concentrations of carbonaceous compounds in UFPs at the RS

	UFPs at the RS					
	OC (μg/m^3)	EC (μg/m^3)	OC/EC	Char-EC (μg/m^3)	Soot-EC (μg/m^3)	Char-EC/soot-EC
	Ave.[a] ± S.D.[b]	Ave.± S.D.	Ave.± S.D.	Ave. ± S.D.	Ave.± S.D.	Ave.± S.D.
Summer (n=15)	1.30 ± 0.26	0.36 ± 0.10	3.73 ± 0.64	0.06 ± 0.04	0.30 ± 0.09	0.23 ± 0.29
STP (n=14)	1.44 ± 0.91	0.45 ± 0.27	3.39 ± 0.82	0.15 ± 0.16	0.30 ± 0.12	0.41 ± 0.39
Winter (n=14)	2.10 ± 0.40	0.59 ± 0.21	3.84 ± 0.83	0.14 ± 0.16	0.45 ± 0.16	0.38 ± 0.38
Average	1.61 ± 0.67	0.46 ± 0.22	3.65 ± 0.77	0.12 ± 0.13	0.35 ± 0.14	0.34 ± 0.35

[a] Average concentration
[b] Standard deviation

The average concentrations of char-EC in UFPs were 0.06 ± 0.04, 0.15 ± 0.16, and 0.14 ± 0.16 μg/m^3 in summer, STP, and winter, respectively. The concentrations of soot-EC were 0.30 ± 0.09, 0.30 ± 0.12, and 0.45 ± 0.16 μg/m^3 in summer, STP, and winter, respectively. Soot-EC, formed at a higher temperature from the gaseous phase, was the main fraction of EC, accounting for approximately 66%–84% of the total EC. In contrast, char-EC, a product of burning carbon materials such as coal or biomass, was responsible for a smaller fraction (16%–34%). The char-EC concentrations were lowest in summer and virtually unchanged from STP to winter (Figure 5.3). It might be associated with biomass burning, which was more frequently observed during the dry season (around STP and winter). However, the minor change in the char-EC concentration between STP and winter indicated that it was not an intensive biomass burning period. According to Thuy et al. (2018), the char-EC concentration significantly increased approximately three times in the Vinacomin sampling site, which was affected by biomass burning during the dry season in Hanoi. Meanwhile, soot-EC reached a peak during winter, suggesting the impact of meteorological factors such as the low mixing height and low precipitation. In this study, the mean char-EC/soot-EC ratio for UFPs at RS was 0.34 ± 0.35. This ratio is comparable with the char-EC/soot-EC ratio in Songkhla, Thailand (0.36) (Phairuang et al., 2020) and slightly lower than the char-EC/soot-EC ratio in Kuala Lumpur, Malaysia (0.67) (Jamhari et al., 2022), and in Bangkok, Thailand (0.72) (Phairuang et al., 2019). It should be noted that the significant impact of vehicular exhaust on air pollution has been reported in these locations, particularly

motorcycle emissions. In contrast, an increased value of the char-EC/soot-EC ratio suggests the effect of biomass burning, such as during the dry season in Hanoi, Vietnam (2.58) (Thuy et al., 2018), or in Chiangmai, Thailand (2.73) (Phairuang et al., 2019, 2020). The low ratio of char-EC/soot-EC for UFPs at the RS was observed in all three sampling periods in this study, indicating the significant contribution of vehicle emissions. Correlations between char-EC, soot-EC and OC, EC in UFPs at RS were plotted in Figure 5.4. Positive correlations (r = 0.72–0.82) between char-EC, soot-EC and OC, EC were observed. This result indicates that the common emission sources of char-EC, soot-EC, OC, and EC, such as vehicular exhaust, might be expected in this sampling site. However, further studies such as the analysis of polycyclic aromatic hydrocarbons or VOCs should be carried out to clarify the contribution of traffic emission to the level of carbon fractions in UFPs near the roadside.

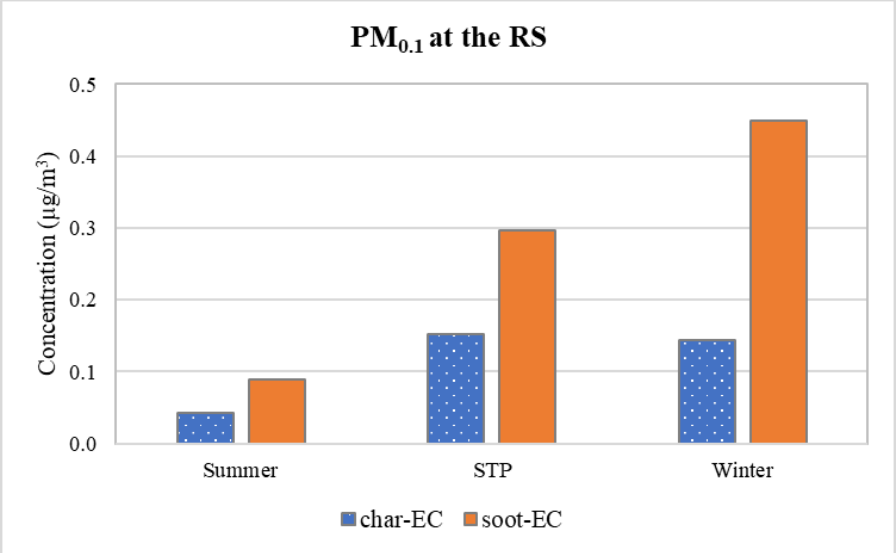

Figure 5.3 Seasonal variation of char-EC and soot-EC in UPFs at the RS

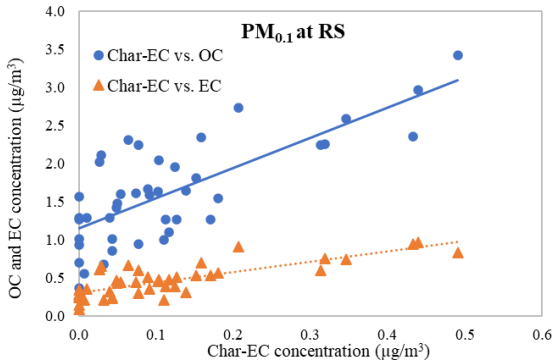

Char-EC vs. OC y = 3.98x + 1.15, r = 0.75, n = 55, p < 0.001
Char-EC vs. EC: y = 1.36x + 0.30, r = 0.79, n = 55, p < 0.001

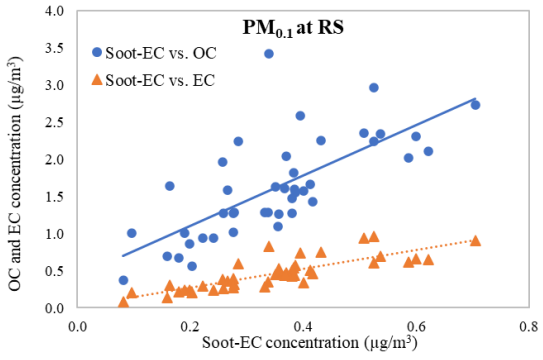

Soot-EC vs. OC: y = 3.40x + 0.42, r = 0.72, n = 55, p < 0.001
Soot-EC vs. EC: y = 1.27x + 0.02, r = 0.82, n = 55, p < 0.001

Figure 5.4 Relationship between char-EC, soot-EC and OC, EC in UPFs at the RS

5.3.1.2 Ionic species and WSOC

The concentrations of WSOC, WIOC, and ionic species in UFPs at RS during different sampling periods are illustrated in Table 5.3. The concentrations of WSOC and WIOC were approximately equal in summer and STP. However, the WSOC concentration was double

that of the WIOC in winter. A higher WSOC concentration or WSOC/OC ratio suggests the formation of secondary organic aerosol (SOA) by photochemical reactions (Miyazaki et al., 2006) or from biomass burning emission (Kudo et al., 2012). However, a poor relationship ($r = 0.43$) between WSOC and K^+, a biomass burning tracer, was observed in UFPs at RS during winter ($r = 0.43$). Furthermore, the intensive period of biomass burning, mainly rice straw, occurs in June and November yearly in the vicinity of Hanoi (Hai & Kim Oanh, 2013). In addition, the variation of ozone concentration could be used to evaluate the secondary emissions by photochemical reactions. One-year ozone observation in Hanoi by Sakamoto et al. (2018) showed that the ozone concentration decreased from summer to winter depending on the photochemical activity. However, the abnormally high ozone concentration was approximately 100 ppb during early winter (in late October), while the highest ozone concentration in summer was 25.7 ppb. The abnormal ozone concentration was supposed to link to the winter monsoon bringing air parcels from northern or northeastern areas associated with other meteorological factors (e.g., low wind speed and temperature inversion). Therefore, during the winter sampling period (December 2–15), the high concentration of WSOC may be because of air mass transportation under adverse meteorological conditions such as low wind speed, temperature inversion, and low mixing height.

Sulfate, nitrate, and ammonium (SNA) were the dominant ions in UFPs, accounting for 50%–89% of the total ion concentration. The concentrations of SNA tended to be higher in winter than in summer, particularly the nitrate ions. In winter, nitrate made up the highest concentration of the SNA ions of 0.40 ± 0.15 μg/m^3, followed by ammonium (0.38 ± 0.17 μg/m^3) and sulfate (0.28 ± 0.12 μg/m^3). In contrast, sulfate accounted for the most significant proportion in the other seasons (summer and STP). The dominance of nitrate in winter may be explained by the formation pathways of nitrate, including the photochemical reactions of precursor gases (NO_x) and hydrolysis of N_2O_5. The photochemical reaction is enhanced by strong sunlight. However, high temperature causes significant volatilization of nitrate and ammonium, leading to lower concentrations of those ions. Xu et al. (2019) showed that the nitrate concentration significantly declined due to volatilization loss when the average temperature reached 26.2 °C. The average temperature of 30.3 °C during the summer sampling resulted in an evaporative loss, and a low nitrate concentration was recorded. In contrast, the low temperature during winter associated with a low mixing layer promoted nitrate formation. Furthermore, the nitrate formation was influenced by the hydrolysis of N_2O_5 at night (Xu et al., 2019). The adverse weather conditions enhanced this process during winter, which prevented the dilution of atmospheric pollutants. The ratios of NO_3^-/SO_4^{2-} are widely used to relatively identify the emission sources as mobile or stationary sources. NOx originated primarily from traffic emissions (mobile sources), while SO_2 came from coal burning (stationary sources). The lower NO_3^-/SO_4^{2-} ratio suggests that the emissions from the stationary sources were more dominant than those of the mobile sources. The ratio of NO_3^-/SO_4^{2-} tended to increase from summer to winter, similar to the trend of the SNA species (Table 5.3). As discussed above, it might be caused by the volatilization of nitrate during summer. The mean ratio of NO_3^-/SO_4^{2-} for all sampling campaigns was 1.07 ± 0.75. This ratio was higher than the ratio of samples at the AS (0.81 ± 0.46) for three seasons (summer, STP, and winter). This result suggests a higher contribution of traffic emissions to the samples at RS than at the AS. The NO_3^-/SO_4^{2-} ratio may provide the first sign of the relative contributions of the stationary and mobile sources; however, further studies such as modeling need to be conducted to quantify the specific contribution of each source.

Other ions, including Cl^- and K^+, accounted for smaller fractions and contributed less than 5% of the total ionic concentration, while Na^+ and Mg^{2+} were not detected in the samples at RS. In contrast, the concentration of Ca^{2+} was highest in the summer sampling at 0.28 ± 0.22 μg/m^3, accounting for approximately 49% of the total concentration of ionic species, followed by STP (0.13 ± 0.13 μg/m^3) and winter (0.07 ± 0.05 μg/m^3). The construction activities near the sampling point could have affected the Ca_2^+ level during summer. Furthermore, the calcium ion concentrations in UFPs at RS were higher than that from the AS in all the seasons, reflecting the impact of the road dust emissions.

Table 5.3 Average concentrations of WSOC, WIOC, and ionic species in UFPs at the RS

	UFPs at the RS		
	Summer (n=15)	STP (n=14)	Winter (n=14)
	Ave.[a] ± S.D.[b]	Ave.± S.D.	Ave.± S.D.
WSOC (μg/m^3)	0.67 ± 0.18	0.78 ± 0.44	1.38 ± 0.34
WIOC(μg/m^3)	0.64 ± 0.23	0.66 ± 0.48	0.72 ± 0.16
Cl^- (μg/m^3)	0.014 ± 0.008	0.007 ± 0.007	0.05 ± 0.02
SO_4^{2-} (μg/m^3)	0.14 ± 0.06	0.19 ± 0.14	0.28 ± 0.12
NO_3^- (μg/m^3)	0.07 ± 0.03	0.15 ± 0.07	0.40 ± 0.17
Na^+ (μg/m^3)	-[c]	-	-
NH_4^+ (μg/m^3)	0.06 ± 0.03	0.10 ± 0.10	0.38 ± 0.17
K^+ (μg/m^3)	-	0.008 ± 0.016	0.006 ± 0.01
Mg^{2+} (μg/m^3)	-	-	-
Ca^{2+} (μg/m^3)	0.28 ± 0.22	0.13 ± 0.13	0.065 ± 0.045
NO_3^-/ SO_4^{2-}	0.54 ± 0.21	1.21 ± 0.99	1.49 ± 0.49

[a] Average concentration
[b] Standard deviation
[c] Below detection limit

5.3.2 Seasonal variation of UFPs and FPs

5.3.2.1 Concentration of UFPs and FPs

The concentrations of the analyzed components, including carbonaceous and ionic species in UFPs and FPs at AS, and the mean $PM_{2.5}$ concentration from the US Embassy are shown in Table 5.4. The total concentration of analyzed components, including carbonaceous and ionic species, was used in this study. Other components such as elements were not included in the actual concentration of particles. For instance, the mean $PM_{2.5}$ concentrations collected by BAM from the US Embassy were higher than those reported in this study, regardless of

the sampling method and location differences. However, data from both sources show a similar trend of variation, i.e., higher concentration in winter than in the other seasons. It is worth mentioning that the carbonaceous and ionic species are the primary chemical compositions of particles, accounting for approximately 70% of the mass of particles (Sardar et al., 2005). In this study, the concentration of analyzed components in FPs accounted for approximately 46.7–74.0% of the mass concentrations monitored by BAM at the US Embassy. The lowest proportion was in summer when frequent rain was observed at the sampling site. A good correlation was found between the measured FPs concentration in this study and the data from the US Embassy (r = 0.89). This result suggests that it is reliable to use the total concentration of analyzed species to observe the seasonal variation in the study area.

The highest concentration of $PM_{0.1}$ was observed in winter (3.24 ± 1.25 μg/m^3), followed by STP (2.65 ± 1.36 μg/m^3), summer (1.91 ± 0.46 μg/m^3), and WTP (1.65 ± 0.61 μg/m^3). Similarly, the level of $PM_{2.5}$ was highest in winter (49.2 ± 21.9 μg/m^3), approximately 4.5 times higher than in summer (10.9 ± 3.53 μg/m^3), 2.4 times higher than in STP (20.9 ± 14.3 μg/m^3), and 1.5 times higher than in WTP (31.7 ± 11.9 μg/m^3). The higher concentration of $PM_{0.1}$ and $PM_{2.5}$ in winter indicated that stable weather conditions possibly affected the concentration of particles. The stable atmospheric conditions (low mixing height, low temperature, and less rain) normally allow the accumulation of air pollution and hinder the dilution processes, leading to a considerably high level of air pollutants. The concentration of $PM_{0.1}$ followed the order of winter > STP > WTP > summer. Meanwhile, $PM_{2.5}$ was highest during winter > WTP > STP > summer. The higher concentration of $PM_{2.5}$ in WTP than in STP was due to the significant increase of ionic species, particularly the concentrations of SNA. It may be due to the drizzle-like weather conditions associated with a high humidity during the WTP sampling, which promoted $PM_{2.5}$ formation by secondary processes on the aerosol surface (Huyen et al., 2021).

The $PM_{0.1}$ concentration at the AS fluctuated slightly, while a significant variation was observed in the $PM_{2.5}$ concentration. It may be explained by the stable emission sources of $PM_{0.1}$ and the different removal processes of $PM_{0.1}$ and $PM_{2.5}$, which depend primarily on the particle size. While bigger particles such as PM_{10} might be removed easily by gravitational forces, FPs ($PM_{2.5}$) are difficult to settle and remove mainly by wet processes. In contrast, the removal and transport of $PM_{0.1}$ was affected by a combination of dilution, evaporation, and coagulation (Jacobson et al., 2005). According to Holmes (2007), UFPs can grow to bigger sizes under suitable conditions, such as the availability of solid surfaces, the presence of VOCs, and favorable weather conditions, leading to the variation of UFPs concentration. However, it may not vary significantly between seasons due to the stable emission of UFPs from the local sources and the minor effect of long-range transportation. Therefore, particles can grow to bigger sizes under suitable conditions, such as the presence of VOCs and favorable weather conditions, leading to a temporary variation in $PM_{0.1}$ concentrations. However, it may not vary significantly due to the stable emission sources of $PM_{0.1}$. These lead to a variation of the particle lifetime, i.e., PM_{10} and $PM_{0.1}$ are not transported over long distances and removed after days or even minutes, while $PM_{2.5}$ may remain in the ambient air for a longer time, from days to weeks (Rönkkö et al., 2018).

The $PM_{2.5}$ concentrations of measured components in this study were lower than the mean $PM_{2.5}$ concentration collected by BAM from the US Embassy. It might be explained by the other components which were not included in this study. However, data from both sources show a similar trend of variation, i.e., higher concentration in winter than in other seasons.

It is worth mentioning that the carbonaceous and ionic species are major chemical components of particles, accounting for approximately 70% of the mass concentration (Sardar et al., 2005). The highest concentrations of both $PM_{0.1}$ and $PM_{2.5}$ in winter indicate that stable weather conditions possibly affected the concentration of particles. The stable atmospheric conditions normally allow the accumulation of air pollution and hinder the dilution process, leading to a high level of pollutants. The $PM_{0.1}$ concentration follows the orders: winter > STP > WTP > summer. Meanwhile, the $PM_{2.5}$ level was winter > WTP > STP > summer. The higher concentration of $PM_{2.5}$ in WTP than in STP was caused by the significant increase of ionic species, particularly the SNA concentrations. It may be explained by the drizzle-like weather conditions associated with high humidity during WTP, which promotes the $PM_{2.5}$ formation by secondary processes on the aerosol surface (Huyen et al., 2021).

Table 5.4 Average concentrations of chemical compositions in UFPs and FPs at the AS

	UFPs at the AS				FPs at the AS			
	Summer (n=15)	STP (n=14)	Winter (n=12)	WTP (n=14)	Summer (n=15)	STP (n=14)	Winter (n=12)	WTP (n=14)
	Ave. ± S.D.[a]	Ave.± S.D.	Ave.± S.D.	Ave.± S.D.	Ave. ± S.D.	Ave.± S.D.	Ave.± S.D.	Ave.± S.D.
OC ($\mu g/m^3$)	1.22 ± 0.31	1.69 ± 0.77	1.97 ± 0.73	1.05 ± 0.31	3.77 ± 0.78	8.59 ± 6.55	14.7 ± 5.78	6.05 ± 1.96
EC ($\mu g/m^3$)	0.29 ± 0.11	0.41 ± 0.26	0.44 ± 0.23	0.24 ± 0.10	1.85 ± 0.49	2.94 ± 2.0	5.14 ± 1.96	2.79 ± 0.98
TC ($\mu g/m^3$)	1.51 ± 0.40	2.10 ± 1.03	2.41 ± 0.96	1.29 ± 0.40	5.62 ± 1.21	11.5 ± 8.53	19.8 ± 7.69	8.84 ± 2.88
WSOC ($\mu g/m^3$)	0.66 ± 0.17	0.87 ± 0.42	1.19 ± 0.36	0.61 ± 0.20	1.86 ± 0.78	4.06 ± 3.14	8.16 ± 3.16	4.61 ± 1.70
WIOC($\mu g/m^3$)	0.56 ± 0.20	0.82 ± 0.36	0.78 ± 0.41	0.44 ± 0.17	1.91 ± 0.79	4.53 ± 3.45	6.53 ± 2.93	1.43 ± 0.96
Cl^- ($\mu g/m^3$)	0.014 ± 0.02	0.008 ± 0.003	0.024 ± 0.01	0.010 ± 0.003	0.24 ± 0.21	0.34 ± 0.34	1.49 ± 0.91	1.37 ± 0.60
SO_4^{2-} ($\mu g/m^3$)	0.16 ± 0.07	0.21 ±0.15	0.24 ± 0.12	0.11 ± 0.08	2.67 ± 1.39	3.87 ± 2.16	10.2 ± 4.98	8.52 ± 3.47
NO_3^- ($\mu g/m^3$)	0.08 ± 0.08	0.12 ± 0.05	0.26 ± 0.09	0.12 ± 0.10	0.71 ± 0.41	1.95 ± 1.85	9.24 ± 6.06	6.32 ± 3.78
Na^+ ($\mu g/m^3$)	-[b]	-	-	-	-	0.06 ± 0.08	0.08 ± 0.09	0.21 ± 0.29
NH_4^+ ($\mu g/m^3$)	0.08 ± 0.04	0.17 ± 0.12	0.25 ± 0.09	0.11 ± 0.08	1.32 ± 0.71	1.48 ± 1.21	5.67 ± 2.84	5.73 ± 2.03
K^+ ($\mu g/m^3$)	-	0.009 ± 0.014	0.009 ± 0.012	-	0.15 ± 0.07	0.52 ± 0.37	0.89 ± 0.34	0.36 ± 0.31
Mg^{2+} ($\mu g/m^3$)	-	-	-	-	0.015 ± 0.004	0.14 ± 0.05	0.22 ± 0.18	0.05 ± 0.03
Ca^{2+} ($\mu g/m^3$)	0.06 ± 0.09	0.03 ± 0.01	0.04 ± 0.01	0.004 ± 0.004	0.20 ± 0.06	0.96 ± 0.79	1.57 ± 1.45	0.28 ± 0.20
Total conc.[c] ($\mu g/m^3$)	**1.91 ± 0.46**	**2.65 ± 1.36**	**3.24 ± 1.25**	**1.65 ± 0.61**	**10.9 ± 3.53**	**20.9 ± 14.3**	**49.2 ± 21.9**	**31.7 ± 11.9**
$PM_{2.5}$ conc.[d] ($\mu g/m^3$)					**23.3**	**40.1**	**69.3**	**45.1**

[a] Average concentration ± Standard deviation
[b] Below detection limit
[c] Sum of the analyzed components
[d] Mean $PM_{2.5}$ concentrations collected by BAM from the US Embassy

5.3.2.2 Seasonal variation of carbonaceous components

Table 5.4 illustrates the OC and EC concentrations in UFPs and FPs during the four sampling periods at AS. The highest concentrations of OC and EC in UFPs were found in winter, followed by STP, summer, and WTP. Similarly, the concentration of those components in FPs was higher in winter and STP and lower in WTP and summer. This result was consistent with the study in Japan by Kim et al. (2011), which indicated higher concentrations of OC and EC in winter and fall (dry season) than in spring and summer. The concentrations of TC in UFPs were 1.51 ± 0.40, 2.10 ± 1.03, 2.41 ± 0.96, and 1.29 ± 0.40 μg/m^3 in summer, STP, winter, and WTP, respectively. In FPs, the concentrations of TC were 5.62 ± 1.21 μg/m^3 in summer, 11.5 ± 8.53 μg/m^3 in STP, 19.8 ± 7.69 μg/m^3 in winter, and 8.84 ± 2.88 μg/m^3 in WTP. TC accounted for approximately 75%–79% of the measured components in UFPs and 28%–55% in FPs, indicating that carbonaceous components were dominant in both particle sizes, particularly in UFPs. The relative contributions of OC and EC to TC in UFPs were virtually unchanged during different seasons, suggesting stable emission sources such as the automobile and motorcycle exhaust. The highest fraction of OC in TC was 82% during winter, while the lowest was 80% during STP. The EC accounted for a lower fraction in the TC of approximately 18%–20% than the OC. Similarly, OC accounted for a higher proportion than EC in FPs, e.g., the contributions of OC and EC to TC were approximately 67%–74% and 26%–33%, respectively.

The average char-EC and soot-EC concentrations in UFPs and FPs in the different sampling periods are shown in Table 6. The mean concentration of soot-EC in UFPs for all the sampling periods was 0.26 ± 0.12 μg/m^3, while that for char-EC was 0.08 ± 0.09 μg/m^3. In contrast, the average char-EC concentration for the four seasons in FPs was 2.65 ± 1.91 μg/m^3, significantly higher than soot-EC of 0.53 ± 0.17 μg/m^3. Soot-EC was more dominant in UFPs, while char-EC accounted for a higher fraction in FPs. The char-EC and soot-EC concentrations in UFPs tended to increase from summer to winter (Figure 5.5-a). Char-EC in FPs showed a similar variation as char-EC and soot-EC in UFPs, indicating that biomass and coal combustion associated with the adverse weather conditions might contribute to the higher char-EC concentration during winter. Meanwhile, soot-EC in FPs reached the highest level in summer and remained relatively stable during other seasons (Figure 5.5-b). A similar result was reported in Japan, where a higher concentration of soot-EC in FPs observed during the summer (Kim et al., 2011).

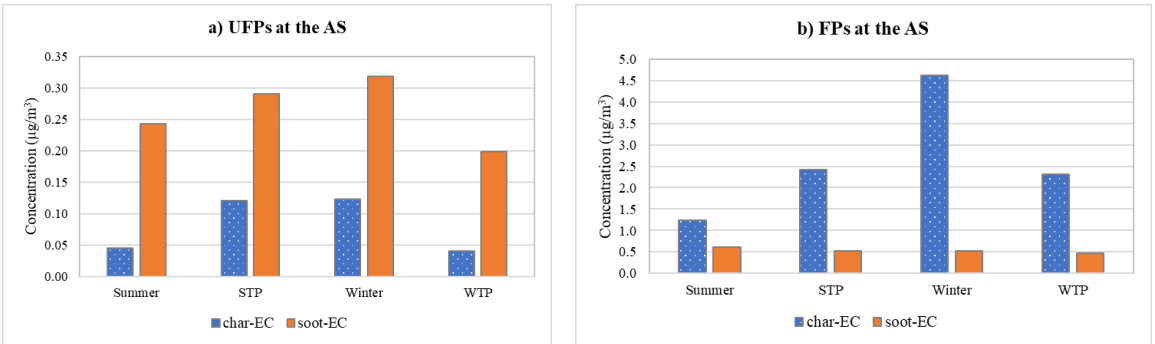

Figure 5.5 Char-EC and soot-EC concentrations in UFPs and FPs at AS

The OC/EC ratio could suggest the possible emission sources and secondary particle formation. In this study, the mean OC/EC ratios of UFPs and FPs for the four sampling periods were 4.87 ± 1.60 (range 2.71–11.4) and 2.50 ± 0.51 (range 1.58–3.73). The

carbonaceous ratios in this study implied the possible emission sources in the study area, i.e., vehicular exhaust, biomass burning, coal combustion, cooking activities, and secondary sources. This result is consistent with the previous studies of the primary emission sources in Hanoi, which were local combustion and traffic-related emissions (vehicle/road dust) (Hien et al., 2004) and automobile, secondary sulfate aerosol, and industry (Cohen et al., 2010).

Table 5.5 shows the OC/EC ratios in UFPs and FPs at AS during the different sampling periods. The OC/EC ratio was lower in summer and WTP and higher in STP and winter in both UFPs and FPs. The higher ratio of OC/EC during winter was also reported elsewhere, such as in Shanghai, China (Feng et al., 2009) and Agra, India (Pachauri et al., 2013). It may be affected by the adverse weather conditions during winter promoting SOA formation. The ratio of char-EC/soot-EC is used to identify the emission sources to avoid the significant bias caused by SOA formation. According to Han et al. (2009), the char-EC/soot-EC ratio of vehicular exhaust, including diesel and gasoline emissions, was lower than 1.0, and coal and biomass burning were 1.9 and more than 10, respectively. A wide range of char-EC/soot-EC ratios for UFPs (0–1.39) and FPs (0.18–22.6) were found in this study, suggesting mixed emission sources including vehicular exhaust, coal combustion, and biomass burning.

The char-EC/soot-EC ratios fluctuated more than the OC/EC ratios, e.g., the char-EC/soot-EC ratio for FPs in winter was approximately fourfold higher than that in summer while OC/EC ratio was virtually unchanged (Table 5.5). The char-EC/soot-EC ratio for FPs was highest in winter (9.37 ± 5.31), followed by WTP (5.13 ± 2.49), STP (4.57 ± 3.70), and summer (2.40 ± 1.75), suggesting the contribution of biomass burning or coal combustion during winter. In contrast, the char-EC/soot-EC ratios for UFPs were similar in WTP and summer (approximately 0.18) and higher in STP (0.34 ± 0.39) and winter (0.35 ± 0.28). The different trends of the char-EC/soot-EC ratios between FPs and UFPs may be due to the char and soot characteristics. Char-EC is formed by the solid residues of combustion and is composed of relatively larger particles, whereas soot-EC is formed through high-temperature condensation of gases and is composed of submicron particles (Han et al., 2009), leading to different residence times, transport mechanisms, and removal processes of particles.

Table 5.5 OC/EC ratios, concentrations of char-EC, soot-EC, and char-/soot-EC ratio in UFPs and FPs at the AS

		OC/EC	Char-EC ($\mu g/m^3$)	Soot-EC ($\mu g/m^3$)	Char-/soot-EC
UFPs at the AS	Summer	4.72 ± 1.55	0.05 ± 0.04	0.24 ± 0.09	0.18 ± 0.14
	STP	5.10 ± 2.35	0.12 ± 0.14	0.29 ± 0.14	0.34 ± 0.39
	Winter	5.05 ± 1.33	0.12 ± 0.09	0.32 ± 0.16	0.35 ± 0.28
	WTP	4.60 ± 0.92	0.04 ± 0.04	0.20 ± 0.06	0.18 ± 0.15
FPs at the AS	Summer	2.04 ± 0.34	1.24 ± 0.48	0.61 ± 0.21	2.40 ± 1.75
	STP	2.92 ± 0.45	2.41 ± 1.99	0.53 ± 0.08	4.57 ± 3.70
	Winter	2.86 ± 0.33	4.62 ± 1.97	0.52 ± 0.10	9.37 ± 5.31
	WTP	2.19 ± 0.34	2.31 ± 0.99	0.48 ± 0.11	5.13 ± 2.49

Values are written as Average concentration ± Standard deviation

The correlations of char-EC, soot-EC and OC and EC were examined to investigate the relationships between these components (Figure 5.6). The strongest association was found between char-EC and EC in FPs for all the seasons (r = 0.997), indicating the significant contribution of char-EC in FPs. A strong relationship was also found between char-EC and OC (r = 0.96), while no correlation was between soot-EC and OC and EC. In contrast, char-EC showed moderate correlations (r = 0.88–0.89) with EC and OC in UFPs. A moderate correlation (r = 0.83) was found between soot-EC and OC, while a good relationship (r = 0.94) was observed between soot-EC and EC. This result implies that soot-EC dominated the EC fraction in UFPs, and OC and EC came from vehicular exhausts. The findings in this study were consistent with previous studies by Han et al. (2009) for China and Kim et al. (2011) for Japan. In addition, the growth of particles due to the condensation of secondary ions on soot particles led to the reduction of the soot-EC concentration. It explained the higher ratio of char-EC/soot-EC in STP and winter and the moderate relationship between OC, a carbonaceous fraction formed by both primary and secondary conversion processes, and soot-EC in UFPs.

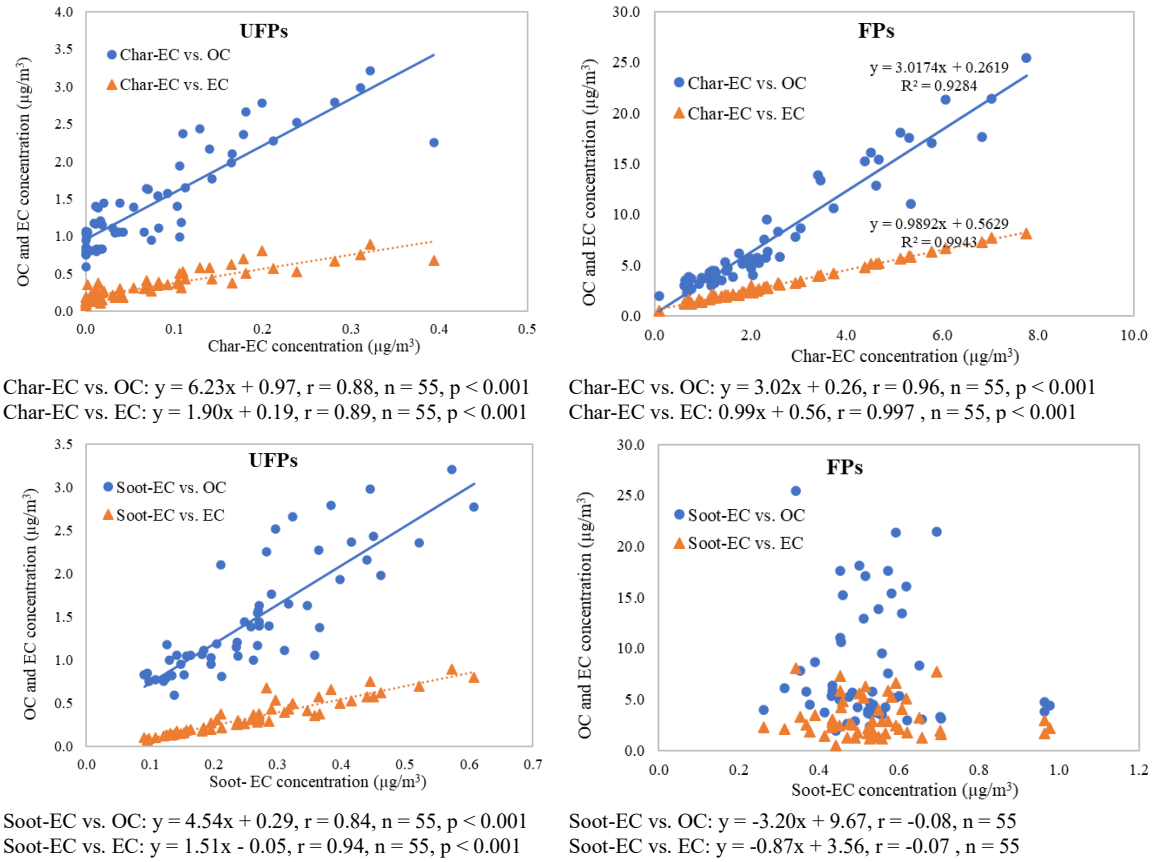

Char-EC vs. OC: y = 6.23x + 0.97, r = 0.88, n = 55, p < 0.001
Char-EC vs. EC: y = 1.90x + 0.19, r = 0.89, n = 55, p < 0.001

Char-EC vs. OC: y = 3.02x + 0.26, r = 0.96, n = 55, p < 0.001
Char-EC vs. EC: 0.99x + 0.56, r = 0.997 , n = 55, p < 0.001

Soot-EC vs. OC: y = 4.54x + 0.29, r = 0.84, n = 55, p < 0.001
Soot-EC vs. EC: y = 1.51x - 0.05, r = 0.94, n = 55, p < 0.001

Soot-EC vs. OC: y = -3.20x + 9.67, r = -0.08, n = 55
Soot-EC vs. EC: y = -0.87x + 3.56, r = -0.07 , n = 55

Figure 5.6 The relationships between OC, EC and char-EC, soot-EC in UFPs and FPs

5.3.2.3 Seasonal variation of ionic species

The seasonal variations of ion concentrations in UFPs and FPs are shown in Figure 5.7. Ionic species accounted for approximately 43%–72% of the analyzed components in FPs and 21%–25% in UFPs. This result indicates that the carbonaceous fraction was more dominant in UFPs, whereas carbonaceous and ionic species were important in FPs. The average concentrations of ionic species in UFPs were 0.41 ± 0.22 µg/m^3 in summer, 0.55 ± 0.34 µg/m^3 in STP, 0.82 ± 0.32 µg/m^3 in winter, and 0.36 ± 0.26 µg/m^3 in WTP. In FPs, the mean

concentrations of ions were 5.30 ± 2.46, 9.32 ± 6.24, 29.4 ± 15.5, and 22.8 ± 9.46 μg/m^3 in summer, STP, winter, and WTP, respectively. The total concentration of ionic species in UFPs increased from summer to winter and declined in WTP when the lowest concentration was recorded. Meanwhile, the mean concentration of ions in FPs reached a peak in winter, followed by WTP, STP, and summer. The daily variations of ionic species are shown in Figure 5.8. Both particle sizes showed fluctuation in ion concentrations during STP and winter. During summer and WTP, a milder daily variation was observed, particularly in FPs.

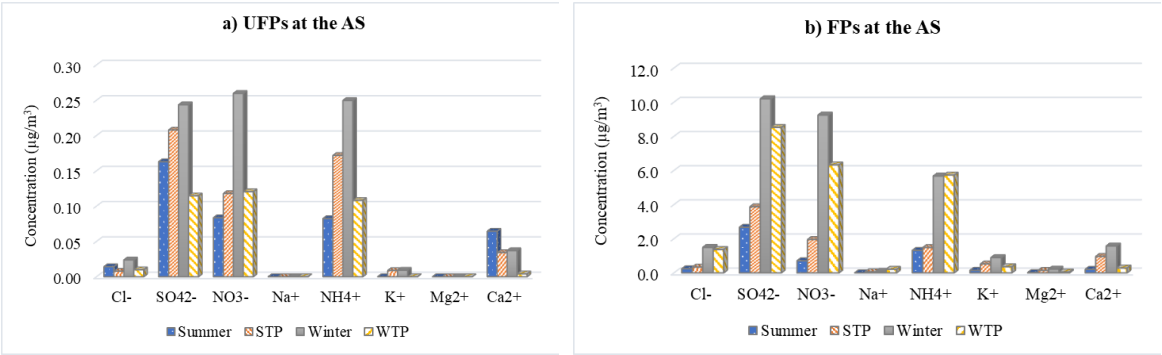

Figure 5.7 Seasonal variations of ion concentrations in UFPs and FPs at the AS

Figure 5.8 Daily variation of ionic species in UFPs and FPs at the AS

In general, the concentration of ionic species in both UFPs and FPs was ranked in following order: $SO_4^{2-} > NO_3^- > NH_4^+ > Ca^{2+} > Cl^- > K^+$. Mg^{2+} and Na^+ were not detected in the UFPs samples and accounted for a minor proportion of the total concentration of ionic species in FPs. SNA were three major ions contributing approximately 80–90% of the total ionic

species concentration in both particle sizes. The large proportion of SNA indicates the contribution of ion condensation to UFPs and FPs. According to Dai et al. (2021), the SNA species appeared in a wide range of particle sizes, from ultrafine to the mode between 0.18 and 0.6 μm (the subclass of FPs). The primary particles emitted from the engines are majority carbonaceous compounds in the solid phase, and may also contain ash, and adsorbed or condensed sulfur compounds (Morawska et al., 2008). The condensation of the hot exhaust gases emitted from vehicles could form the secondary particles, which are in the ultrafine mode of less than 30 nm and contain mainly hydrocarbons and hydrated sulfuric acid (Morawska et al., 2008). Furthermore, transformations of precursor gases (SO_2, NO_x) to secondary ions (SO_4^{2-}, NO_3^-. NH_4^+) in the atmosphere are crucial to the secondary formation of particles. The condensation of secondary ionic species on freshly emitted particles could lead to the growth of particles from ultrafine to the fine size range.

In UFPs, the mean concentration of SNA tended to increase from summer to winter and then lowered in WTP. The SNA concentrations in UFPs were 0.33 ± 0.14 μg/m^3 in summer, 0.50 ± 0.32 μg/m^3 in STP, 0.75 ± 0.31 μg/m^3 in winter, and 0.34 ± 0.26 μg/m^3 in WTP. In contrast, the mean concentration of SNA in FPs was lowest in summer at 4.70 ± 2.41 μg/m^3, while that was approximately twofold in STP of 7.31 ± 4.98 μg/m^3, fourfold in WTP of 20.6 ± 8.75 μg/m^3, and fivefold in winter of 25.1 ± 13.6 μg/m^3. The high concentration of SNA species in both particle sizes indicates the contribution of secondary formations. Higher concentrations in winter might result from the oxidation of precursor gases such as SO_2 and NO_x from vehicular exhaust or industry under the stagnant condition of the atmosphere, which lengthened the reaction time and hindered the dispersion of the air pollutants. A study by Sakamoto et al. (2018) indicated that Hanoi's NO_2 and NOx concentrations increased from summer to winter. Furthermore, the higher NO_2 and SO_2 concentrations were higher at traffic and industry hotspots, and the background NO_2 concentration was highest in the populated area, downtown Hanoi (Hien et al., 2014).

WSOC and WIOC accounted for approximately equal fractions of OC in summer and STP in both particle sizes. Meanwhile, the concentration of WSOC was higher than that of the WIOC during winter and WTP, e.g., the concentration of WSOC in FPs during WTP was 4.61 ± 1.70 μg/m^3, which was threefold higher than WIOC concentration. The seasonal variation of WSOC concentration was similar to the total ionic species in both particle sizes. In UFPs, the variation of WSOC followed the pattern: winter > STP > summer > WTP, and that in FPs was winter > WTP > STP > summer. The variability in the WIOC concentration in FPs was the same as that of WSOC in UFPs, while that in UFPs was STP > winter > summer > WTP. The correlations between WSOC and secondary ions (SO_4^{2-}, NO_3^-, and NH_4^+) and inorganic tracer of biomass burning (K^+) were examined to identify the sources of the WSOC (Table 5.6). WSOC correlated well with secondary ions in STP, winter, and WTP, particularly sulfate ions in UFPs during STP (r = 0.99). This result indicates that WSOC might be formed by secondary processes and condensed in the atmosphere, similar to SNA ions. In summer, poor correlation coefficients (r < 0.3) were found between WSOC and other ions. The frequent rain may explain it during the summer sampling (11 per 15 sampling days), which promoted washout and rainout in the atmosphere. A strong relationship was found between WSOC and K^+ in FPs during STP (r = 0.98) and winter (r = 0.90), while a moderate relationship was found in WTP and a negative correlation coefficient in summer. A higher correlation coefficient was found in UFPs during STP than during winter. In contrast, no K^+ was recorded in the summer and WTP. The significant correlation between WSOC and K^+ demonstrates that combustion activities may contribute to the WSOC level in FPs during STP and winter. In addition, moderate and good association (r =

0.7–0.92) between WIOC and soot-EC in UFPs was found in all the seasons, while no relationship was observed in FPs (Table 5.7). This result implies that WIOC and soot-EC could be products from the exhaust gases of the fuels and oils of vehicles. Therefore, particles were stably emitted from vehicles such as automobiles and motorcycles. Biomass burning and secondary sources also contributed to the UFPs and FPs levels in the sampling sites. The condensation of chemical components in the atmosphere may lead to new UFPs that may grow to the fine size range. Notably, those emission sources were marked as predominant sources in Hanoi, also mentioned in other studies (Hai & Kim Oanh, 2013; Hien et al., 2004; Hopke et al., 2008; Nghiem et al., 2020).

The correlations between WSOC and SNA and inorganic tracer of biomass burning (K^+) show that WSOC might be formed by secondary processes and condensed in the atmosphere similar to SNA ions. In summer, very poor correlation coefficients were found between WSOC and other ions ($r < 0.3$). It might be explained by the frequent rain observed during summer sampling (11 per 15 sampling days) which promoted the washout and rainout processes. The significant correlation between WSOC and K^+ ($r > 0.9$) demonstrates that combustion activities might contribute to the WSOC level in FPs during STP and winter. In addition, the moderate and very good relationships between WIOC and soot-EC in UFPs were found in all seasons ($r = 0.7 – 0.92$) while there was no relationship was observed in FPs. This result implies that both WIOC and soot-EC could be the products in the exhaust gases caused by fuels and oils of vehicles. Therefore, it hypothesized that particles were stably emitted from vehicles such as automobiles and motorcycles. Biomass burning and secondary sources also contributed to the UFPs and FPs levels in the sampling site. The condensation of chemical components in the atmosphere might lead to the formation of new particles in ultrafine mode and the growth to the fine size range. It should be noted that those sources were marked as predominant sources in Hanoi, which were mentioned in other studies (Hai & Kim Oanh, 2013; Hien et al., 2004; Hopke et al., 2008; Nghiem et al., 2020).

Table 5.6 Correlation coefficient (r) between WSOC and ionic species in UFPs and FPs at the AS

	WSOC in UFPs				**WSOC in FPs**			
	Summer	STP	Winter	WTP	Summer	STP	Winter	WTP
SO_4^{2-}	0.27	**0.99**	**0.91**	**0.80**	0.30	**0.77**	**0.90**	0.69
NO_3^-	0.27	**0.91**	**0.89**	**0.77**	-0.16	**0.91**	**0.79**	**0.82**
NH_4^+	0.25	**0.97**	**0.94**	**0.84**	0.26	0.62	**0.85**	**0.77**
K^+	-	**0.88**	0.41	-	-0.21	**0.98**	**0.90**	**0.75**

Bold values indicated $p < 0.01$

Table 5.7 Correlation coefficient (r) between WIOC and carbonaceous components in UFPs and FPs at the AS

	WSIC in UFPs				WIOC in FPs			
	Summer	STP	Winter	WTP	Summer	STP	Winter	WTP
OC	**0.88**	**0.98**	**0.95**	**0.86**	0.51	**0.99**	**0.94**	0.50
EC	0.70	**0.95**	**0.85**	**0.76**	0.44	**0.98**	**0.93**	0.38
Char-EC	0.32	**0.82**	**0.92**	0.70	0.57	**0.97**	**0.93**	0.37
Soot-EC	0.71	**0.92**	0.70	0.73	-0.28	0.25	0.07	0.03

Bold values indicated $p < 0.01$

5.3.3 Relationship between particles from RS and AS

5.3.3.1 Difference in UFPs concentration at the RS and AS

The total concentration of the measured components in UFPs differed between the RS and AS in three seasons, summer, STP, and winter. In general, slightly higher concentrations of the analyzed components were found in the samples at the RS (Figure 5.9). For example, UFPs at the RS had higher concentrations of EC than the AS in all sampling periods (Figure 5.9). Suppose the traffic emissions at the RS (emissions by vehicles from Tran Dai Nghia St.) were hypothesized as a single emission source in the sampling site, and there were no other significant sources during the sampling periods. In that case, the samples at the AS could be affected by traffic emissions at the RS. According to Zhu et al. (2002), the total particle number concentration in the size range of 6 to 25 nm, which accounted for approximately 70% of the total UFPs number concentration, dropped sharply to around 80% after 100 m. Particles in the size range of 25–50 and 50–100 nm decreased and approached the background concentration at approximately 150 m from the emission point. The study by Jeong et al. (2015) found a gradual decrease of non-volatile particles, and the effect of the emissions was still apparent at a distance of 300 m. Fujitani et al. (2012) also reported that both mass and particle number concentration exponentially declined with distance from the traffic emission source. Since the distance between the RS and AS in this study was approximately 200 m, the exponential decrease in the concentration of UFPs at the AS was expected to observe. However, the total concentrations of measured components and the levels of single composition in UFPs at the AS varied slightly compared with UFPs samples from the RS. The emissions from two other main roads (Dai Co Viet and Giai Phong St.) and other sources, such as biomass or coal burning, and cooking activities in the surrounding areas may provide a reason for the concentration differences. Further studies should be conducted to measure the concentration and chemical compositions in UFPs and FPs at increasing distances from major roads in the study area to clarify the contribution of traffic-related emission sources.

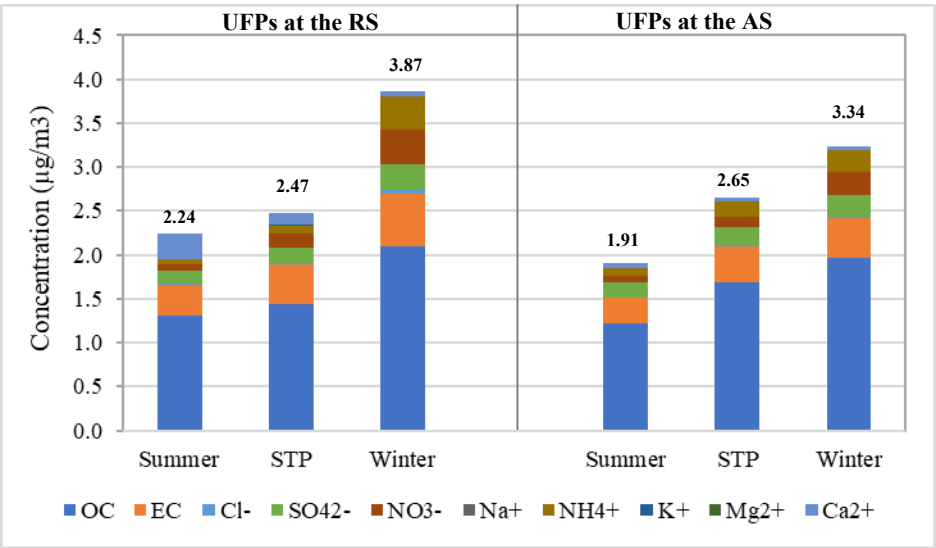

Figure 5.9 Comparison of UFPs concentration between the RS and AS in different seasons

5.3.3.2 Possibility of particle growth

The relationship between carbonaceous components and secondary ions (SNA) in UFPs from RS and FPs from AS was examined to assess the transport of particles and their growth processes in different microenvironments. Table 5.8 shows the relationship between major components (OC, EC, and SNA) from those two sites. An exceptional relationship was seen only during winter and the transitional period, while low correlations were found for all components in summer, except ammonium. A moderate correlation was found between OC in UFPs at RS and FPs at AS during STP ($r = 0.89$) and winter ($r = 0.85$); it was very low in summer ($r = 0.36$). A similar trend was observed in the relationship of EC between these two sampling sites. In contrast, the relationships of SNA from the UFPs and FPs from RS and AS differed. A moderate correlation coefficient ($r = 0.63–0.72$) was found in winter for SNA. In other sampling periods (summer and STP), the relationship of sulfate between the two sites was unchanged ($r = 0.53$), suggesting the stable development of this ion irrespective of the season change. However, a very poor correlation ($r = 0.18$) was found in the nitrate relationship during summer. In contrast, the ammonium in UFPs at RS correlated better with FPs at AS in summer ($r = 0.64$) than in the transitional period ($r = 0.45$). In general, moderate and poor relationships of each component between UFPs at the RS and FPs at the AS were found. A number of reasons may lead to the poor correlations between chemical components in two particle sizes, including the sources and spatial differences, and the contribution of particle growth. Under a high concentration of UFPs and other pollutants (SO_2, NO_x, VOCs) in Hanoi (Hien et al., 2014; Thuy et al., 2018), which means the presence of large surface area and the availability of gas-phase pollutants, the evolution of particles is possibly found (Holmes, 2007). The effect of emission sources of UFPs and FPs, and the spatial difference may be significant. However, based on the chemical compositions and their relationships in particle sizes, we initially investigated the possibility of particle growth in this area. Further investigation is needed to explain the contribution of particle growth to FPs concentrations. However, this result may be vital for investigating particle evolution under highly polluted conditions in big cities in Vietnam in the future.

Table 5.8 Correlation coefficient (r) of OC, EC and SNA between UFPs at RS and FPs at the AS

	UFPs at the RS vs. FPs at the AS		
	Summer (n=15)	STP (n=14)	Winter (n=14)
OC	0.36	**0.89**	**0.85**
EC	0.30	**0.89**	0.66
SO_4^{2-}	0.53	0.53	0.63
NO_3^-	0.18	0.72	**0.72**
NH_4^+	0.64	0.45	**0.70**

Bold values indicated $p < 0.01$

5.4 Conclusion

Higher concentrations of carbonaceous components in UFPs at the RS were found compared to at the AS and other published studies. A higher EC fraction, and the lower OC/EC ratio in UFPs at the RS indicate that the effect of the primary emissions such as vehicular exhausts might be more substantial than at the AS. The mean ratio of NO_3^-/SO_4^{2-} used to identify the relative contributions of the stationary and mobile sources was higher in UFPs at the RS, suggesting the contribution of traffic emissions.

The UFPs and FPs concentrations at the AS increased from summer to winter and dropped in the winter-to-summer transitional period. The adverse weather conditions (low mixing height, temperature inversion, less rain) may allow the accumulation of air pollutants, leading to higher concentrations of both particle sizes in winter. During two transitional periods, the concentration of UPFs was higher in STP than in WTP, while that of FPs was higher in WTP than in STP. The difference is probably due to secondary processes which formed FPs under drizzle and foggy conditions during the WTP sampling. This finding provides useful information for policy maker and stakeholders in building up the related policies and air pollution control measures, especially during highly polluted seasons.

Carbonaceous compounds (OC and EC) were the major components of particles, contributing up to 55% and 80% of the concentration of FPs and UFPs at the AS, respectively. The ratios of OC/EC and char-EC/soot-EC suggest that the possible emission sources in the study area were vehicular exhaust, biomass burning, coal combustion, cooking activities, and secondary sources. High levels of SO_4^{2-}, NO_3^-, and NH_4^+ were found in both UFPs and FPs, and the unique relationship between WSOC and SNA species suggested the influence of secondary particle formation.

Under the high concentration of UFPs and other presence of gas-phase pollutants in Hanoi, the relationships of OC, EC and SNA ions between the roadside UFPs and ambient FPs suggest the possibility of particle growth from ultrafine to the fine-size range. Further investigation should be conducted to evaluate and quantify the contribution of particle growth to the chemical composition and size distribution of particles.

Chapter 6

Chemical characterization of indoor and outdoor particles

6.1 Introduction

According to the World Health Organization (WHO, 2020), air pollution is a major environmental risk to human health. In 2016, there was an estimated 7 million deaths caused by outdoor and indoor air pollution while in 2012 was 6.5 million (WHO, 2016, 2020). The exposure and impact of air pollution are different in low-, middle-, and high-income countries. People in low- and middle-income countries are more vulnerable, accounting for more than 90% of fatalities caused by air pollution in 2016 (WHO, 2020). People in those countries have relied mainly on polluting cooking fuel which is one of the primary sources of indoor air pollution. According to WHO (2020), less than 20% of Africans in the WHO Region used clean cooking fuel while that was more than 90% in the European and Americas region. Besides, the high pollution levels from the outdoor environment could transport into the indoor environment by ventilation and infiltration airflows, leading to high concentrations of indoor pollutants.

In Vietnam, the high level of air pollution in big cities has been reported in the last some decades, particularly high concentrations of $PM_{2.5}$ caused poor or very poor air quality. According to Green Innovation and Development Centre GreenID (2018), in 2017, the levels of $PM_{2.5}$ in Hanoi exceeded the Vietnamese National Standard for annual $PM_{2.5}$ (25 $\mu g/m^3$) for 85 days compared to 14 days in Ho Chi Minh City. The high level of PM in the ambient air, together with other indoor emission sources are the reasons for poor indoor air quality. The high concentrations of indoor pollutants pose even higher risks to human health than outdoor ones because people spend approximately 90% of their time in indoor environments such as houses, offices, and schools. However, indoor air pollutants and indoor particles in Vietnam have not yet been paid attention to in comparison with outdoor particles. It is due to the limitation of monitoring data and the accessibility of field sampling.

Very few studies on indoor air pollution in Vietnam have been published, such as the study on the impact of incense burning on $PM_{2.5}$ concentration (Tran et al., 2021), indoor trace elements compositions in coarse, fine, and ultrafine particles in school environments (Tran et al., 2020), indoor trace elements and PAHs in the residential houses (Ha et al., 2020; Vo et al., 2022), parabens in indoor dust at private houses, laboratories, and medical stores (Tran et al., 2021) indoor particle number concentration in a household in Hanoi (Quang et al., 2017). A limited number of studies on ultrafine particles and their chemical components have been published. The effects of indoor and outdoor emission sources have not been comprehensively studied.

In this chapter, $PM_{2.5}$ and $PM_{0.1}$ were simultaneously collected in a residential house and an unused classroom in Hanoi during different seasons. The chemical components including the carbonaceous and ionic components were analyzed to observe the characteristics of indoor and outdoor particles. The relationships between indoor and outdoor emission sources were also investigated to understand the contribution of each emission source.

6.2 Methods

Two selected sampling sites were in Hanoi, including a residential house located in Truong Dinh St., Hoang Mai District (21˚28′59″N, 105˚24′49″E) and Hanoi University of Science and Technology (HUST), Hai Ba Trung District, Hanoi, Vietnam (21˚0′20″N, 105˚50′39″E). The distance between the two sampling sites is approximately 2 km. The sampling was done simultaneously at both sites during different seasons. The residential house is in Truong Dinh St., a two-traffic lanes (inbound and outbound) street. Both sides of the street have a pavement of about 1.5-2m in width and are bordered by residential buildings. At the residential house, the indoor (RI) and outdoor (RO) samples were monitored on the fourth floor of a terraced house, approximately 9m from the ground. (Figure 6.1). The AI sampling site is on the rooftop of a four-story building of the School of Materials Science and Engineering, HUST, approximately 11 m from the ground. This site is around 200 m from Dai Co Viet St., 250 m from Giai Phong St., 200 m from Tran Dai Nghia St., and surrounded by diverse institutional and residential areas (Figure 6.1). Devices in both sites were placed approximately 1.5m in height from the floor.

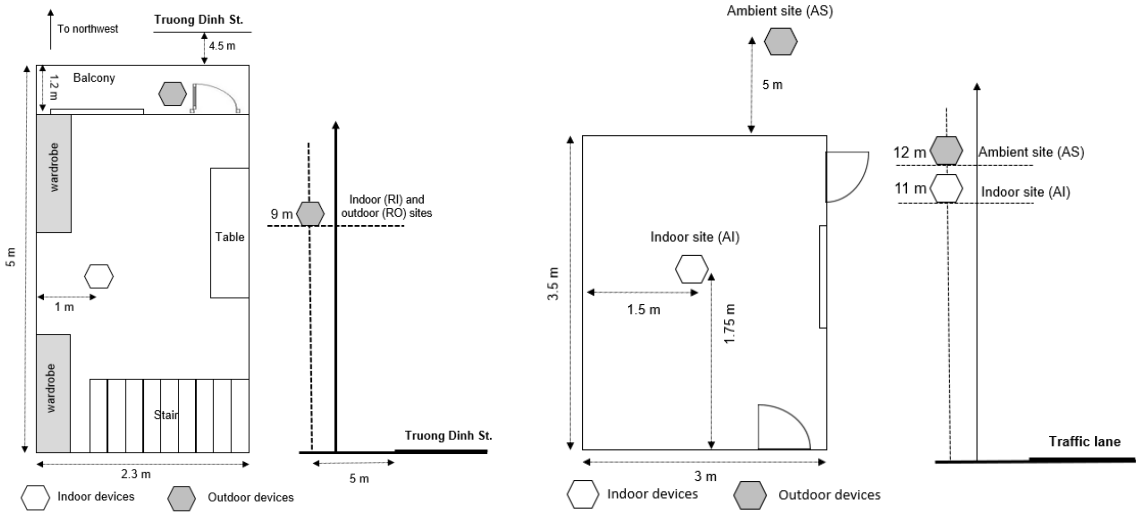

Figure 6.1 Sketch of sampling site at the residential house (a) and classroom (b)

At the residential house, the indoor (RI) and outdoor (RO) FPs samples were collected in summer (August 10 – 16), winter (December 2 – 15) in 2020, and both UFPs and FPs were collected in the summer of 2021 (July 9 – 24). The first sampling period in summer lasted only 6 days due to the covid-19 situation at the sampling site. At HUST, due to the limitation of the devices, only indoor (AI) UFPs were sampled in three different periods summer (August 10 – 24), winter (December 2 – 15) in 2020, and the transitional period from winter to summer 2021 (March 24 – April 7). The real-time data of $PM_{2.5}$, temperature and humidity were recorded by sensors at RI, AI, and AS during all sampling periods, except the final sampling in the summer of 2021. Furthermore, the data of hourly $PM_{2.5}$ measured by BAM from the AirNow website, the US Embassy located approximately 3.5 km from HUST, was also obtained.

$PM_{2.5}$ was collected by cyclone (URG-2000-30EH, University Research Glassware Corp., Chapel Hill, NC, USA), operated at a flow rate of 16 L/min while $PM_{0.1}$ was sampled by a Nanosampler (Model 3182, KANOMAX) at 40 L/min. Both $PM_{2.5}$ and $PM_{0.1}$ were collected

in 23.5 h by a quartz fiber filter (2500 QAT-UP, Pall Corp., USA), with a diameter of 55 mm for Nanosampler and 47 mm for cyclone. Further details of sampling devices and sampling methods were discussed in Section 3.2. $PM_{2.5}$ sensor (P-sensor, Industrial Hygiene Device Calibration, Inc.) was hung in the same place as other sampling devices and set up to get data every 10 seconds. The temperature and humidity in the sampling sites were also recorded by a thermo recorder (TR-72bwb, TECPEL CO., LTD.). The data of hourly $PM_{2.5}$ measured by BAM from AirNow, the US Embassy located approximately 3.5 km from HUST, was obtained as well to compare to the real-time data.

Carbonaceous and ionic species were analyzed for all indoor and outdoor samples. A 0.503 cm^2 punch-out filter was used to measure carbonaceous compounds by a carbon analyzer (DRI model 2001, Atmoslytic Inc., Calabasas, CA, USA). The Interagency Monitoring of Protected Visual Environments (IMPROVE) method was used to analyze OC and EC fractions (Chow et al., 2001). Ionic components were analyzed by ion chromatography (ICS-1600, Dionex Corp., Sunnyvale, CA, USA) and water-soluble organic carbon (WSOC) by a total carbon analyzer (Multi N/C 3100, Analytik Jena, Jena, Germany). Before analysis, the samples were extracted with 20 mL ultrapure water for 20 min in an ultrasonic bath. Details of carbonaceous and ionic species analysis were further discussed in Section 3.3.

6.3 Results and Discussion

6.3.1 $PM_{2.5}$ and meteorological data

$PM_{2.5}$ concentrations from the US Embassy and recorded by a P-sensor in this study show a similar trend of seasonal variation, which is higher in winter than in other seasons. The real-time $PM_{2.5}$ concentration in this study correlated well with the mean $PM_{2.5}$ concentration from the US Embassy (r = 0.67 – 0.86), except in winter (r = 0.54). The real-time data of indoor and outdoor $PM_{2.5}$ shows that indoor concentration was lower than outdoor in all seasons (Figure 6.2). The $PM_{2.5}$ concentration was significantly higher than the Vietnamese national standard for an annual average of 25 $\mu g/m^3$, except in summer. The $PM_{2.5}$ levels at RI were higher than at AI in both summer and winter. It may be due to the other emission sources at RI, such as cooking activities or incense burning, while there were no other indoor sources at AI. It should be noted that the indoor site at AI was an unused classroom at HUST. The real-time PM2.5 data collected by a sensor at the outdoor site at AS was consistent with data from the US Embassy, which were higher in winter than in other seasons.

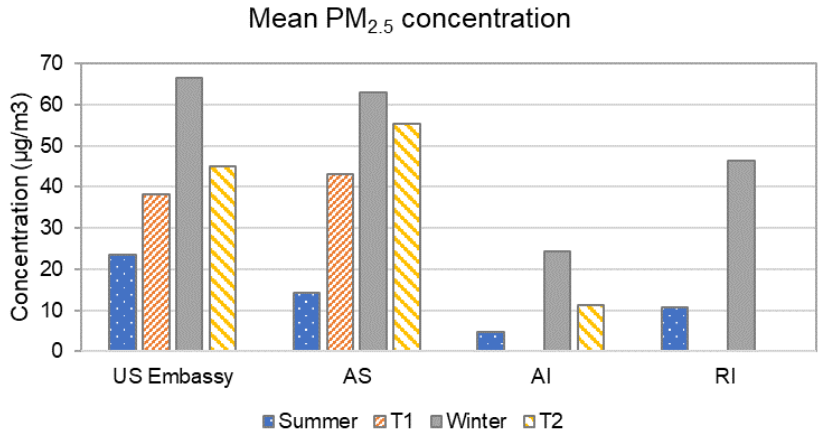

Figure 6.2 Mean $PM_{2.5}$ concentration at different sites

Temperature and humidity recorded by the thermos recorder at AS, AI, and RI are illustrated in Table 6.1. The variation in temperature and humidity among the sampling sites was insignificant. In contrast, it was a remarkable change in temperature and humidity in different seasons. Higher temperature and humidity, and frequent rainy days were observed in summer. Temperature and humidity gradually decreased from summer to winter, then increased in WTP. In winter, lower temperatures are associated with stable weather conditions (low mixing layer and less rain) may be the reason for the high $PM_{2.5}$ level.

Table 6.1 Meteorological conditions during the sampling periods

Season	AS		AI		RI		No. of rainy days	Wind speed (m/s)
	T (ºC)	H (%)	T (ºC)	H (%)	T (ºC)	H (%)		
Summer August 10 - 24, 2020	30.3	76.0	31.5	71.1	31.9	72.4	11/15	2.9 (0 – 7.2)
STP October 15 - 27, 2020	24.4	67.4					3/14	2.9 (0 – 7.2)
Winter December 02 - 15, 2020	20.6	62.8	22.1	58.3	21.4	54.3	2/14	2.9 (0 – 7.7)
WTP March 24 – April 07, 2021	25.2	82.1	26.7	76.8			4/14	3.1 (1 – 6.2)

T: Temperature
H: Relative humidity
No. of rainy days: Number of rainy days per total sampling days
Wind speed: Average wind speed and wind speed range

6.3.2 Indoor and outdoor particles at the residential house

6.3.2.1 FPs

The total concentration of analyzed components in FPs at RI was higher than at RO, and in winter than in summer (Figure 6.3). The total concentrations of FPs were 20.8 ± 11.5 μg/m^3, 37.4 ± 13.7 μg/m^3, 20.2 ± 4.2 μg/m^3 at RI and 15.6 ± 3.25 μg/m^3, 33.1 ± 14.9 μg/m^3, 13.9 ± 2.63 μg/m^3 at RO in summer 2020, winter 2020, and summer 2021, respectively. Indoor and outdoor FPs concentrations significantly varied between summer and winter. The concentration of FPs in winter was approximately twofold higher than in summer. The seasonal variation of indoor and outdoor FPs was similar to the FPs variation at AS, which was mentioned in Section 4.3.2 of this study. The higher concentrations of FPs during winter may be due to adverse weather conditions, such as low mixing layer, and less rain, which led to the accumulation of air pollutants and hinder the dilution. Furthermore, the similar variation of indoor and outdoor FPs may be explained by the air circulation between indoor and outdoor environments. In contrast, the FPs concentrations between the two sampling periods in the summer of 2020 and 2021 were insignificant fluctuations in both indoor and outdoor samples. This result implies stable emissions of particles in the sampling sites.

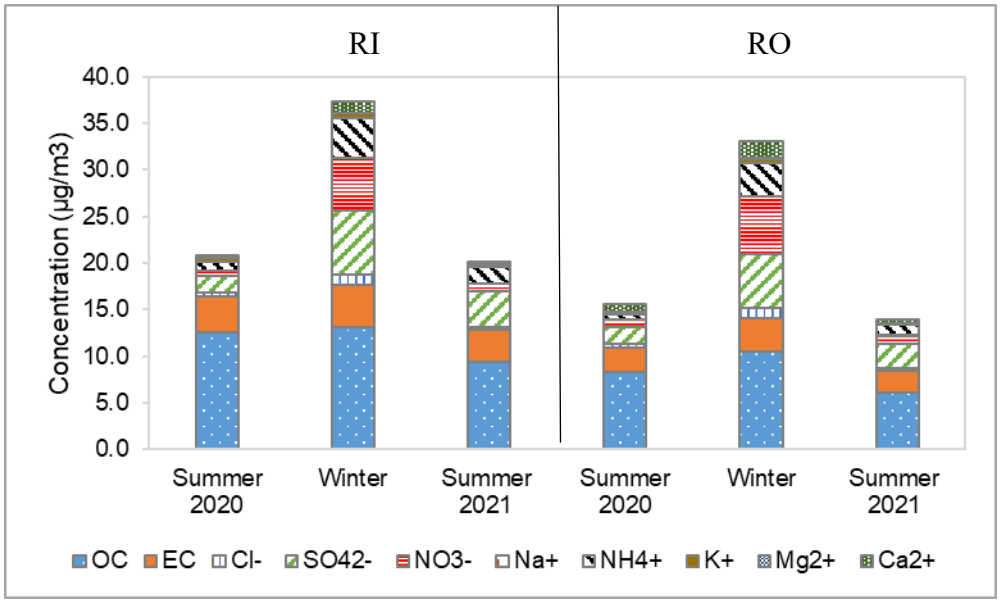

Figure 6.3 Concentration of carbonaceous and ionic species in FPs at RI and RO

The indoor/outdoor (I/O) ratio for the total concentration of FPs suggests the influence of indoor or outdoor emission sources. The I/O ratio of less than 1.0 presents the predominance of outdoor sources, while the ratio is higher than 1.0, indicating the influence of indoor sources. In this study, the average I/O ratios varied from 1.13 to 1.45, suggesting the contribution of indoor sources such as cooking and incense burning. The I/O ratio variation was insignificant between the summer and winter periods. The average I/O ratios were 1.28, 1.27, and 1.46 in summer 2020, winter 2020, and summer 2021. This result confirms the stable emission sources of particles at RI and RO. The daily variation in the I/O ratio shows that the indoor emission sources remarkably influenced the ratio (Figure 6.4). The high I/O ratio was recorded when burning incense in the residential house. The indoor FPs concentration significantly increased during the incense burning event, particularly the OC concentration. For example, the OC concentration was 16.6 µg/m^3 on the incense burning day compared to the average OC concentration of 9.34 µg/m^3.

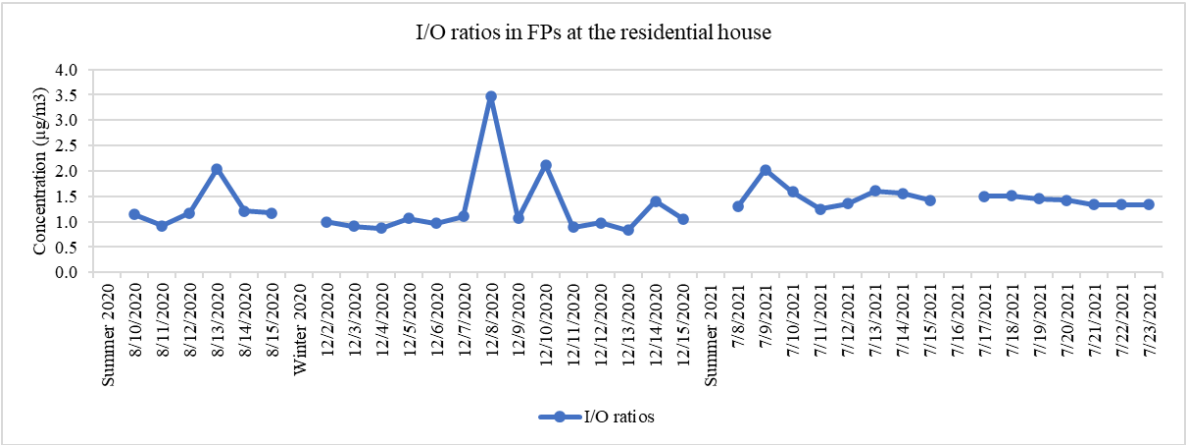

Figure 6.4 The daily variation of I/O ratio at the residential house

Table 6.2 illustrates the concentrations of carbonaceous compounds and their ratios in FPs at RI and RO. The TC concentration was higher at RI than RO in both seasons. However, the contribution of each carbon fraction to the TC concentration was similar in both sites and seasons. OC and EC accounted for approximately 72 – 77% and 23 – 28% of TC in FPs at both RI and RO, respectively. Similarly, the OC/EC ratios slightly varied between two seasons in both indoor and outdoor FPs. The OC/EC ratios in FPs at RI varied from 2.80 to 3.24, while in FPs at RO were 2.73 – 3.28. The OC/EC ratios suggest the contributions of cooking activities, biomass and coal burning, and traffic emissions. This result is consistent with the results in Section 4.3.2. The contribution of OC and EC to TC and minor variation of OC/EC ratios indicate the stable emission sources of carbonaceous compounds.

Char-EC was more dominant in EC, accounting for approximately 80% of the EC concentration. The mean concentrations of char-EC and soot-EC for all the sampling periods at RI were 3.35 μg/m^3 and 0.60 μg/m^3, respectively. Meanwhile, the average char-EC and soot-EC concentrations at RO were 2.25 μg/m^3 and 0.57 μg/m^3, respectively. Soot-EC concentrations in FPs at RI and RO were approximately the same, while the higher char-EC concentration was observed in FPs at RI. It may be due to incense burning events in the indoor environment. As the result, a higher char-EC/soot-EC ratio was found in the indoor FPs than in the outdoor samples.

Table 6.2 Carbonaceous concentrations, OC/EC, and char-EC/soot-EC ratios in FPs

	FPs at RI			FPs at RO		
	Summer 2020 (n=6)	Winter 2020 (n=14)	Summer 2021 (n=15)	Summer 2020 (n=6)	Winter 2020 (n=14)	Summer 2021 (n=15)
OC (μg/m^3)	12.6 ± 10.2	13.2 ± 3.89	9.35 ± 2.48	8.03 ± 2.98	10.5 ± 3.36	6.12 ± 0.90
EC (μg/m^3)	3.84 ± 0.97	4.52 ± 1.45	3.51 ± 1.25	2.57 ± 0.35	3.55 ± 1.27	2.34 ± 0.72
TC (μg/m^3)	16.4 ± 10.5	17.7 ± 5.27	12.9 ± 3.39	10.9 ± 2.95	14.1 ± 4.60	8.46 ± 2.54
OC/EC	3.24 ± 2.31	2.95 ± 0.37	2.80 ± 0.67	3.28 ± 1.29	3.01 ± 0.28	2.73 ± 0.41
Char-EC (μg/m^3)	3.34 ± 1.09	3.81 ± 1.49	2.91 ± 1.26	2.10 ± 0.40	2.85 ± 1.30	1.81 ± 0.82
Soot-EC (μg/m^3)	0.50 ± 0.18	0.70 ± 0.12	0.60 ± 0.11	0.48 ± 0.20	0.69 ± 0.08	0.53 ± 0.17
Char-EC/soot-EC	8.08 ± 5.05	5.78 ± 3.31	5.04 ± 2.43	5.15 ± 2.27	4.26 ± 2.23	3.06 ± 1.71

Value is written as Average concentration ± Standard deviation

Total ion concentration was significantly higher in winter than in summer, e.g., the total ion concentration in FPs at RI was 19.7 ± 9.13 μg/m^3 in winter while that in summer was 7.34 ± 2.75 μg/m^3 (Table 6.3). The rise in the total ion concentration is primarily caused by the increase in SNA concentration. The SNA concentration in winter was approximately three to nine times higher than in summer. Particularly the nitrate concentration increased significantly in the winter sampling. The sharp increase in the SNA concentration suggests that the contribution of secondary particles may be crucial in the FPs concentration in these sampling sites. However, the variation in the total ion concentration between the two sampling sites was minor. For example, the total ion concentrations in FPs at RI and RO in

winter were 19.7 ± 9.13 μg/m^3 and 19.0 ± 10.8 μg/m^3, respectively. More significant daily variation of ions in outdoor FPs was observed compared to the indoor samples. It may be because of secondary particles under adverse weather conditions, which impact outdoor FPs more than indoor FPs.

Table 6.3 Ion concentrations in FPs at RI and RO

	FPs at RI			**FPs at RO**		
	Summer 2020 (n=6)	Winter 2020 (n=14)	Summer 2021 (n=15)	Summer 2020 (n=6)	Winter 2020 (n=14)	Summer 2021 (n=15)
Cl^- (μg/m^3)	0.42 ± 0.43	1.11 ± 0.69	0.27 ± 0.19	0.50 ± 0.42	1.17 ± 0.70	0.26 ± 0.17
SO_4^{2-} (μg/m^3)	1.78 ± 0.25	6.82 ± 2.99	3.79 ± 1.51	1.69 ± 0.34	5.77 ± 3.08	2.61 ± 0.99
NO_3^- (μg/m^3)	0.59 ± 0.12	5.63 ± 3.61	0.90 ± 0.56	0.86 ± 0.20	6.14 ± 4.58	0.85 ± 0.39
Na^+ (μg/m^3)	0.01 ± 0.02	0.02 ± 0.04	0.03± 0.04	-	0.01 ± 0.02	0.05 ± 0.08
NH_4^+ (μg/m^3)	0.89 ± 0.22	4.27 ± 1.97	1.69 ± 0.81	0.54 ± 0.27	3.59 ± 2.10	1.10 ± 0.49
K^+ (μg/m^3)	0.42 ± 0.61	0.57 ± 0.27	0.30 ± 0.10	0.26 ± 0.22	0.41 ± 0.22	0.20 ± 0.09
Mg^{2+} (μg/m^3)	0.02 ± 0.003	0.08 ± 0.04	0.04 ± 0.02	0.05 ± 0.005	0.12 ± 0.12	0.04 ± 0.01
Ca^{2+} (μg/m^3)	0.26 ± 0.06	1.20 ± 0.35	0.32 ± 0.20	0.81 ± 0.21	1.81 ± 0.66	0.35 ± 0.16
Total ion concentration (μg/m^3)	4.38 ± 1.16	19.7 ± 9.13	7.34 ± 2.75	4.69 ± 1.25	19.0 ± 10.8	5.47 ± 1.70

Values are written as Average concentration ± Standard deviation

6.3.2.2 UFPs

Due to the limitation of sampling devices, indoor and outdoor UFPs were sampled in the summer of 2021 (July 9 – 24). The total concentration of UFPs at RI was 3.53 ± 0.84 μg/m^3, higher than at RO of 2.93 ± 0.59 μg/m^3. OC and EC concentrations in UFPs at RI were 2.65 ± 0.70 μg/m^{3}and 0.51 ± 0.20 μg/m^3, respectively. Meanwhile, the OC and EC concentrations in UFPs at RO were 2.04 ± 0.45 μg/m^{3}and 0.47 ± 0.15 μg/m^3, respectively, which were slightly lower than at RI. The higher OC concentration in UFPs at RI may be the result of burning incense in the indoor environment. In contrast, the total ion concentration in UFPs at RI was 0.38 ± 0.09 μg/m^3, slightly lower than that in UFPs at RO (0.42 ± 0.10 μg/m^3). The SNA concentration at RO was higher than at RI. It may be explained by the effect of photochemical reactions, which impact outdoor UFPs more than indoor UFPs. Meanwhile, the higher concentration of chloride and potassium ions, which are used as biomass burning markers, in indoor samples indicates the impact of incense burning.

Daily I/O ratios for the total concentration of measured components in UFPs follow a similar trend of FPs in these sampling sites, which is higher than 1.0 and significantly increase during the incense burning days (Figure 6.5). The average I/O ratio was 1.22 (range 0.81 – 2.01) indicating the contribution of indoor emission sources. The highest I/O ratio was found during the incense burning day (I/O ratio ~ 2.05).

Table 6.4 Carbonaceous and ionic concentrations in UFPs at RI and RO

	UFPs at RI	**UFPs at RO**
	Summer 2021 (n = 16)	Summer 2021 (n = 16)
OC (μg/m^3)	2.65 ± 0.70	2.04 ± 0.45
EC (μg/m^3)	0.51 ± 0.20	0.47 ± 0.15
WSOC (μg/m^3)	0.93 ± 0.32	0.83 ± 0.15
WIOC(μg/m^3)	1.72 ± 0.40	1.21 ± 0.34
Cl^- (μg/m^3)	0.012 ± 0.005	0.009 ± 0.004
SO_4^{2-} (μg/m^3)	0.12 ± 0.04	0.16 ± 0.05
NO_3^- (μg/m^3)	0.08 ± 0.003	0.09 ± 0.04
Na^+ (μg/m^3)	-	-
NH_4^+ (μg/m^3)	0.09 ± 0.04	0.09 ± 0.04
K^+ (μg/m^3)	0.004 ± 0.009	-
Mg^{2+} (μg/m^3)	-	-
Ca^{2+} (μg/m^3)	0.07 ± 0.02	0.08 ± 0.04
Total concentration (μg/m^3)	**3.53 ± 0.84**	**2.93 ± 0.59**

Values are written as Average concentration ± Standard deviation

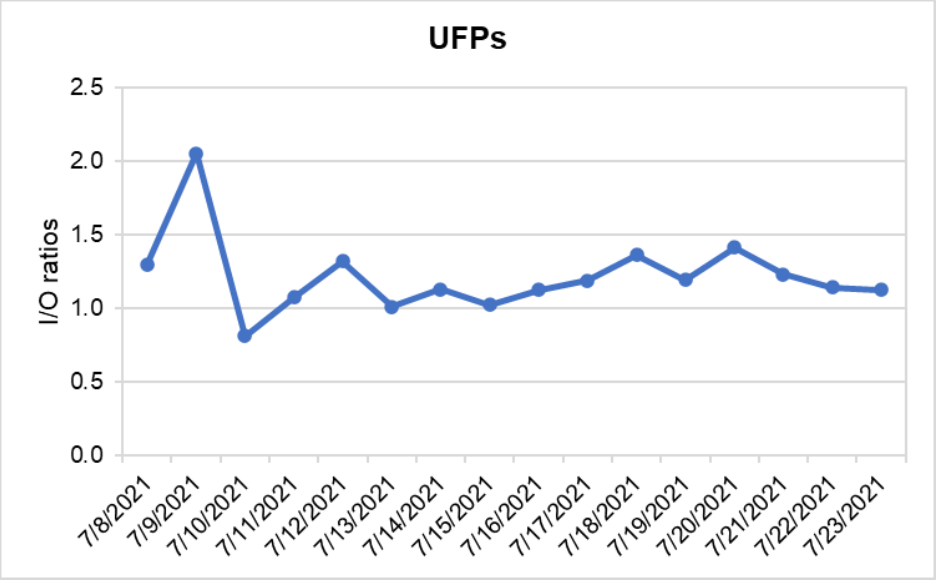

Figure 6.5 I/O ratio for UFPs at the residential house

6.3.3 UFPs at AI

The total concentrations of analyzed components in UFPs were highest in winter, followed by WTP and summer. The UFPs concentrations at AI were slightly higher than at AS, as mentioned in Section 5.3.2 (Figure 6.6). The concentration of carbonaceous compounds was also slightly higher in the indoor UFPs. However, the FPs recorded by the sensor showed

that the FPs concentration at AI was significantly lower than at AS. This result may be explained by the difference in the characteristic of UFPs. UFPs can penetrate the room by infiltration through the gaps or cracks, which may be easier than particles in the fine-size range. It should be noted that there were no human activities at AI except the sampling activity. However, both UFPs and FPs samples are expected to conduct in future studies to clarify the impact of infiltration on the concentration and composition of UFPs and FPs

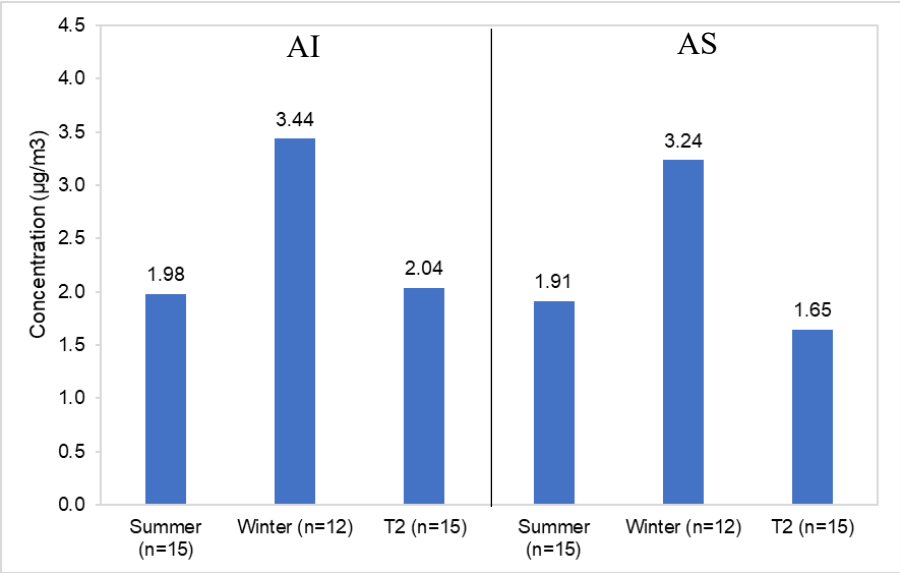

Figure 6.6 The total UFPs concentration at AI and AS

6.4 Conclusion

The real-time $PM_{2.5}$ concentrations were highest in winter, followed by WTP, STP, and summer. The real-time showed a good correlation with the $PM_{2.5}$ concentrations measured by BAM. Both data illustrated a similar variation trend of $PM_{2.5}$ concentrations.

The real-time $PM_{2.5}$ levels at RI were higher than at AI in both summer and winter, suggesting the contribution of indoor emissions such as cooking activities or incense burning, while there was no human activity in an unused classroom at AI.

The total concentration of analyzed compounds in FPs at RI was higher than at RO, and in winter than in summer. The concentration of FPs in winter was approximately twofold higher than in summer. This result may be due to the adverse weather conditions (low mixing height layer, and less rain), which led to the accumulation of air pollutants and hinder the dilution.

The variation of indoor and outdoor UFPs was similar in this study. It may be explained by the air circulation between indoor and outdoor environments. In contrast, the FPs concentration between the two sampling periods in the summer of 2020 and 2021 were insignificant fluctuations in both indoor and outdoor samples, indicating stable emissions of particles in the sampling sites.

The average I/O ratio in FPs was greater than 1.0 (1.13 – 1.45), suggesting the contribution of indoor sources such as cooking or incense burning. The variation of the I/O ratio was

insignificant between the summer and winter periods, while the daily I/O ratio variation shows the influence of indoor emission sources.

The sharp increase in the SNA concentration suggests the contribution of secondary particles. However, the variation of the total ion concentration between the two sampling sites was minor. More significant daily variation of ions in outdoor FPs was observed compared to the indoor samples. It may be because of secondary particles under adverse weather conditions, which impact outdoor FPs more than indoor FPs.

Similar to the FPs concentration, the higher UFPs concentration was found in indoor samples. The higher OC concentration in UFPs at RI was due to the incense burning, while the ion concentration was slightly lower in UFPs at RI, particularly SNA species. It may be explained by the effect of photochemical reactions, which impact outdoor UFPs more than indoor UFPs. Daily I/O ratios in UFPs follow a similar trend of FPs variation, which is higher than 1.0 and significantly increases due to incense burning.

The total concentrations of UFPs at AI were highest in winter, followed by WTP and summer. However, the FPs recorded by the sensor at the same sampling site show that the FPs concentration at AI was significantly lower than at AS. This result may be due to the difference in the characteristic of UFPs. However, both UFPs and FPs samples are expected to conduct in future studies to clarify the impact of infiltration on the concentration and composition of UFPs and FPs.

Chapter 7

Conclusions and recommendations

7.1 Conclusions

In this study, UFPs and FPs were collected in different locations in Hanoi, Vietnam, including the roadside, ambient, and indoor environment. Monitoring was conducted in different seasons according to the variation of the weather conditions from 2020 to 2021. The chemical compositions (carbonaceous and ionic compounds) of particles were analyzed to investigate the characteristics of particles and the contribution of different emission sources to particle concentrations. The real-time data of FPs, temperature, and humidity were recorded to get an overview of the daily and seasonal variation of FPs concentrations in different locations. This is the first study that monitored the indoor and outdoor UFPs, FPs in a residential house with normal human activities and in a school environment without human activity. Furthermore, this is also a pioneer study that conducted the roadside UFPs samples in Hanoi and the possibility of particle growth from the ultrafine to fine-size range particles. Based on the results, the following conclusions can be drawn:

- The good correlation between AH and particle components was found in this study, while the relationship between RH and particle components was not observed. It may be due to the very high RH (>85%) and rainy conditions that occur in summer in the study region. The strong correlations between AH and other components during summer might be related to secondary transformation processes involving water molecules, regardless of temperature. Therefore, it is necessary to consider the particle formation via water molecules that can occur in highly contaminated areas under high humidity conditions. A different influence of AH on the WSOC concentration was found in FPs and UFPs.

- The higher concentration of carbonaceous components, higher EC fraction, and the lower OC/EC ratio in UFPs at RS indicate that the effect of the primary emissions such as vehicular exhausts might be more substantial than that at AS. The mean ratio of NO3-/SO42- in UFPs at RS was higher than that at AS, suggesting the higher contribution of traffic emissions. A significantly higher concentration of calcium ions was found during summer, which might be due to the construction site near the sampling point. The higher concentration of calcium ions at the roadside may reflect the impact of road dust emissions.

- The UFPs and FPs concentrations at AS increased from summer to winter and dropped in the transitional period from winter to summer. The stable weather conditions (low mixing height, and low precipitation) may allow the accumulation of air pollutants, leading to higher concentrations of both particle sizes during winter. However, the different order of the UFPs and FPs concentrations is probably due to secondary processes, which formed FPs under drizzle-like conditions associated with high humidity during the WTP sampling.

- The relationship between particle compositions in UFPs at the RS and FPs at the AS indicates the possibility of particle growth from the ultra- to the fine-size range. It may be crucial to explain the secondary emission sources and the chemical compositions and size distribution of particles in different sampling locations.

- The higher real-time FPs concentrations were found in the residential house with human activity (cooking, incense burning, cleaning, etc.). In contrast, lower FPs levels were found in the unused classroom in the school environment. The real-time data also show the highest concentration of FPs in winter, followed by WTP, STP, and summer. This result was consistent with the FPs concentrations measured by BAM from the US Embassy and the total concentration of all analyzed components in this study.

- The total concentration of analyzed compounds in FPs at RI was higher than at RO, and in winter than in summer. A similar variation was found in the indoor and outdoor UFPs, which was higher in the indoor samples. The I/O ratio was greater than 1.0 for both UFPs and FPs, suggesting the contribution of indoor sources such as cooking and incense burning. The similar variation of indoor and outdoor FPs indicates the air circulation between indoor and outdoor environments in the residential house.

7.2 Recommendations

The findings of this study contribute to the understanding of particle compositions in different size ranges and the characteristics of particles in multiple locations. This is a pioneer study to get an overview of particle composition in the urban areas in Vietnam, which may be vital to assess the human health effects and significantly contribute to the decision-making in air pollution control measures in Vietnam. However, some recommendations are expected to fill up as follows:

- A longer sampling period is expected to conduct in future studies, e.g., one month continuously for each season or one full year should be done to acquire comprehensive data on the variation of particle chemical composition and concentration.

- More than two sampling locations and the different determined distances from the traffic emission source should be conducted to investigate the effect of vehicular exhaust and its contribution to the particle in different size ranges in the ambient air.

- More types of residential houses (e.g., apartments or private houses with different numbers of rooms or residents) should be included to evaluate the contribution of indoor and outdoor emission sources.

- PAHs should be analyzed in the indoor and ambient samples to clarify the effects of traffic-related emissions on particles. It is also crucial to evaluate the human health impacts.

- Both UFPs and FPs should be monitored at the same time in the indoor and outdoor environments for determining the effect of infiltration and ventilation of particles and investigating the difference in characteristics of particles in different size ranges.

- The particle number concentration should be included together with the chemical characteristics to get a comprehensive understanding of size distribution and its chemical composition in different environments, such as indoor, outdoor, or near roadways environments.

- Other chemical compounds, such as trace elements should be included to get comprehensive data on chemical compounds in particles.

- Impact of meteorological parameters, such as solar radiation or wind direction should be further clarified to get insights into weather conditions on particle characteristics and concentrations.

References

Agudelo-Castañeda, D. M., Teixeira, E. C., Braga, M., Rolim, S. B. A., Silva, L. F. O., Beddows, D. C. S., Harrison, R. M., & Querol, X. (2019). Cluster analysis of urban ultrafine particles size distributions. *Atmospheric Pollution Research*, *10*(1), 45–52. https://doi.org/10.1016/j.apr.2018.06.006

Anderson, H. R., Atkinson, R. W., Peacock, J. L., Sweeting, M. J., & Marston, L. (2005). Ambient particulate matter and health effects: Publication bias in studies of short-term associations. *Epidemiology*, *16*(2), 155–163. https://doi.org/10.1097/01.ede.0000152528.22746.0f

Cao, J. J., Wu, F., Chow, J. C., Lee, S. C., Li, Y., Chen, S. W., An, Z. S., Fung, K. K., Watson, J. G., Zhu, C. S., & Liu, S. X. (2005). Characterization and source apportionment of atmospheric organic and elemental carbon during fall and winter of 2003 in Xi'an, China. *Atmospheric Chemistry and Physics*, *5*(11), 3127–3137. https://doi.org/10.5194/acp-5-3127-2005

Chen, C., Zhao, B., Zhou, W., Jiang, X., & Tan, Z. (2012). A methodology for predicting particle penetration factor through cracks of windows and doors for actual engineering application. *Building and Environment*, *47*(1), 339–348. https://doi.org/10.1016/j.buildenv.2011.07.004

Chen, S. C., Tsai, C. J., Chou, C. C. K., Roam, G. D., Cheng, S. S., & Wang, Y. N. (2010). Ultrafine particles at three different sampling locations in Taiwan. *Atmospheric Environment*, *44*(4), 533–540. https://doi.org/10.1016/j.atmosenv.2009.10.044

Chen, Y., Zhi, G., Feng, Y., Fu, J., Feng, J., Sheng, G., & Simoneit, B. R. T. (2006). Measurements of emission factors for primary carbonaceous particles from residential raw-coal combustion in China. *Geophysical Research Letters*, *33*(20), 2–5. https://doi.org/10.1029/2006GL026966

Cheng, Z., Luo, L., Wang, S., Wang, Y., Sharma, S., Shimadera, H., Wang, X., Bressi, M., de Miranda, R. M., Jiang, J., Zhou, W., Fajardo, O., Yan, N., & Hao, J. (2016). Status and characteristics of ambient PM2.5 pollution in global megacities. *Environment International*, *89–90*, 212–221. https://doi.org/10.1016/j.envint.2016.02.003

Choochuay, C., Pongpiachan, S., Tipmanee, D., Deelaman, W., Suttinun, O., Wang, Q., Xing, L., Li, G., Han, Y., Palakun, J., Poshyachinda, S., Aukkaravittayapun, S., Surapipith, V., & Cao, J. (2020a). Long-range transboundary atmospheric transport of polycyclic aromatic hydrocarbons, carbonaceous compositions, and water-soluble ionic species in southern thailand. *Aerosol and Air Quality Research*, *20*(7), 1591–1606. https://doi.org/10.4209/aaqr.2020.03.0120

ChooChuay, C., Pongpiachan, S., Tipmanee, D., Suttinun, O., Deelaman, W., Wang, Q., Xing, L., Li, G., Han, Y., Palakun, J., & Cao, J. (2020b). Impacts of PM2.5 sources on variations in particulate chemical compounds in ambient air of Bangkok, Thailand. *Atmospheric Pollution Research*, *11*(9), 1657–1667. https://doi.org/10.1016/j.apr.2020.06.030

Chow, J. C., Watson, J. G., Chen, L. W. A., Arnott, W. P., Moosmüller, H., & Fung, K. (2004). Equivalence of elemental carbon by thermal/optical reflectance and transmittance with different temperature protocols. *Environmental Science and Technology*, *38*(16), 4414–4422. https://doi.org/10.1021/es034936u

Chow, J. C., Watson, J. G., Crow, D., Lowenthal, D. H., & Merrifield, T. (2001). Comparison of IMPROVE and NIOSH Carbon Measurements. *Aerosol Science and Technology*, *34*(1), 23–34. https://doi.org/10.1080/02786820119073

Cohen, D. D., Crawford, J., Stelcer, E., & Bac, V. T. (2010). Characterisation and source apportionment of fine particulate sources at Hanoi from 2001 to 2008. *Atmospheric Environment*, *44*(3), 320–328. https://doi.org/10.1016/j.atmosenv.2009.10.037

Corsini, E., Vecchi, R., Marabini, L., Fermo, P., Becagli, S., Bernardoni, V., Caruso, D., Corbella, L., Dell'Acqua, M., Galli, C. L., Lonati, G., Ozgen, S., Papale, A., Signorini, S., Tardivo, R., Valli, G., & Marinovich, M. (2017). The chemical composition of ultrafine particles and associated biological effects at an alpine town impacted by wood burning. *Science of the Total Environment*, *587–588*, 223–231. https://doi.org/10.1016/j.scitotenv.2017.02.125

Dai, Q., Ding, J., Song, C., Liu, B., Bi, X., Wu, J., Zhang, Y., Feng, Y., & Hopke, P. K. (2021). Changes in source contributions to particle number concentrations after the COVID-19 outbreak: Insights from a dispersion normalized PMF. *Science of the Total Environment*, *759*, 143548. https://doi.org/10.1016/j.scitotenv.2020.143548

Derudi, M., Gelosa, S., Sliepcevich, A., Cattaneo, A., Cavallo, D., Rota, R., & Nano, G. (2014). Emission of air pollutants from burning candles with different composition in indoor environments. *Environmental Science and Pollution Research*, *21*(6), 4320–4330. https://doi.org/10.1007/s11356-013-2394-2

Dumkova, J., Vrlikova, L., Vecera, Z., Putnova, B., Docekal, B., Mikuska, P., Fictum, P., Hampl, A., & Buchtova, M. (2016). Inhaled cadmium oxide nanoparticles: Their in Vivo fate and effect on target organs. *International Journal of Molecular Sciences*, *17*(6). https://doi.org/10.3390/ijms17060874

Feng, Y., Chen, Y., Guo, H., Zhi, G., Xiong, S., Li, J., Sheng, G., & Fu, J. (2009). Characteristics of organic and elemental carbon in PM2.5 samples in Shanghai, China. *Atmospheric Research*, *92*(4), 434–442. https://doi.org/10.1016/j.atmosres.2009.01.003

Fujitani, Y., Kumar, P., Tamura, K., Fushimi, A., Hasegawa, S., Takahashi, K., Tanabe, K., Kobayashi, S., & Hirano, S. (2012). Science of the Total Environment Seasonal differences of the atmospheric particle size distribution in a metropolitan area in Japan. *Science of the Total Environment, The*, *437*, 339–347. https://doi.org/10.1016/j.scitotenv.2012.07.085

Furuuchi, M., Eryu, K., Nagura, M., Hata, M., Kato, T., Tajima, N., Sekiguchi, K., Ehara, K., Seto, T., & Otani, Y. (2010). Development and performance evaluation of air sampler with inertial filter for nanoparticle sampling. *Aerosol and Air Quality Research*, *10*(2), 185–192. https://doi.org/10.4209/aaqr.2009.11.0070

Gatari, M., Wagner, A., & Boman, J. (2005). Elemental composition of tropospheric aerosols in Hanoi, Vietnam and Nairobi, Kenya. *Science of the Total Environment*, *341*(1–3), 241–249. https://doi.org/10.1016/j.scitotenv.2004.09.031

Goyal, R., & Kumar, P. (2013). Indoor-outdoor concentrations of particulate matter in nine microenvironments of a mix-use commercial building in megacity Delhi. *Air Quality, Atmosphere and Health*, *6*(4), 747–757. https://doi.org/10.1007/s11869-013-0212-0

GreenID. (2018). Air Quality Report. *Air Quality in Vietnam in 2017*, *2*, 1–20.

Gu, J., Bai, Z., Liu, A., Wu, L., Xie, Y., Li, W., Dong, H., & Zhang, X. (2010).

Characterization of atmospheric organic carbon and element carbon of PM2.5 and PM10 at Tianjin, China. *Aerosol and Air Quality Research*, *10*(2), 167–176. https://doi.org/10.4209/aaqr.2009.12.0080

Ha, N., Hien, T., Dung, N. T., Anh, N. L., Vinh, T. H., & Yoneda, M. (2020). *PM 2 . 5 - BOUND PAHs IN THE INDOOR AND OUTDOOR AIR OF NURSERY SCHOOLS IN HA NOI , VIET NAM AND HEALTH*. *58*(3), 319–327. https://doi.org/10.15625/2525-2518/58/3/14224

Hai, C. D., & Kim Oanh, N. T. (2013). Effects of local, regional meteorology and emission sources on mass and compositions of particulate matter in Hanoi. *Atmospheric Environment*, *78*, 105–112. https://doi.org/10.1016/j.atmosenv.2012.05.006

Hama, S. M. L., Cordell, R. L., & Monks, P. S. (2017). Quantifying primary and secondary source contributions to ultrafine particles in the UK urban background. *Atmospheric Environment*, *166*, 62–78. https://doi.org/10.1016/j.atmosenv.2017.07.013

Han, Y., Cao, J., Chow, J. C., Watson, J. G., An, Z., Jin, Z., Fung, K., & Liu, S. (2007). Evaluation of the thermal/optical reflectance method for discrimination between char- and soot-EC. *Chemosphere*, *69*(4), 569–574. https://doi.org/10.1016/j.chemosphere.2007.03.024

Han, Y. M., Lee, S. C., Cao, J. J., Ho, K. F., & An, Z. S. (2009). Spatial distribution and seasonal variation of char-EC and soot-EC in the atmosphere over China. *Atmospheric Environment*, *43*(38), 6066–6073. https://doi.org/10.1016/j.atmosenv.2009.08.018

Hanoi Statistical Office. (2021). *Hanoi statistical yearbook 2020*. Statistical publishing house.

Hien, P. D., Bac, V. T., Tham, H. C., Nhan, D. D., & Vinh, L. D. (2002). Influence of meteorological conditions on PM2.5 and PM2.5-10 concentrations during the monsoon season in Hanoi, Vietnam. *Atmospheric Environment*, *36*(21), 3473–3484. https://doi.org/10.1016/S1352-2310(02)00295-9

Hien, P. D., Bac, V. T., & Thinh, N. T. H. (2004). PMF receptor modelling of fine and coarse PM10 in air masses governing monsoon conditions in Hanoi, northern Vietnam. *Atmospheric Environment*, *38*(2), 189–201. https://doi.org/10.1016/j.atmosenv.2003.09.064

Hien, P. D., Hangartner, M., Fabian, S., & Tan, P. M. (2014). Concentrations of NO2, SO2, and benzene across Hanoi measured by passive diffusion samplers. *Atmospheric Environment*, *88*(2), 66–73. https://doi.org/10.1016/j.atmosenv.2014.01.036

Hofmann, W. (2011). Modelling inhaled particle deposition in the human lung-A review. *Journal of Aerosol Science*, *42*(10), 693–724. https://doi.org/10.1016/j.jaerosci.2011.05.007

Höllbacher, E., Ters, T., Rieder-Gradinger, C., & Srebotnik, E. (2017). Emissions of indoor air pollutants from six user scenarios in a model room. *Atmospheric Environment*, *150*, 389–394. https://doi.org/10.1016/j.atmosenv.2016.11.033

Hopke, P. K., Cohen, D. D., Begum, B. A., Biswas, S. K., Ni, B., Pandit, G. G., Santoso, M., Chung, Y. S., Davy, P., Markwitz, A., Waheed, S., Siddique, N., Santos, F. L., Pabroa, P. C. B., Seneviratne, M. C. S., Wimolwattanapun, W., Bunprapob, S., Vuong, T. B., Duy Hien, P., & Markowicz, A. (2008). Urban air quality in the Asian region. *Science of the Total Environment*, *404*(1), 103–112. https://doi.org/10.1016/j.scitotenv.2008.05.039

Hussein, T., Puustinen, A., Aalto, P. P., Mäkelä, J. M., Hämeri, K., & Kulmala, M. (2003). Urban aerosol number size distributions. *Atmospheric Chemistry and Physics Discussions*, *3*(5), 5139–5184. https://doi.org/10.5194/acpd-3-5139-2003

Huyen, T. T., Yamaguchi, R., Kurotsuchi, Y., Sekiguchi, K., Dung, N. T., Thuy, N. T. T., & Thuy, L. B. (2021). Characteristics of Chemical Components in Fine Particles (PM2.5) and Ultrafine Particles (PM0.1) in Hanoi, Vietnam: a Case Study in Two Seasons with Different Humidity. *Water, Air, and Soil Pollution*, *232*(5), 1–21. https://doi.org/10.1007/s11270-021-05108-0

Jacobson, M. Z., Kittelson, D. B., & Watts, W. F. (2005). Enhanced coagulation due to evaporation and its effect on nanoparticle evolution. *Environmental Science and Technology*, *39*(24), 9486–9492. https://doi.org/10.1021/es0500299

Jeong, C., Evans, G. J., Healy, R. M., Jadidian, P., Wentzell, J., Liggio, J., & Brook, J. R. (2015). Rapid physical and chemical transformation of traffic–related atmospheric particles near a highway. *Atmospheric Pollution Research*, *6*(4), 662–672. https://doi.org/10.5094/APR.2015.075

Karagulian, F., Belis, C. A., Dora, C. F. C., Prüss-Ustün, A. M., Bonjour, S., Adair-Rohani, H., & Amann, M. (2015). Contributions to cities' ambient particulate matter (PM): A systematic review of local source contributions at global level. *Atmospheric Environment*, *120*, 475–483. https://doi.org/10.1016/j.atmosenv.2015.08.087

Keogh, D. U., Ferreira, L., & Morawska, L. (2009). Development of a particle number and particle mass vehicle emissions inventory for an urban fleet. *Environmental Modelling and Software*, *24*(11), 1323–1331. https://doi.org/10.1016/j.envsoft.2009.05.003

Khalek, I. A., Blanks, M. G., Merritt, P. M., & Zielinska, B. (2015). Regulated and unregulated emissions from modern 2010 emissions-compliant heavy-duty on-highway diesel engines. *Journal of the Air and Waste Management Association*, *65*(8), 987–1001. https://doi.org/10.1080/10962247.2015.1051606

Kim, K. H., Sekiguchi, K., Furuuchi, M., & Sakamoto, K. (2011). Seasonal variation of carbonaceous and ionic components in ultrafine and fine particles in an urban area of Japan. *Atmospheric Environment*, *45*(8), 1581–1590. https://doi.org/10.1016/j.atmosenv.2010.12.037

Kim, K. H., Sekiguchi, K., Kudo, S., Kinoshita, M., & Sakamoto, K. (2013). Carbonaceous and ionic components in ultrafine and fine particles at four sampling sites in the vicinity of roadway intersection. *Atmospheric Environment*, *74*, 83–92. https://doi.org/10.1016/j.atmosenv.2013.03.016

Kim, K. H., Sekiguchi, K., Kudo, S., & Sakamoto, K. (2011). Characteristics of atmospheric elemental carbon (char and soot) in ultrafine and fine particles in a roadside environment, Japan. *Aerosol and Air Quality Research*, *11*(1), 1–12. https://doi.org/10.4209/aaqr.2010.07.0061

Kim Oanh, N. T., Upadhyay, N., Zhuang, Y. H., Hao, Z. P., Murthy, D. V. S., Lestari, P., Villarin, J. T., Chengchua, K., Co, H. X., Dung, N. T., & Lindgren, E. S. (2006). Particulate air pollution in six Asian cities: Spatial and temporal distributions, and associated sources. *Atmospheric Environment*, *40*(18), 3367–3380. https://doi.org/10.1016/j.atmosenv.2006.01.050

Kittelson, D. B., Watts, W. F., & Johnson, J. P. (2004). Nanoparticle emissions on Minnesota highways. *Atmospheric Environment*, *38*(1), 9–19.

https://doi.org/10.1016/j.atmosenv.2003.09.037

Komppula, M., Laakso, L., & Hussein, T. (2003). *Diurnal and annual characteristics of particle mass and number concentrations in urban , rural and Arctic environments in Finland*. *37*, 2629–2641. https://doi.org/10.1016/S1352-2310(03)00206-1

Kozáková, J., Pokorná, P., Černíková, A., Hovorka, J., Braniš, M., Moravec, P., & Schwarz, J. (2017). The association between intermodal (PM1-2.5) and PM1, PM2.5, coarse fraction and meteorological parameters in various environments in central Europe. *Aerosol and Air Quality Research*, *17*(5), 1234–1243. https://doi.org/10.4209/aaqr.2016.06.0242

Kudo, S., Sekiguchi, K., Kim, K. H., Kinoshita, M., Möller, D., Wang, Q., Yoshikado, H., & Sakamoto, K. (2012). Differences of chemical species and their ratios between fine and ultrafine particles in the roadside environment. *Atmospheric Environment*, *62*, 172–179. https://doi.org/10.1016/j.atmosenv.2012.08.039

Kudo, S., Sekiguchi, K., Kim, K. H., & Sakamoto, K. (2011). Spatial distributions of ultrafine particles and their behavior and chemical composition in relation to roadside sources. *Atmospheric Environment*, *45*(35), 6403–6413. https://doi.org/10.1016/j.atmosenv.2011.08.021

Kulmala, M., & Kerminen, V. M. (2008). On the formation and growth of atmospheric nanoparticles. *Atmospheric Research*, *90*(2–4), 132–150. https://doi.org/10.1016/j.atmosres.2008.01.005

Kumagai, K., Iijima, A., Shimoda, M., Saitoh, Y., Kozawa, K., Hagino, H., & Sakamoto, K. (2010). Determination of dicarboxylic acids and levoglucosan in fine particles in the kanto plain, japan, for source apportionment of organic aerosols. *Aerosol and Air Quality Research*, *10*(3), 282–291. https://doi.org/10.4209/aaqr.2009.11.0075

Kumagai, K., Iijima, A., Tago, H., Tomioka, A., Kozawa, K., & Sakamoto, K. (2009). Seasonal characteristics of water-soluble organic carbon in atmospheric particles in the inland Kanto plain, Japan. *Atmospheric Environment*, *43*(21), 3345–3351. https://doi.org/10.1016/j.atmosenv.2009.04.008

Kumar, P., Morawska, L., Birmili, W., Paasonen, P., Hu, M., Kulmala, M., Harrison, R. M., Norford, L., & Britter, R. (2014). Ultrafine particles in cities. *Environment International*, *66*, 1–10. https://doi.org/10.1016/j.envint.2014.01.013

Kuo, S. C., Tsai, Y. I., & Sopajaree, K. (2015). Emission identification and health risk potential of allergy-causing fragrant substances in PM2.5 from incense burning. *Building and Environment*, *87*, 23–33. https://doi.org/10.1016/j.buildenv.2015.01.012

Li, T., Cao, S., Fan, D., Zhang, Y., Wang, B., Zhao, X., Leaderer, B. P., Shen, G., Zhang, Y., & Duan, X. (2016). Household concentrations and personal exposure of PM2.5 among urban residents using different cooking fuels. *Science of the Total Environment*, *548–549*, 6–12. https://doi.org/10.1016/j.scitotenv.2016.01.038

Lim, S., Lee, M., Lee, G., Kim, S., Yoon, S., & Kang, K. (2012). Ionic and carbonaceous compositions of PM10, PM2.5 and PM1.0 at Gosan ABC Superstation and their ratios as source signature. *Atmospheric Chemistry and Physics*, *12*(4), 2007–2024. https://doi.org/10.5194/acp-12-2007-2012

Lin, C. C., Chen, S. J., Huang, K. L., Lee, W. J., Lin, W. Y., Liao, C. J., Chaung, H. C., & Chiu, C. H. (2007). Water-soluble ions in nano/ultrafine/fine/coarse particles collected near a busy road and at a rural site. *Environmental Pollution*, *145*(2), 562–570.

https://doi.org/10.1016/j.envpol.2006.04.023

Ly, B. T., Matsumi, Y., Nakayama, T., Sakamoto, Y., Kajii, Y., & Nghiem, T. D. (2018). Characterizing PM2.5 in Hanoi with new high temporal resolution sensor. *Aerosol and Air Quality Research*, *18*(9), 2487–2497. https://doi.org/10.4209/aaqr.2017.10.0435

Mayol-Bracero, O. L., Guyon, P., Graham, B., Roberts, G., Andreae, M. O., Decesari, S., Facchini, M. C., Fuzzi, S., & Artaxo, P. (2002). Water-soluble organic compounds in biomass burning aerosols over Amazonia Apportionment of the chemical composition and importance of the polyacidic fraction. *Journal of Geophysical Research Atmospheres*, *107*(20), LBA 59-1-LBA 59-15. https://doi.org/10.1029/2001JD000522

McGarry, P., Morawska, L., He, C., Jayaratne, R., Falk, M., Tran, Q., & Wang, H. (2011). Exposure to particles from laser printers operating within office workplaces. *Environmental Science and Technology*, *45*(15), 6444–6452. https://doi.org/10.1021/es200249n

Mendes, L., Gini, M. I., Biskos, G., Colbeck, I., & Eleftheriadis, K. (2018). Airborne ultrafine particles in a naturally ventilated metro station: Dominant sources and mixing state determined by particle size distribution and volatility measurements. *Environmental Pollution*, *239*, 82–94. https://doi.org/10.1016/j.envpol.2018.03.067

Meng, Z. Y., Jiang, X. M., Yan, P., Lin, W. L., Zhang, H. D., & Wang, Y. (2007). Characteristics and sources of PM2.5 and carbonaceous species during winter in Taiyuan, China. *Atmospheric Environment*, *41*(32), 6901–6908. https://doi.org/10.1016/j.atmosenv.2007.07.049

Minoura, H., Takekawa, H., & Terada, S. (2009). Roadside nanoparticles corresponding to vehicle emissions during one signal cycle. *Atmospheric Environment*, *43*(3), 546–556. https://doi.org/10.1016/j.atmosenv.2008.10.004

Miyazaki, Y., Kondo, Y., Takegawa, N., Komazaki, Y., Fukuda, M., Kawamura, K., Mochida, M., Okuzawa, K., & Weber, R. J. (2006). Time-resolved measurements of water-soluble organic carbon in Tokyo. *Journal of Geophysical Research Atmospheres*, *111*(23). https://doi.org/10.1029/2006JD007125

Mönkkönen, P., Koponen, I. K., Lehtinen, K. E. J., Hämeri, K., Uma, R., & Kulmala, M. (2004). Measurements in a highly polluted Asian mega city: observations of aerosol number size distribution, modal parameters and nucleation events. *Atmospheric Chemistry and Physics Discussions*, *4*(5), 5407–5431. https://doi.org/10.5194/acpd-4-5407-2004

MONRE. (2015). *VietNam- National Environmental Performance Assessment (EPA) Report*. https://doi.org/10.1017/CBO9781107415324.004

MONRE. (2017). *National state of environment report 2016 on air quality*. Vietnam publishing house of natural resources, environment and cartography.

Morawska, L., Ristovski, Z., Jayaratne, E. R., Keogh, D. U., & Ling, X. (2008). Ambient nano and ultrafine particles from motor vehicle emissions: Characteristics, ambient processing and implications on human exposure. *Atmospheric Environment*, *42*(35), 8113–8138. https://doi.org/10.1016/j.atmosenv.2008.07.050

Nghiem, T., Thu, T., Nguyen, T., Thu, T., Nguyen, H., Ly, B., & Sekiguchi, K. (2020). *Chemical characterization and source apportionment of ambient nanoparticles : a case study in Hanoi , Vietnam*.

Nhat, T., Nguyen, T., Le, H. A., Minh, T., Mac, T., Trang, T., Nguyen, N., Pham, V. H., & Bui, Q. H. (2018). Current Status of PM 2 . 5 Pollution and its Mitigation in Vietnam. *Global Environmental Research*, 65–72.

Oberdörster, G., Sharp, Z., Atudorei, V., Elder, A., Gelein, R., Kreyling, W., & Cox, C. (2004). Translocation of inhaled ultrafine particles to the brain. *Inhalation Toxicology*, *16*(6–7), 437–445. https://doi.org/10.1080/08958370490439597

Otani, Y., Eryu, K., Furuuchi, M., Tajima, N., & Tekasakul, P. (2007). Inertial Classification of Nanoparticles with Fibrous Filters. *Aerosol and Air Quality Research*, *7*(3), 343–352. https://doi.org/10.4209/aaqr.2007.03.0021

Paasonen, P. (2013). *Aerosol particle number emissions and size distributions : Implementation in the GAINS model and initial results Approved by*.

Pachauri, T., Satsangi, A., Singla, V., Lakhani, A., & Maharaj Kumari, K. (2013). Characteristics and sources of carbonaceous aerosols in PM2.5 during wintertime in Agra, India. *Aerosol and Air Quality Research*, *13*(3), 977–991. https://doi.org/10.4209/aaqr.2012.10.0263

Pakkanen, T. A., Kerminen, V. M., Korhonen, C. H., Hillamo, R. E., Aarnio, P., Koskentalo, T., & Maenhaut, W. (2001). Urban and rural ultrafine (PM0.1) particles in the Helsinki area. *Atmospheric Environment*, *35*(27), 4593–4607. https://doi.org/10.1016/S1352-2310(01)00167-4

Panicker, A. S., Ali, K., Beig, G., & Yadav, S. (2015). Characterization of particulate matter and carbonaceous aerosol over two urban environments in Northern India. *Aerosol and Air Quality Research*, *15*(7), 2584–2595. https://doi.org/10.4209/aaqr.2015.04.0253

Phairuang, W., Inerb, M., Furuuchi, M., Hata, M., Tekasakul, S., & Tekasakul, P. (2020). Size-fractionated carbonaceous aerosols down to PM0.1 in southern Thailand: Local and long-range transport effects. *Environmental Pollution*, *260*, 114031. https://doi.org/10.1016/j.envpol.2020.114031

Phan, H. Y. T., Yano, T., Sato, T., & Nishimura, T. (2010). Characteristics of road traffic noise in Hanoi and Ho Chi Minh City, Vietnam. *Applied Acoustics*, *71*(5), 479–485. https://doi.org/10.1016/j.apacoust.2009.11.008

Phuc, N. H., & Kim Oanh, N. T. (2018). Determining factors for levels of volatile organic compounds measured in different microenvironments of a heavy traffic urban area. *Science of the Total Environment*, *627*, 290–303. https://doi.org/10.1016/j.scitotenv.2018.01.216

Pio, C., Cerqueira, M., Harrison, R. M., Nunes, T., Mirante, F., Alves, C., Oliveira, C., Sanchez de la Campa, A., Artíñano, B., & Matos, M. (2011). OC/EC ratio observations in Europe: Re-thinking the approach for apportionment between primary and secondary organic carbon. *Atmospheric Environment*, *45*(34), 6121–6132. https://doi.org/10.1016/j.atmosenv.2011.08.045

Plaza, J., Artíñano, B., Salvador, P., Gómez-Moreno, F. J., Pujadas, M., & Pio, C. A. (2011). Short-term secondary organic carbon estimations with a modified OC/EC primary ratio method at a suburban site in Madrid (Spain). *Atmospheric Environment*, *45*(15), 2496–2506. https://doi.org/10.1016/j.atmosenv.2011.02.037

Pokhrel, A. K., Bates, M. N., Acharya, J., Valentiner-Branth, P., Chandyo, R. K., Shrestha, P. S., Raut, A. K., & Smith, K. R. (2015). PM2.5 in household kitchens of Bhaktapur,

Nepal, using four different cooking fuels. *Atmospheric Environment*, *113*, 159–168. https://doi.org/10.1016/j.atmosenv.2015.04.060

Pongpiachan, S., Choochuay, C., Chonchalar, J., Kanchai, P., Phonpiboon, T., Wongsuesat, S., Chomkhae, K., Kittikoon, I., Hiranyatrakul, P., Cao, J., & Thamrongthanyawong, S. (2013). Chemical characterisation of organic functional group compositions in pm2.5 collected at nine administrative provinces in northern thailand during the haze episode in 2013. *Asian Pacific Journal of Cancer Prevention*, *14*(6), 3653–3661. https://doi.org/10.7314/APJCP.2013.14.6.3653

Quang, T. N., Hue, N. T., Thai, P., Mazaheri, M., & Morawska, L. (2017). Exploratory assessment of indoor and outdoor particle number concentrations in Hanoi households. *Science of the Total Environment*, *599–600*, 284–290. https://doi.org/10.1016/j.scitotenv.2017.04.154

Ristovski, Z., Morawska, L., Ayoko, G. A., Johnson, G., Gilbert, D., & Greenaway, C. (2004). Emissions from a vehicle fitted to operate on either petrol or compressed natural gas. *Science of the Total Environment*, *323*(1–3), 179–194. https://doi.org/10.1016/j.scitotenv.2003.10.023

Rivas, I., Beddows, D. C. S., Amato, F., Green, D. C., Järvi, L., Hueglin, C., Reche, C., Timonen, H., Fuller, G. W., Niemi, J. V., Pérez, N., Aurela, M., Hopke, P. K., Alastuey, A., Kulmala, M., Harrison, R. M., Querol, X., & Kelly, F. J. (2020). Source apportionment of particle number size distribution in urban background and traffic stations in four European cities. *Environment International*, *135*(November 2019), 105345. https://doi.org/10.1016/j.envint.2019.105345

Rönkkö, T. J., Jalava, P. I., Happo, M. S., Kasurinen, S., Sippula, O., Leskinen, A., Koponen, H., Kuuspalo, K., Ruusunen, J., Väisänen, O., Hao, L., Ruuskanen, A., Orasche, J., Fang, D., Zhang, L., Lehtinen, K. E. J., Zhao, Y., Gu, C., Wang, Q., … Hirvonen, M. R. (2018). Emissions and atmospheric processes influence the chemical composition and toxicological properties of urban air particulate matter in Nanjing, China. *Science of the Total Environment*, *639*, 1290–1310. https://doi.org/10.1016/j.scitotenv.2018.05.260

Saha, P. K., Khlystov, A., Snyder, M. G., & Grieshop, A. P. (2018). Characterization of air pollutant concentrations, fleet emission factors, and dispersion near a North Carolina interstate freeway across two seasons. *Atmospheric Environment*, *177*(April 2017), 143–153. https://doi.org/10.1016/j.atmosenv.2018.01.019

Sakamoto, Y., Shoji, K., Bui, M. T., Phạm, T. H., Vu, T. A., Ly, B. T., & Kajii, Y. (2018). Air quality study in Hanoi, Vietnam in 2015–2016 based on a one-year observation of NOx, O3, CO and a one-week observation of VOCs. *Atmospheric Pollution Research*, *9*(3), 544–551. https://doi.org/10.1016/j.apr.2017.12.001

Sardar, S. B., Fine, P. M., Mayo, P. R., & Sioutas, C. (2005). Size-fractionated measurements of ambient ultrafine particle chemical composition in Los Angeles using the NanoMOUDI. *Environmental Science and Technology*, *39*(4), 932–944. https://doi.org/10.1021/es049478j

Sleiman, M., Logue, J. M., Pankow, J. F., Gundel, L. A., & Destaillats, H. (2014). Chemical characterization and health impact assessment of VOCs and particles in thirdhand tobacco smoke. *Indoor Air 2014 - 13th International Conference on Indoor Air Quality and Climate*, 177–178.

Stölzel, M., Breitner, S., Cyrys, J., Pitz, M., Wölke, G., Kreyling, W., Heinrich, J.,

Wichmann, H. E., & Peters, A. (2007). Daily mortality and particulate matter in different size classes in Erfurt, Germany. *Journal of Exposure Science and Environmental Epidemiology*, *17*(5), 458–467. https://doi.org/10.1038/sj.jes.7500538

Tang, X., Zhang, X., Wang, Z., & Ci, Z. (2016). Water-soluble organic carbon (WSOC) and its temperature-resolved carbon fractions in atmospheric aerosols in Beijing. *Atmospheric Research*, *181*, 200–210. https://doi.org/10.1016/j.atmosres.2016.06.019

Thuy, N. T. T., Dung, N. T., Sekiguchi, K., Thuy, L. B., Hien, N. T. T., & Yamaguchi, R. (2018). Mass concentrations and carbonaceous compositions of pm0.1, pm2.5, and pm10 at urban locations in hanoi, vietnam. *Aerosol and Air Quality Research*, *18*(7), 1591–1605. https://doi.org/10.4209/aaqr.2017.11.0502

Thuy, N. T. T., Dung, N. T., Sekiguchi, K., Yamaguchi, R., Thuy, P. C., & Bang, H. Q. (2017). Characteristics of Elemental and Organic Carbon in Atmospheric Nanoparticles At Different Sampling Locations in Vietnam. *Journal of Science and Technology*, *55*(3), 305–315. https://doi.org/10.15625/2525-2518/55/3/8820

Tran, L. K., Morawska, L., Quang, T. N., Jayaratne, R. E., Hue, N. T., Dat, M. V., Phi, T. H., & Thai, P. K. (2021). The impact of incense burning on indoor PM2.5 concentrations in residential houses in Hanoi, Vietnam. *Building and Environment*, *205*(August), 108228. https://doi.org/10.1016/j.buildenv.2021.108228

Tran, T. D., Nguyen, P. M., Nghiem, D. T., Le, T. H., Tu, M. B., Alleman, L. Y., Nguyen, V. M., Pham, D. T., Ha, N. M., Dang, M. N., Van Le, C., & Van Nguyen, N. (2020). Assessment of air quality in school environments in Hanoi, Vietnam: A focus on mass-size distribution and elemental composition of indoor-outdoor ultrafine/fine/coarse particles. *Atmosphere*, *11*(5), 1–21. https://doi.org/10.3390/atmos11050519

Tran, T. M., Tran-Lam, T. T., Mai, H. H. T., Bach, L. H. T., Nguyen, H. M. N., Trinh, H. T., Dang, L. T., Minh, T. B., Quan, T. C., & Hoang, A. Q. (2021). Parabens in personal care products and indoor dust from Hanoi, Vietnam: Temporal trends, emission sources, and non-dietary exposure through dust ingestion. *Science of the Total Environment*, *761*, 143274. https://doi.org/10.1016/j.scitotenv.2020.143274

Trang, T. T., Van, H. H., & Oanh, N. T. K. (2015). Traffic emission inventory for estimation of air quality and climate co-benefits of faster vehicle technology intrusion in Hanoi, Vietnam. *Carbon Management*, *6*(3–4), 117–128. https://doi.org/10.1080/17583004.2015.1093694

Truc, V. T. Q., & Kim Oanh, N. T. (2007). Roadside BTEX and other gaseous air pollutants in relation to emission sources. *Atmospheric Environment*, *41*(36), 7685–7697. https://doi.org/10.1016/j.atmosenv.2007.06.003

Tuch, T. H., Brand, P., Wichmann, H. E., & Heyder, J. (1997). Variation of particle number and mass concentration in various size ranges of ambient aerosols in Eastern Germany. *Atmospheric Environment*, *31*(24), 4193–4197. https://doi.org/10.1016/S1352-2310(97)00260-4

Turpin, B. J., & Huntzicker, J. J. (1995). Identification of secondary organic aerosol episodes and quantitation of primary and secondary organic aerosol concentrations during SCAQS. *Atmospheric Environment*, *29*(23), 3527–3544. https://doi.org/10.1016/1352-2310(94)00276-Q

USEPA. (1999). Nitrogen oxides (NOx), why and how they are controlled. *Epa-456/F-99-*

006R, *November*, 48. http://www.epa.gov/ttncatc1/dir1/fnoxdoc.pdf

USEPA. (2012). *Report to Congress on Black Carbon: Department of the Interior, Environment, and Related Agencies Appropriations Act, 2010*. *March*, 388. www.epa.gov/blackcarbon

Vecchi, R., Marcazzan, G., Valli, G., Ceriani, M., & Antoniazzi, C. (2004). The role of atmospheric dispersion in the seasonal variation of PM1 and PM2.5 concentration and composition in the urban area of Milan (Italy). *Atmospheric Environment*, *38*(27), 4437–4446. https://doi.org/10.1016/j.atmosenv.2004.05.029

Vietnam Register (VR). (2019). *Vietnam transportation statistical book.* Hanoi, Vietnam: Author

Vo, L. H. T., Yoneda, M., Nghiem, T. D., Shimada, Y., Van, D. A., Nguyen, T. H. T., & Nguyen, T. T. (2022). Indoor PM0.1 and PM2.5 in Hanoi: Chemical characterization, source identification, and health risk assessment. *Atmospheric Pollution Research*, *13*(2). https://doi.org/10.1016/j.apr.2022.101324

Vu, T. V., Delgado-Saborit, J. M., & Harrison, R. M. (2015). Review: Particle number size distributions from seven major sources and implications for source apportionment studies. *Atmospheric Environment*, *122*, 114–132. https://doi.org/10.1016/j.atmosenv.2015.09.027

Wang, X., Wang, W., Yang, L., Gao, X., Nie, W., Yu, Y., Xu, P., Zhou, Y., & Wang, Z. (2012). The secondary formation of inorganic aerosols in the droplet mode through heterogeneous aqueous reactions under haze conditions. *Atmospheric Environment*, *63*, 68–76. https://doi.org/10.1016/j.atmosenv.2012.09.029

Wang, Ying, Zhuang, G., Tang, A., Yuan, H., Sun, Y., Chen, S., & Zheng, A. (2005). The ion chemistry and the source of PM2.5 aerosol in Beijing. *Atmospheric Environment*, *39*(21), 3771–3784. https://doi.org/10.1016/j.atmosenv.2005.03.013

Wang, Yungang, Hopke, P. K., & Utell, M. J. (2012). Urban-scale seasonal and spatial variability of ultrafine particle number concentrations. *Water, Air, and Soil Pollution*, *223*(5), 2223–2235. https://doi.org/10.1007/s11270-011-1018-z

Watson, J. G., Chow, J. C., & Houck, J. E. (2001). PM2.5 chemical source profiles for vehicle exhaust, vegetative burning, geological material, and coal burning in Northwestern Colorado during 1995. *Chemosphere*, *43*(8), 1141–1151. https://doi.org/10.1016/S0045-6535(00)00171-5

Wehner, B., & Wiedensohler, A. (2003). Long term measurements of submicrometer urban aerosols: Statistical analysis for correlations with meteorological conditions and trace gases. *Atmospheric Chemistry and Physics*, *3*(3), 867–879. https://doi.org/10.5194/acp-3-867-2003

Westerdahl, D., Fruin, S., Sax, T., Fine, P. M., & Sioutas, C. (2005). Mobile platform measurements of ultrafine particles and associated pollutant concentrations on freeways and residential streets in Los Angeles. *Atmospheric Environment*, *39*(20), 3597–3610. https://doi.org/10.1016/j.atmosenv.2005.02.034

WHO. (2016). World health statistics 2016: monitoring health for the SDGs. *World Health Organization*, 1.121.

WHO. (2020). World health statistics 2020: monitoring health for the SDGs. In *Composites Part A: Applied Science and Manufacturing* (Vol. 68, Issue 1).

Xiang, P., Zhou, X., Duan, J., Tan, J., He, K., Yuan, C., Ma, Y., & Zhang, Y. (2017). Chemical characteristics of water-soluble organic compounds (WSOC) in PM2.5 in Beijing, China: 2011–2012. *Atmospheric Research*, *183*, 104–112. https://doi.org/10.1016/j.atmosres.2016.08.020

Xu, Q., Wang, S., Jiang, J., Bhattarai, N., Li, X., Chang, X., Qiu, X., Zheng, M., Hua, Y., & Hao, J. (2019). Nitrate dominates the chemical composition of PM2.5 during haze event in Beijing, China. *Science of the Total Environment*, *689*, 1293–1303. https://doi.org/10.1016/j.scitotenv.2019.06.294

Yan, G., Zhang, P., Yang, J., Zhang, J., Zhu, G., Cao, Z., Fan, J., Liu, Z., & Wang, Y. (2021). Chemical characteristics and source apportionment of PM2.5 in a petrochemical city: Implications for primary and secondary carbonaceous component. *Journal of Environmental Sciences (China)*, *103*, 322–335. https://doi.org/10.1016/j.jes.2020.11.012

Yang, S., Liu, Z., Li, J., Zhao, S., Xu, Z., Gao, W., Hu, B., & Wang, Y. (2021). Insights into the chemistry of aerosol growth in Beijing: Implication of fine particle episode formation during wintertime. *Chemosphere*, *274*. https://doi.org/10.1016/j.chemosphere.2021.129776

Yassin, M. F., AlThaqeb, B. E. Y., & Al-Mutiri, E. A. E. (2012). Assessment of indoor PM 2.5 in different residential environments. *Atmospheric Environment*, *56*, 65–68. https://doi.org/10.1016/j.atmosenv.2012.03.051

Zhang, L., Cheng, Y., Zhang, Y., He, Y., Gu, Z., & Yu, C. (2017). Impact of air humidity fluctuation on the rise of PM mass concentration based on the high-resolution monitoring data. *Aerosol and Air Quality Research*, *17*(2), 543–552. https://doi.org/10.4209/aaqr.2016.07.0296

Zhang, Y., Liu, X., Zhang, L., Tang, A., Goulding, K., & Collett, J. L. (2021). Evolution of secondary inorganic aerosols amidst improving PM2.5 air quality in the North China plain. *Environmental Pollution*, *281*, 117027. https://doi.org/10.1016/j.envpol.2021.117027

Zhu, C. S., Chen, C. C., Cao, J. J., Tsai, C. J., Chou, C. C. K., Liu, S. C., & Roam, G. D. (2010). Characterization of carbon fractions for atmospheric fine particles and nanoparticles in a highway tunnel. *Atmospheric Environment*, *44*(23), 2668–2673. https://doi.org/10.1016/j.atmosenv.2010.04.042

Zhu, Y., Hinds, W. C., Kim, S., Shen, S., & Sioutas, C. (2002). Study of ultrafine particles near a major highway with heavy-duty diesel traffic. *Atmospheric Environment*, *36*(27), 4323–4335. https://doi.org/10.1016/S1352-2310(02)00354-0

Zhu, Y., Pudota, J., Collins, D., Allen, D., Clements, A., DenBleyker, A., Fraser, M., Jia, Y., McDonald-Buller, E., & Michel, E. (2009). Air pollutant concentrations near three Texas roadways, Part I: Ultrafine particles. *Atmospheric Environment*, *43*(30), 4513–4522. https://doi.org/10.1016/j.atmosenv.2009.04.018